

# Final-state rescattering mechanism of double-charm baryon decays: $\mathcal{B}_{cc} \rightarrow \mathcal{B}_c P$

Xiao-Hui Hu,<sup>1,2,\*</sup> Cai-Ping Jia,<sup>3,†</sup> Ye Xing,<sup>1,‡</sup> and Fu-Sheng Yu<sup>2,4,§</sup>

<sup>1</sup>*The College of Materials and physics,  
China University of mining and technology, Xuzhou 221116, China*

<sup>2</sup>*Lanzhou Center for Theoretical Physics and Key  
Laboratory of Theoretical Physics of Gansu Province,  
Lanzhou University, Lanzhou 730000, China*

<sup>3</sup>*Center for High Energy Physics, Peking University, Beijing 100871, China*

<sup>4</sup>*Frontiers Science Center for Rare Isotopes,  
and School of Nuclear Science and Technology,  
Lanzhou University, Lanzhou 730000, China*

(Dated: March 25, 2025)

## Abstract

The doubly charmed baryon,  $\Xi_{cc}^{++}$ , was first observed by LHCb through the non-leptonic decay modes of  $\Xi_{cc}^{++} \rightarrow \Lambda_c^+ K^- \pi^+ \pi^+$  and  $\Xi_c^+ \pi^+$ . Following this discovery, researchers shifted their focus to identifying other doubly charmed baryons, specifically  $\Xi_{cc}^+$  and  $\Omega_{cc}^+$ . In this study, we examine the non-leptonic weak decays of doubly charmed baryons, denoted as  $\mathcal{B}_{cc} \rightarrow \mathcal{B}_c P$ , where  $\mathcal{B}_{cc}$  represents the doubly charmed baryons, specifically  $(\Xi_{cc}^{++}, \Xi_{cc}^+, \Omega_{cc}^+)$ . The notation  $\mathcal{B}_c$  denotes the singly charmed baryons, specifically  $(\mathcal{B}_3, \mathcal{B}_6)$ , while  $P$  signifies the light pseudoscalar. These terms are pertinent to the non-leptonic decay modes under discussion. While the short-distance contributions can be precisely estimated through theoretical calculations, addressing the long-distance contributions for final-state-interaction effects presents a significant challenge. In order to address this issue, we utilize the rescattering mechanism of final state interaction effects to compute the long-distance contributions. We initially derive the entire hadronic loop contributions for these two-body nonleptonic decays of doubly charmed baryons. In subsequent analyses, we are able to calculate relative strong phases. As a result, we can provide predictions for their decay asymmetry parameters and CP violations. Furthermore, we employ experimental data from the LHCb collaboration, specifically the ratio  $Br(\Xi_{cc}^{++} \rightarrow \Xi_c'^+ \pi^+)/Br(\Xi_{cc}^{++} \rightarrow \Xi_c^+ \pi^+) = (1.41 \pm 0.17 \pm 0.10)$ , to ascertain the model parameters  $\eta = 0.9 \pm 0.2$ . Consequently, we present the predictions of branching ratios and decay asymmetry parameters for 67 distinct decay processes and CP violations for the singly Cabibbo suppressed channels. This not only strengthens the validity of our theoretical predictions, but also provides a more comprehensive theoretical framework for the future identification of other doubly charmed baryons.

PACS numbers:

\*huxiaohui@cumt.edu.cn, corresponding author

†jiacp@pku.edu.cn, corresponding author

‡xingye.guang@cumt.edu.cn, corresponding author

§yufsh@lzu.edu.cn, corresponding author

## I. INTRODUCTION

Over the past two decades, a significant number of new hadrons with the heavy quark have been identified experimentally [1]. These encompass both exotic states and conventional heavy baryons, offering an optimal opportunity to explore and establish traditional baryon spectroscopy. Until now, most candidates of conventional baryons are accommodated into the singly heavy baryons, while the experimental observations for doubly heavy baryons are still scarce. In 2002, the SELEX collaboration initially reported the detection of  $\Xi_{cc}^+$ . However, subsequent experiments have yet to corroborate this discovery [2–5]. In 2017, the LHCb Collaboration made a remarkable discovery, revealing a significant structure,  $\Xi_{cc}^{++}(3621)$ , within the invariant mass spectrum of the  $\Lambda_c^+ K^- \pi^+ \pi^+$  [6]. Also, the existence of  $\Xi_{cc}^{++}$  was confirmed by them through the decay channel  $\Xi_{cc}^{++} \rightarrow \Xi_c^+ \pi^+$  [7]. The LHCb Collaboration has conducted precise measurements of its mass and lifetime [8, 9], and also measured the branching fraction of  $\Xi_{cc}^{++} \rightarrow \Xi_c'^+ \pi^+$  decay relative to  $\Xi_{cc}^{++} \rightarrow \Xi_c^+ \pi^+$  decay as  $Br(\Xi_{cc}^{++} \rightarrow \Xi_c'^+ \pi^+)/Br(\Xi_{cc}^{++} \rightarrow \Xi_c^+ \pi^+) = \mathcal{B}'/\mathcal{B} = (1.41 \pm 0.17 \pm 0.10)$  [10]. The other doubly heavy baryons, such as  $\Xi_{cc}^+$  [11, 12],  $\Omega_{cc}^+$  [13],  $\Xi_{bc}^+$  [14],  $\Xi_{bc}^0$  [15, 16] and  $\Omega_{bc}^0$  [16], have also been investigated by the LHCb Collaboration; however, no signals have been detected to date. The doubly charmed tetraquark  $T_{cc}^+(3875)$  was also identified by the LHCb Collaboration, which may provide insights into the nature of doubly heavy baryons [17, 18]. Prior to the experimental discovery of  $\Xi_{cc}^{++}$ , theoretical studies had already suggested that the most likely discovery of these doubly charmed baryons would occur via two decay channels:  $\Xi_{cc}^{++} \rightarrow \Lambda_c^+ K^- \pi^+ \pi^+$  and  $\Xi_{cc}^{++} \rightarrow \Xi_c^+ \pi^+$  [19]. Therefore, pre-theoretical studies of their decays are crucial for the experimental research of doubly heavy baryons.

Numerous theoretical investigations have been conducted on the production, mass spectra, and both strong and weak or radiative decays of doubly heavy baryons, utilizing a variety of methodologies [19–67]. Theoretical studies on the weak decays of doubly heavy baryons have been mostly focused on semileptonic weak decays, while nonleptonic weak decays have received relatively less attention. This is mainly due to the large number of nonleptonic decay channels. In addition, unlike semi-leptonic decays, non-leptonic decays include not only factorizable contributions but also non-factorizable ones, which are difficult to systematically study using QCD methods. At present, there appears to be a notable dearth of research on the nonleptonic weak decays of doubly heavy baryons, which also lacks a systematic approach [46, 68–74]. Aside from an SU(3) symmetry analysis [68, 69] and a phenomenological study [46], there is no research on the non-factorizable contribution in doubly charmed baryon decays that is based on QCD or is model-independent. The predominant technique for evaluating such a contribution is the pole-model [70–74]. For example, the factorizable and non-factorizable contributions from the pole-model give a ratio  $\mathcal{B}'/\mathcal{B}$  in the range  $0.81 - 0.83$  [70, 71]. This implies that the branching fraction of the decay into  $\Xi_c'^+$  is suppressed, in direct contradiction with experiment data [10]. In addition, when the interference between the W-emission and W-exchange contributions is considered, the ratio  $\mathcal{B}'/\mathcal{B}$  increases to about 6.74 [72]. By integrating the factorizable amplitudes derived from heavy quark effective theory with the W-exchange contribution ascertained through light-cone sum rules (LCSR), the ratio  $\mathcal{B}'/\mathcal{B}$  can be determined to be  $1.42 \pm 0.78$  [75], which is align with the experimental results, within the acceptable margin of error. So the investigation of non-leptonic weak decays is profoundly impacted by non-factorizable contributions, such as the W-exchange contribution. In the prior research [19], the authors calculated the short-distance contributions of decay amplitudes using a factorization approach. Conversely, the long-distance contributions were initially examined in double-charm-baryon decays, taking into account the rescattering mechanism. It is found that these long-distance contributions are significantly enhanced and play a crucial role in the non-leptonic weak decays. Subsequently, they utilized this framework to examine the two-body non-leptonic weak decays of doubly heavy baryons  $\mathcal{B}_{cc} \rightarrow \mathcal{B}_c P(V)$  [76, 77],  $\mathcal{B}_{cc} \rightarrow \mathcal{B} D^{(*)}$  [78], and

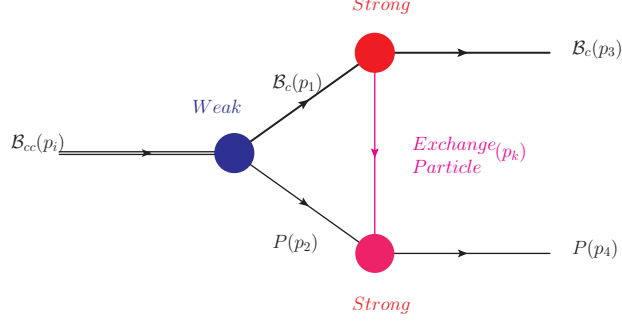


Figure 1: The diagram description of the rescattering mechanism at the hadron level.  $p_i$ ,  $p_1$  and  $p_2$  are the momentum of the initial and final states,  $p_1$ ,  $p_2$  and  $p_k$  are the ones of intermediate states. The blue ball represents the weak vertex, and the red one denotes the strong vertex.

$\mathcal{B}_{bc} \rightarrow \mathcal{B}_b P$  [79]. The long-distance contributions were calculated using the cutting rule for the imaginary component of the hadronic triangle diagram. It is worth noting that final-state interaction effects have been reasonably addressed for singly charmed baryon decays in recent work [80], which explores long-distance contributions within the framework of hadronic loop integrals. This method computes both the real and imaginary parts of the amplitudes comprehensively, providing strong phases that enhance our understanding of decay asymmetries and  $CP$  asymmetries. In this paper, we will adopt this method to improve the understanding of double-charmed baryon by calculating the cumulative triangle-diagram contribution including real and imaginary parts.

In the following, we will explain the theoretically improved framework of two-body nonleptonic decay of double-charmed baryons  $\mathcal{B}_{cc} \rightarrow \mathcal{B}_c P$ .

- Firstly, the factorizable contributions are computed using the factorization method, which comprises two components: the non-perturbative transition matrix element  $\langle \mathcal{B}_c | (V - A)_\mu | \mathcal{B}_{cc} \rangle$ , characterized by form factors, and the matrix element  $\langle P | (V - A)_\mu | 0 \rangle$ , represented by the decay constant of meson  $P$ . The non-perturbative form factors have been assessed in a variety of theoretical studies, utilizing LCSR [81–85], light-front quark model (LFQM) [72, 86–90], QCD sum rules [91], QCD factorization [70, 71], diquark effective theory [92], constituent quark model [73, 93], and heavy quark effective theory [70, 74]. In this work, we adopt the theoretical predictions of form factors within LFQM [86] as inputs. The decay constants of mesons have been accurately calculated and measured [94–96].
- Secondly, we will show how the computation of non-factorizable long-distance contributions is achieved via the rescattering mechanism briefly. The final states of the nonleptonic weak decays of the doubly charmed baryons,  $\mathcal{B}_c$  and  $P$ , involve their mutual scattering via the exchange of one particle, resulting in a triangle diagram at the hadron level, as depicted in Fig. 1. The triangle diagram mechanism has been widely studied in recent works about exotic hadrons [97–113]. To circumvent the issue of double-counting, contributions from both short and long distances are segregated into the tree emission process  $\mathcal{B}_{cc}(p_i) \rightarrow \mathcal{B}_c(p_1)P(p_2)$  and final state interaction effects. In this study, we employ the effective Lagrangian at the hadronic level of the strong vertex in the rescattering mechanism to compute the final state interaction effects. Previous literature [19, 76–79] have utilized the optical theorem and Cutkosky cutting rules to compute triangle diagrams. However, these calculations only yield the imaginary component of the amplitude, making it challenging to accurately represent the strong phase. In this paper, we corrected this issue by employing the comprehensive analytical expression of loop integrals, which allows us to ascertain both the magnitude and

strong phase of triangle diagrams. While in the calculations of the final states interaction effects, the non-perturbative parameters such as the cut-off  $\Lambda$  in the loop calculation will bring large theoretical uncertainties on the branching ratios. Unlike the case of B meson [114, 115], there are not enough data to determine the non-perturbative parameters of doubly charmed baryons. Therefore, the main problem in the calculations of long-distance contribution is how to control the theoretical uncertainties. Due to the ratios of the branching fractions are not sensitive to the non-perturbative parameters, we will calculate the ratios to control the uncertainties of the theoretical prediction.

The remainder of this paper is organized as follows. In the section II, we will introduce the theoretical framework of the final states rescattering mechanism and factorization approach. In the section III, the input parameters, numerical results of observations including branching ratios, decay asymmetry parameters and CP violation, and the corresponding theoretical analysis are presented. In the section IV, we give a brief summary. In the Appendix A, the amplitudes of each modes are listed. In the Appendix B, the strong coupling constants of  $g_{VVP}$ ,  $g_{VPP}$ ,  $g_{PBB}$  and  $g_{VBB}$  are collected.

## II. THEORETICAL FRAMEWORK

In this section, we will present a topological analysis of each nonleptonic weak decay channel of doubly charmed baryons, as detailed in Sec. II A. Subsequently, we present the general framework for calculating the short-distance and long-distance dynamics of all topological diagrams in Sec. II B and Sec. II C, respectively.

### A. Topological analysis

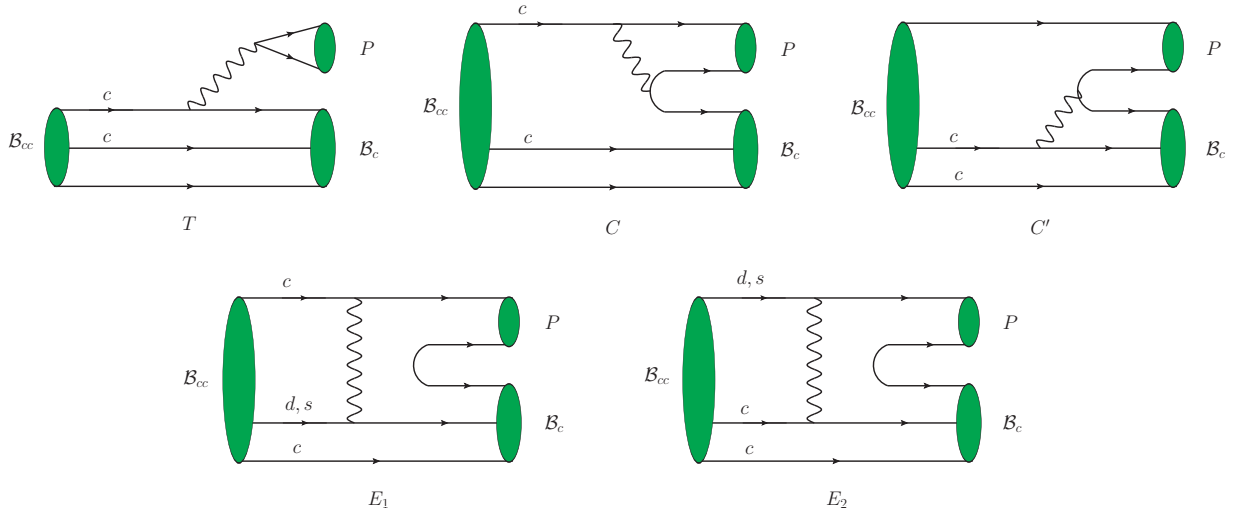


Figure 2: The five tree level topological diagrams for two body non leptonic decays  $\mathcal{B}_{cc} \rightarrow \mathcal{B}_c P$  of the doubly charmed baryons  $\mathcal{B}_{cc} = (\Xi_{cc}^{++}, \Xi_{cc}^+, \Omega_{cc}^+)$ .

In this work, we will investigate the exclusive channels of nonleptonic weak decay of doubly charmed baryons  $\mathcal{B}_{cc} \rightarrow \mathcal{B}_c P$ . The initial state is characterized by a doubly charmed baryon triplet  $\mathcal{B}_{cc} = (\Xi_{cc}^{++}, \Xi_{cc}^+, \Omega_{cc}^+)$ , while the final state encompasses the singly charmed baryon  $\mathcal{B}_c =$

$(\mathcal{B}_3, \mathcal{B}_6)$ , and the light pseudoscalar mesons  $P = (\pi, K, \eta_{1,8})$ , as shown in Appendix B. Based on the symmetry analysis of the initial and final states of particles, we will study forty-nine decay processes.

The tree-level contributions to the nonleptonic weak decay of doubly charmed baryons  $\mathcal{B}_{cc} \rightarrow \mathcal{B}_c P$  are shown in Fig. 2, where each diagram contains both short-distance and long-distance contributions. Due to their distinct topologies, the five diagrams can be categorized into three types:  $T$ ,  $C(C')$  and  $E_1(E_2)$ .  $T$  represents the color-favored external  $W$  emission diagram. Both  $C$  and  $C'$  are color-suppressed internal  $W$ -emission diagrams. The difference between them is whether both quarks of the final light meson come from the weak vertex. In the  $C$  diagram, all constituent quarks of the final light meson come from the weak vertex. In the  $C'$  diagram, one constituent quark of the final light meson comes from the initial state baryon, and only its antiquark comes from the weak vertex. The contributions of  $W$ -exchange can be divided into two cases. In the  $E_1$  diagram, the light quark which comes from the decay of charmed quark is taken by the final light meson. In the  $E_2$  diagram, it is taken by the final charmed baryon.

The topology analysis for each nonleptonic weak decay channel can be concluded in Tab. I. The topological amplitudes for the channels with the sextet single charmed baryons are distinguished from anti-triplet baryons by adding a *tilde*, e.g.  $\tilde{T}$ . The short-distance dominated modes are listed in the first part of Tab. I. The following three parts are the long-distance dynamics dominated modes, which can be divided into three groups based on the CKM matrix elements: the Cabibbo-favored (CF) decays induced by  $c \rightarrow s\bar{u}\bar{d}$ , (ii) the singly Cabibbo-suppressed (SCS) ones induced by  $c \rightarrow d\bar{u}\bar{d}$  or  $c \rightarrow s\bar{u}\bar{s}$ , the doubly Cabibbo-suppressed (DCS) ones induced by  $c \rightarrow d\bar{u}\bar{s}$ . The topological diagram  $T$ , dominated by the factorizable short-distance contributions [116], can be determined using the factorization hypothesis. While the contribution of the  $C(C')$  diagram is markedly diminished at the charm scale, primarily due to the color factor  $a_2(m_c) = C_1(m_c) + C_2(m_c)/N_c$  [19]. At the charm quark mass scale, the long-distance contribution in the  $E_1(E_2)$  diagram exceeds that of the short-distance contribution, which is suppressed by at least one order [116]. Based on the topology analysis, we can determine that the ratio  $Br(\Xi_{cc}^{++} \rightarrow \Xi_c'^+ \pi^+)/Br(\Xi_{cc}^{++} \rightarrow \Xi_c^+ \pi^+)$  is approximate to 0.5. This finding contrasts with the experimental data [10]. Since the non-factorizable long-distance contributions may predominantly influence the calculation of the  $C(C')$  diagram, potentially exerting a significant impact on the final result of the decay branching ratio. So we need more investigation on the nonfactorizable long distance contributions. The inclusion of non-factorizable contributions, such as final state interaction effects mediated by loop mechanisms, into our model allows for the improvement of theoretical predictions through parameter and assumption refinement. This ensures a more precise congruence with experimental data. The calculation of the factorizable short-distance and non-factorizable long-distance contributions will be introduced in detail in the following subsections.

## B. Calculation of short-distance amplitudes under the factorization hypothesis

At the tree level, the non-leptonic weak decay of doubly charmed baryons are induced by the decay of the charm quark. The effective Hamiltonian can be represented as follows,

$$\mathcal{H}_{eff} = \frac{G_F}{\sqrt{2}} \sum_{q'=d,s} V_{cq'}^* V_{uq} [C_1(\mu) O_1(\mu) + C_2(\mu) O_2(\mu)] + h.c.. \quad (1)$$

Here  $V_{cq'}$  and  $V_{uq}$  represent the Cabibbo-Kobayashi-Maskawa (CKM) matrix elements. And the four-fermion operators  $O_1$  and  $O_2$  can be expressed as,

$$O_1 = (\bar{u}_\alpha q_\beta)_{V-A} (\bar{q}'_\beta c_\alpha)_{V-A}, \quad O_2 = (\bar{u}_\alpha q_\alpha)_{V-A} (\bar{q}'_\beta c_\beta)_{V-A}, \quad (2)$$

Table I: The topological analysis of each nonleptonic weak decay channel.

Decay	Topology	Decay	Topology	Decay	Topology
$\Xi_{cc}^{++} \rightarrow \Xi_c^+ \pi^+$	$\lambda_s d(T + C')$	$\Xi_c^+ \rightarrow \Xi_c^0 \pi^+$	$\lambda_s d(T - E_2)$	$\Omega_{cc}^+ \rightarrow \Omega_c^0 \pi^+$	$\lambda_s d T$
$\Xi_{cc}^{++} \rightarrow \Xi_c^+ \pi^0$	$\frac{1}{\sqrt{2}} \lambda_s d(\tilde{T} + \tilde{C}')$	$\Xi_{cc}^+ \rightarrow \Xi_c^0 \pi^0$	$\frac{1}{\sqrt{2}} \lambda_s d(\tilde{T} + \tilde{E}_2)$	$\Omega_{cc}^+ \rightarrow \Xi_c^0 \pi^0$	$-\lambda_d T - \lambda_s E_2$
$\Xi_{cc}^{++} \rightarrow \Sigma_c^+ \pi^+$	$\frac{1}{\sqrt{2}} \lambda_d(\tilde{T} + \tilde{C}')$	$\Xi_{cc}^+ \rightarrow \Sigma_c^0 \pi^+$	$\lambda_d(\tilde{T} + \tilde{E}_2)$	$\Omega_{cc}^+ \rightarrow \Xi_c^0 \pi^+$	$\frac{1}{\sqrt{2}}(\lambda_d \tilde{T} + \lambda_s \tilde{E}_2)$
$\Xi_{cc}^{++} \rightarrow \Lambda_c^+ \pi^+$	$\lambda_d(T + C')$	$\Xi_{cc}^+ \rightarrow \Xi_c^0 K^+$	$\frac{1}{\sqrt{2}}(\lambda_s \tilde{T} + \lambda_d \tilde{E}_2)$	$\Omega_{cc}^+ \rightarrow \Omega_c^0 K^+$	$\lambda_s(\tilde{T} + \tilde{E}_2)$
$\Xi_{cc}^{++} \rightarrow \Xi_c^+ K^0$	$\frac{1}{\sqrt{2}} \lambda_s(\tilde{T} + \tilde{C}')$	$\Xi_{cc}^+ \rightarrow \Xi_c^0 K^0$	$\lambda_s T + \lambda_d E_2$	$\Omega_{cc}^+ \rightarrow \Xi_c^0 K^0$	$\lambda_{ds}(-T + E_2)$
$\Xi_{cc}^{++} \rightarrow \Xi_c^+ K^+$	$\lambda_s(T + C')$	$\Xi_{cc}^+ \rightarrow \Sigma_c^0 K^+$	$\lambda_{ds} \tilde{T}$	$\Omega_{cc}^+ \rightarrow \Xi_c^0 K^+$	$\frac{1}{\sqrt{2}} \lambda_{ds}(\tilde{T} + \tilde{E}_2)$
$\Xi_{cc}^{++} \rightarrow \Lambda_c^+ K^+$	$\lambda_{ds}(T + C')$	$\Xi_{cc}^{++} \rightarrow \Sigma_c^+ K^+$	$\frac{1}{\sqrt{2}} \lambda_{ds}(\tilde{T} + \tilde{C}')$		
$\Xi_{cc}^{++} \rightarrow \Sigma_c^{++} \bar{K}^0$	$\tilde{C}$	$\Xi_{cc}^+ \rightarrow \Xi_c^+ \pi^0$	$\frac{1}{2}(-\tilde{C}' + \tilde{E}_2)$	$\Xi_{cc}^+ \rightarrow \Xi_c^+ \eta_8$	$\frac{1}{\sqrt{6}}(C' - 2E_1 - E_2)$
$\Xi_{cc}^+ \rightarrow \Omega_c^0 K^+$	$\tilde{E}_2$	$\Xi_{cc}^+ \rightarrow \Xi_c^+ \eta_1$	$\frac{1}{\sqrt{6}}(\tilde{C}' + \tilde{E}_1 + \tilde{E}_2)$	$\Omega_{cc}^+ \rightarrow \Xi_c^+ \bar{K}^0$	$\frac{1}{\sqrt{2}}(\tilde{C} + \tilde{C}')$
$\Xi_{cc}^+ \rightarrow \Sigma_c^+ \bar{K}^0$	$\frac{1}{\sqrt{2}}(\tilde{C} + \tilde{E}_1)$	$\Xi_{cc}^+ \rightarrow \Xi_c^+ \eta_8$	$\frac{1}{2\sqrt{3}}(\tilde{C}' - 2\tilde{E}_1 + \tilde{E}_2)$	$\Omega_{cc}^+ \rightarrow \Xi_c^+ \bar{K}^0$	$-C + C'$
$\Xi_{cc}^+ \rightarrow \Lambda_c^+ \bar{K}^0$	$-C + E_1$	$\Xi_{cc}^+ \rightarrow \Xi_c^+ \pi^0$	$-\frac{1}{\sqrt{2}}(C' + E_2)$		
$\Xi_{cc}^+ \rightarrow \Sigma_c^{++} K^-$	$\tilde{E}_1$	$\Xi_{cc}^+ \rightarrow \Xi_c^+ \eta_1$	$\frac{1}{\sqrt{3}}(C' + E_1 - E_2)$		
$\Xi_{cc}^{++} \rightarrow \Sigma_c^{++} \pi^0$	$-\frac{1}{\sqrt{2}} \tilde{C}$	$\Xi_{cc}^+ \rightarrow \Xi_c^+ K^0$	$\frac{1}{\sqrt{2}}(\lambda_s C' + \lambda_d \tilde{E}_1)$	$\Omega_{cc}^+ \rightarrow \Sigma_c^{++} K^-$	$\lambda_s \tilde{E}_1$
$\Xi_{cc}^{++} \rightarrow \Sigma_c^{++} \eta_1$	$\frac{1}{\sqrt{3}}(\lambda_d + \lambda_s) \tilde{C}$	$\Xi_{cc}^+ \rightarrow \Xi_c^+ K^0$	$\lambda_s C' + \lambda_d E_1$	$\Omega_{cc}^+ \rightarrow \Xi_c^+ \pi^0$	$\frac{1}{2}(-\lambda_d \tilde{C} + \lambda_s \tilde{E}_2)$
$\Xi_{cc}^{++} \rightarrow \Sigma_c^{++} \eta_8$	$\frac{1}{\sqrt{6}}(\lambda_d - 2\lambda_s) \tilde{C}$	$\Xi_{cc}^+ \rightarrow \Lambda_c^+ \pi^0$	$\frac{\lambda_d}{\sqrt{2}}(C - C' - E_1 - E_2)$	$\Omega_{cc}^+ \rightarrow \Xi_c^+ \pi^0$	$\frac{1}{\sqrt{2}}(\lambda_d C - \lambda_s E_2)$
$\Xi_{cc}^+ \rightarrow \Sigma_c^+ \pi^0$	$\frac{\lambda_d}{2}(\tilde{C} - \tilde{C}' + \tilde{E}_1 + \tilde{E}_2)$	$\Xi_{cc}^+ \rightarrow \Lambda_c^+ \eta_1$	$\frac{1}{\sqrt{3}}[\lambda_d(C' - C + E_1 - E_2) - \lambda_s C]$	$\Omega_{cc}^+ \rightarrow \Xi_c^+ \eta_1$	$\frac{1}{\sqrt{6}}[\lambda_s(\tilde{C} + \tilde{C}' + \tilde{E}_1 + \tilde{E}_2) + \lambda_d \tilde{C}]$
$\Xi_{cc}^+ \rightarrow \Sigma_c^+ \eta_1$	$\frac{1}{\sqrt{6}}[\lambda_d(\tilde{C} + \tilde{C}' + \tilde{E}_1 + \tilde{E}_2) + \lambda_s \tilde{C}]$	$\Xi_{cc}^+ \rightarrow \Lambda_c^+ \eta_8$	$\frac{1}{\sqrt{6}}[\lambda_s(2C - 2C' + E_1 - E_2) + 2\lambda_s C]$	$\Omega_{cc}^+ \rightarrow \Xi_c^+ \eta_8$	$\frac{1}{2\sqrt{3}}[\lambda_s(\tilde{E}_2 - 2\tilde{C} - 2\tilde{C}' - 2\tilde{E}_1) + \lambda_d \tilde{C}]$
$\Xi_{cc}^+ \rightarrow \Sigma_c^+ \eta_8$	$\frac{1}{2\sqrt{3}}[\lambda_d(\tilde{C} + \tilde{C}' + \tilde{E}_1 + \tilde{E}_2) - 2\lambda_s \tilde{C}]$	$\Omega_{cc}^+ \rightarrow \Xi_c^+ \eta_8$	$\frac{1}{\sqrt{6}}[\lambda_s(2C - 2C' + 2E_1 - E_2) - \lambda_d C]$	$\Omega_{cc}^+ \rightarrow \Xi_c^+ \eta_1$	$\frac{1}{\sqrt{3}}[\lambda_s(C' - C + E_1 - E_2) - \lambda_d C]$
$\Xi_{cc}^+ \rightarrow \Sigma_c^{++} \pi^-$	$\lambda_d \tilde{E}_1$	$\Omega_{cc}^+ \rightarrow \Sigma_c^+ \bar{K}^0$	$\frac{1}{\sqrt{2}}(\lambda_d \tilde{C} + \lambda_s \tilde{E}_1)$	$\Omega_{cc}^+ \rightarrow \Lambda_c^+ \bar{K}^0$	$\lambda_d C' + \lambda_s E_1$
$\Xi_{cc}^{++} \rightarrow \Sigma_c^{++} K^0$	$\tilde{C}$	$\Omega_{cc}^+ \rightarrow \Sigma_c^+ \eta_8$	$\frac{1}{2\sqrt{3}}(-2\tilde{C}' + \tilde{E}_1 + \tilde{E}_2)$	$\Omega_{cc}^+ \rightarrow \Sigma_c^{++} \pi^-$	$\tilde{E}_1$
$\Xi_{cc}^+ \rightarrow \Sigma_c^+ K^0$	$\frac{1}{\sqrt{2}}(\tilde{C} + \tilde{C}')$	$\Omega_{cc}^+ \rightarrow \Lambda_c^+ \pi^0$	$-\frac{1}{\sqrt{2}}(E_1 + E_2)$	$\Omega_{cc}^+ \rightarrow \Xi_c^+ K^0$	$\frac{1}{\sqrt{2}}(\tilde{C} + \tilde{E}_1)$
$\Xi_{cc}^+ \rightarrow \Lambda_c^+ K^0$	$-C + C'$	$\Omega_{cc}^+ \rightarrow \Lambda_c^+ \eta_1$	$\frac{1}{\sqrt{3}}(C' + E_1 - E_2)$	$\Omega_{cc}^+ \rightarrow \Xi_c^+ K^0$	$-C + E_1$
$\Omega_{cc}^+ \rightarrow \Sigma_c^+ \pi^0$	$\frac{1}{2}(-\tilde{E}_1 + \tilde{E}_2)$	$\Omega_{cc}^+ \rightarrow \Lambda_c^+ \eta_8$	$-\frac{1}{\sqrt{6}}(2C' - E_1 + E_2)$		
$\Omega_{cc}^+ \rightarrow \Sigma_c^+ \eta_1$	$\frac{1}{\sqrt{6}}(\tilde{C}' + \tilde{E}_1 + \tilde{E}_2)$	$\Omega_{cc}^+ \rightarrow \Sigma_c^0 \pi^+$	$\tilde{E}_2$		

with the color indices  $\alpha$  and  $\beta$ . And  $C_{1,2}(\mu)$  are the relevant Wilson coefficients. After inserting the effective Hamiltonian as Eq. (1), the amplitude of the non-leptonic weak decay of doubly charmed baryons  $\mathcal{B}_{cc} \rightarrow \mathcal{B}_c P$  can be evaluated with the hadronic matrix element,

$$\langle \mathcal{B}_c P | \mathcal{H}_{eff} | \mathcal{B}_{cc} \rangle = \frac{G_F}{\sqrt{2}} V_{cq'} V_{uq} \sum_{i=1,2} C_i \langle \mathcal{B}_c P | O_i | \mathcal{B}_{cc} \rangle. \quad (3)$$

In this work, we neglect the penguin operators for the strong suppression of CKM matrix elements in charmed hadron decays. According to the factorization hypothesis, the matrix elements  $\langle \mathcal{B}_c M | O_i | \mathcal{B}_{cc} \rangle$  in Eq. (3) can be factorized into two parts. The first part is parameterized with the decay constant of the emitted meson, while the second part can be evaluated using the heavy-light transition form factors. The short-distance contribution of the  $T$  diagram can be expressed as:

$$\langle \mathcal{B}_c M | \mathcal{H}_{eff} | \mathcal{B}_{cc} \rangle_{SD}^T = \frac{G_F}{\sqrt{2}} V_{cq'}^* V_{uq} a_1(\mu) \langle M | \bar{u} \gamma^\mu (1 - \gamma_5) q | 0 \rangle \langle \mathcal{B}_c | \bar{q}' \gamma_\mu (1 - \gamma_5) c | \mathcal{B}_{cc} \rangle, \quad (4)$$

here  $a_1(\mu) = C_1(\mu) + C_2(\mu)/3$  is the effective Wilson coefficients. For color suppressed  $C$  diagram, its short-distance contribution can be given via its relation to the  $T$  diagram after Fierz transformation. And under the charm scale  $\mu = m_c$ , the Wilson coefficients are taken as  $C_1(\mu) = 1.21$  and  $C_2(\mu) = -0.42$  [117].  $M$  represents both pseudoscalar meson( $P$ ) and vector meson( $V$ ). The vector meson also contributes to long-distance dynamics as an intermediate state in the next subsections.

By utilizing the heavy-light transition form factors  $f_{1,2,3}$  and  $g_{1,2,3}$ , the transition matrix ele-

ments of  $\mathcal{B}_{cc} \rightarrow \mathcal{B}_c$  can be effectively parameterized as,

$$\begin{aligned} & \langle \mathcal{B}_c(p', s'_z) | \bar{q}' \gamma_\mu (1 - \gamma_5) c | \mathcal{B}_{cc}(p, s_z) \rangle \\ &= \bar{u}(p', s'_z) \left[ \gamma_\mu f_1(q^2) + i \sigma_{\mu\nu} \frac{q^\nu}{M_{\mathcal{B}_{cc}}} f_2(q^2) + \frac{q^\mu}{M_{\mathcal{B}_{cc}}} f_3(q^2) \right] u(p, s_z) \\ &- \bar{u}(p', s'_z) \left[ \gamma_\mu g_1(q^2) + i \sigma_{\mu\nu} \frac{q^\nu}{M_{\mathcal{B}_{cc}}} g_2(q^2) + \frac{q^\mu}{M_{\mathcal{B}_{cc}}} g_3(q^2) \right] \gamma_5 u(p, s_z). \end{aligned} \quad (5)$$

Here  $q = p - p'$ ,  $M_{\mathcal{B}_{cc}}$  is the mass of doubly charmed baryons.

The first matrix element in Eq. (4) are defined using the decay constants of the emitted mesons  $P$  and  $V$ , denoted by  $f_P$  and  $f_V$ , respectively.

$$\langle P(p) | \bar{u} \gamma^\mu (1 - \gamma_5) q | 0 \rangle = -i f_P p^\mu, \quad (6)$$

$$\langle V(p) | \bar{u} \gamma^\mu (1 - \gamma_5) q | 0 \rangle = m_V f_V \epsilon^{*\mu}, \quad (7)$$

where  $\epsilon^\mu$  represents the polarization vector of the vector meson.

Substituting Eqs. (5-7) into Eq. (4), the short-distance amplitudes of the weak decays  $\mathcal{B}_{cc} \rightarrow \mathcal{B}_c P$  and  $\mathcal{B}_{cc} \rightarrow \mathcal{B}_c V$  can be written as,

$$\mathcal{A}(\mathcal{B}_{cc} \rightarrow \mathcal{B}_c P) = i \bar{u}_{\mathcal{B}_c} (A_{SD} + B_{SD} \gamma_5) u_{\mathcal{B}_{cc}}, \quad (8)$$

$$\mathcal{A}(\mathcal{B}_{cc} \rightarrow \mathcal{B}_c V) = \epsilon^{*\mu} \bar{u}_{\mathcal{B}_c} \left[ A_{SD}^1 \gamma_\mu \gamma_5 + A_{SD}^2 \frac{p_\mu(\mathcal{B}_c)}{M_{\mathcal{B}_{cc}}} \gamma_5 + B_{SD}^1 \gamma_\mu + B_{SD}^2 \frac{p_\mu(\mathcal{B}_c)}{M_{\mathcal{B}_{cc}}} \right] u_{\mathcal{B}_{cc}}. \quad (9)$$

Here the short distance amplitudes  $A_{SD}$ ,  $B_{SD}$  and  $A_{SD}^{1,2}$ ,  $B_{SD}^{1,2}$  are specifically designated to encapsulate the strong interaction information via factorization.

$$A_{SD} = \lambda f_P (M_{\mathcal{B}_{cc}} - M_{\mathcal{B}_c}) f_1(m^2), \quad B_{SD} = \lambda f_P (M_{\mathcal{B}_{cc}} + M_{\mathcal{B}_c}) g_1(m^2), \quad (10)$$

$$A_{SD}^1 = -\lambda f_V m \left( g_1(m^2) + g_2(m^2) \frac{M_{\mathcal{B}_{cc}} - M_{\mathcal{B}_c}}{M_{\mathcal{B}_{cc}}} \right), \quad A_{SD}^2 = -2\lambda f_V m g_2(m^2), \quad (11)$$

$$B_{SD}^1 = \lambda f_V m \left( f_1(m^2) - f_2(m^2) \frac{M_{\mathcal{B}_{cc}} + M_{\mathcal{B}_c}}{M_{\mathcal{B}_{cc}}} \right), \quad B_{SD}^2 = 2\lambda f_V m f_2(m^2), \quad (12)$$

where the parameter  $\lambda$  is  $\frac{G_F}{\sqrt{2}} V_{CKM} a_{1,2}(\mu)$ , and  $m$  is the mass of pseudoscalar or vector meson. We exclude  $f_3$  and  $g_3$  terms in Eq. (5) due to  $m^2/M_{\mathcal{B}_{cc}}^2$  suppression.

### C. Calculation of long-distance contributions using the final states rescattering mechanism

The long-distance contributions are large and very difficult to evaluate. In this work, we employ the rescattering mechanism of final states to perform the calculation of the long-distance contributions, as done in Ref. [19]. The rescattering mechanism of final states can be constructed through the rescattering of two intermediate particles, as depicted in Fig. 1. In the following, we explain the detail of our calculation of the amplitudes of the nonleptonic decays  $\mathcal{B}_{cc} \rightarrow \mathcal{B}_c P$ . These decays can proceed as shown in Fig. 3. At the quark level, the first weak vertex of the triangle diagram is induced by the external  $W$  emission diagram  $T$  to avoid double counting, which is dominated by the factorization contribution. The upcoming scattering process can occur via either an  $s$  channel or a  $t/u$  channel. The diagram of  $s$  channel would make a sizable contribution when the mass of the exchanged particle is the sequel to the ones of the mother particle  $\mathcal{B}_{cc}$ . While the heaviest discovered singly charmed baryon is approximately 500 MeV lighter than  $m_{\Xi_{cc}^+}$ . So the contribution of the  $s$ -channel diagram is supposed to be highly suppressed by the off-shell effect and can be safely

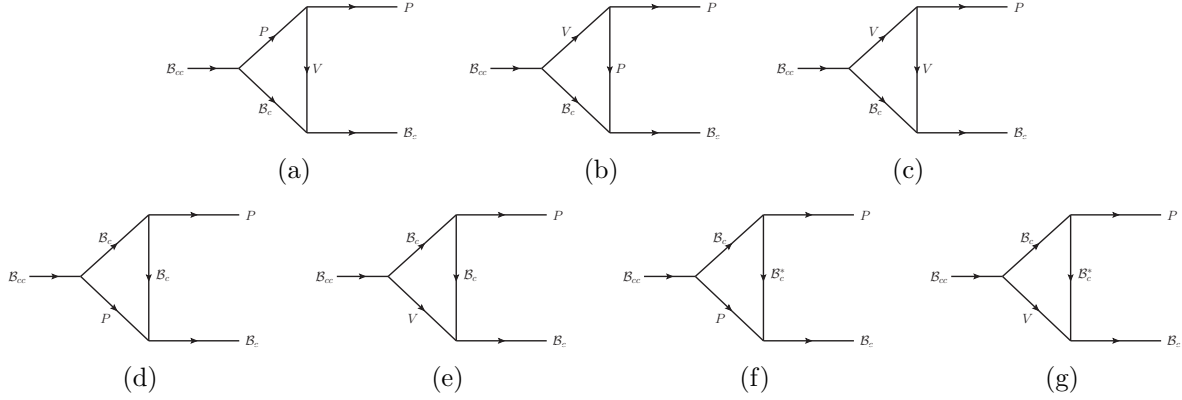


Figure 3: The long-distance rescattering contributions to  $\mathcal{B}_{cc} \rightarrow \mathcal{B}_c P$  manifested at hadron level.

neglected. As a result, we only consider the contribution of the  $t/u$ -channel triangle diagram, as depicted in Fig. 3. The remaining two strong interaction vertices, as depicted in Fig. 3, can be assessed utilizing the hadronic strong interaction Lagrangians [118–123] presented as following.

$$\mathcal{L}_{VPP} = ig_{VP_1P_2}[V^\mu P_1 \partial_\mu P_2 - V^\mu P_2 \partial_\mu P_1], \quad (13)$$

$$\mathcal{L}_{VVP} = \frac{g_{V_1V_2P}}{\sqrt{m_{V_1}m_{V_2}}} \varepsilon_{\mu\nu\alpha\beta} \text{Tr}[\partial^\mu V_1^\nu \partial^\alpha P V_2^\beta], \quad (14)$$

$$\mathcal{L}_{P\mathcal{B}_c\mathcal{B}_c} = g_{P\mathcal{B}_c\mathcal{B}_c} \text{Tr}[\bar{\mathcal{B}}_c i\gamma_5 P \mathcal{B}_c], \quad (15)$$

$$\mathcal{L}_{V\mathcal{B}_c\mathcal{B}_c} = f_{1V\mathcal{B}_c\mathcal{B}_c} \text{Tr}[\bar{\mathcal{B}}_c \gamma_\mu V^\mu \mathcal{B}_c] + \frac{f_{2V\mathcal{B}_c\mathcal{B}_c}}{m_{\mathcal{B}_c} + m_{\mathcal{B}_c}} \text{Tr}[\bar{\mathcal{B}}_c \sigma_{\mu\nu} \partial^\mu V^\nu \mathcal{B}_c], \quad (16)$$

$$\mathcal{L}_{P\mathcal{B}_c\mathcal{B}_c^*} = g_{P\mathcal{B}_c\mathcal{B}_c^*} \epsilon^{ijk} (\bar{\mathcal{B}}_c)_i^j (\mathcal{B}_c^*)_\mu^{kl} \partial^\mu P_m^i, \quad (17)$$

$$\mathcal{L}_{V\mathcal{B}_c\mathcal{B}_c^*} = -ig_{V\mathcal{B}_c\mathcal{B}_c^*} [\bar{\mathcal{B}}_c^{*\mu} \gamma^5 \gamma^\nu \mathcal{B}_c + \bar{\mathcal{B}}_c \gamma^5 \gamma^\nu \mathcal{B}_c^*] (\partial_\mu V_\nu - \partial_\nu V_\mu). \quad (18)$$

There are various ways to compute the triangle amplitude [114, 115, 124–128]. The main point of distinction between them is their approach towards the integration of hadronic loops. In work [76], the authors adopting the optical theorem and Cutkosky cutting rule as in Ref. [115], only calculate the absorptive (imaginary) part of these diagrams. The real component of the triangle diagram can be theoretically derived from the dispersion relation. However, due to significant ambiguity, it is challenging to reliably describe the amplitude across the entire region. Consequently, this effect is often neglected in numerous studies. To accurately determine the complete amplitude of the triangle diagram, the most direct method involves calculating the loop integrals. In this study, we employ the Passarino-Veltman method to simplify the tensor integrals and utilize the method of integral by parts to derive expressions with master integrals.

To clarify, we want to determine the amplitude of the decay mode for  $\mathcal{B}_{cc}(p_i) \rightarrow \mathcal{B}_c(p_4)P(p_3)$ . The Fig. 3(a) shows a triangle diagram with intermediate states  $\{P, \mathcal{B}_c; V\}$ , involving a weak vertex  $\mathcal{B}_{cc}(p_i) \rightarrow \mathcal{B}_c(p_2)P(p_1)$ , as well as a rescattering amplitude of  $\mathcal{B}_c(p_2)P(p_1) \rightarrow \mathcal{B}_c(p_4)P(p_3)$ . The factorization approach in Eq. (8) can calculate the weak vertex, while the rescattering amplitude is computed using the hadronic effective Lagrangian. We use the symbol  $\mathcal{M}[P_1, P_2; P_k]$  to represent a triangle amplitude in this work. The amplitudes of the diagrams shown in Fig. 3 can be expressed



as follows,

$$\begin{aligned}\mathcal{M}[P, \mathcal{B}_c, V] = & - \int \frac{d^4 p_1}{(2\pi)^4} \bar{u}(p_4, s_4) (f_{1\mathcal{B}_c \mathcal{B}_c V} \gamma_\nu - \frac{i f_{2\mathcal{B}_c \mathcal{B}_c V}}{m_2 + m_4} \sigma_{\mu\nu} p_k^\mu) (\not{p}_2 + m_2) \\ & \times (A_{SD} + B_{SD} \gamma_5) u(p_i, s_i) g_{VPP} (-g^{\alpha\nu} + \frac{p_k^\alpha p_k^\nu}{m_k^2}) (p_1 + p_3)_\alpha \mathcal{P}\mathcal{F},\end{aligned}\quad (19)$$

$$\begin{aligned}\mathcal{M}[V, \mathcal{B}_c; P] = & - \int \frac{d^4 p_1}{(2\pi)^4} g_{P\mathcal{B}_c \mathcal{B}_c} \bar{u}(p_4, s_4) \gamma_5 (\not{p}_2 + m_2) \\ & \times (-g^{\rho\alpha} + \frac{p_1^\rho p_1^\alpha}{m_1^2}) (A_1 \gamma_\rho \gamma_5 + A_2 \frac{p_{2\rho}}{m_i} \gamma_5 + B_1 \gamma_\rho + B_2 \frac{p_{2\rho}}{m_i}) u(p_i, s_i) \\ & \times g_{VPP} (p_3 - p_k)_\alpha \mathcal{P}\mathcal{F},\end{aligned}\quad (20)$$

$$\begin{aligned}\mathcal{M}[V, \mathcal{B}_c; V] = & -i \int \frac{d^4 p_1}{(2\pi)^4} \bar{u}(p_4, s_4) (f_{1\mathcal{B}_c \mathcal{B}_c V} \gamma^\nu - \frac{i f_{2\mathcal{B}_c \mathcal{B}_c V}}{m_2 + m_4} \sigma^{\mu\nu} p_{k\mu}) \\ & \times (\not{p}_2 + m_2) (A_1 \gamma^\rho \gamma_5 + A_2 \frac{p_2^\rho}{m_i} \gamma_5 + B_1 \gamma^\rho + B_2 \frac{p_2^\rho}{m_i}) u(p_i, s_i) \\ & \times \frac{g_{VVP}}{\sqrt{m_1 m_k}} \epsilon^{\alpha\beta\delta\sigma} p_{k\alpha} p_{3\delta} (-g_{\rho\sigma} + \frac{p_{1\rho} p_{1\sigma}}{m_1^2}) (-g_{\nu\beta} + \frac{p_{k\nu} p_{k\beta}}{m_k^2}) \mathcal{P}\mathcal{F},\end{aligned}\quad (21)$$

$$\begin{aligned}\mathcal{M}[V, \mathcal{B}_c; V] = & i \int \frac{d^4 p_1}{(2\pi)^4} \bar{u}(p_4, s_4) (f_{1\mathcal{B}_c \mathcal{B}_c V} \gamma^\nu - \frac{i f_{2\mathcal{B}_c \mathcal{B}_c V}}{m_2 + m_4} \sigma^{\mu\nu} p_{k\mu}) \\ & \times (\not{p}_2 + m_2) (A_1 \gamma^\rho \gamma_5 + A_2 \frac{p_2^\rho}{m_i} \gamma_5 + B_1 \gamma^\rho + B_2 \frac{p_2^\rho}{m_i}) u(p_i, s_i) \\ & \times \frac{4g_{VVP}}{f_P} \epsilon^{\alpha\beta\delta\sigma} p_{k\alpha} p_{1\delta} (-g_{\rho\sigma} + \frac{p_{1\rho} p_{1\sigma}}{m_1^2}) (-g_{\nu\beta} + \frac{p_{k\nu} p_{k\beta}}{m_k^2}) \mathcal{P}\mathcal{F},\end{aligned}\quad (22)$$

$$\begin{aligned}\mathcal{M}[\mathcal{B}_c, P; \mathcal{B}_c] = & \int \frac{d^4 p_1}{(2\pi)^4} g_{P\mathcal{B}_c \mathcal{B}_c} \bar{u}(p_4, s_4) \gamma_5 (\not{p}_k + m_k) g_{P\mathcal{B}_c \mathcal{B}_c} \gamma_5 (\not{p}_1 + m_1) \\ & \times (A_{SD} + B_{SD} \gamma_5) u(p_i, s_i) \mathcal{P}\mathcal{F},\end{aligned}\quad (23)$$

$$\begin{aligned}\mathcal{M}[\mathcal{B}_c, V; \mathcal{B}_c] = & - \int \frac{d^4 p_1}{(2\pi)^4} \bar{u}(p_4, s_4) (f_{1V\mathcal{B}_c \mathcal{B}_c} \gamma_\nu - \frac{i f_{2V\mathcal{B}_c \mathcal{B}_c}}{m_k + m_4} \sigma_{\mu\nu} p_2^\mu) \\ & \times (\not{p}_k + m_k) g_{P\mathcal{B}_c \mathcal{B}_c} \gamma_5 (\not{p}_1 + m_1) (-g^{\nu\rho} + \frac{p_2^\nu p_2^\rho}{m_2^2}) \\ & \times (A_1 \gamma_\rho \gamma_5 + A_2 \frac{p_{1\rho}}{m_i} \gamma_5 + B_1 \gamma_\rho + B_2 \frac{p_{1\rho}}{m_i}) u(p_i, s_i) \mathcal{P}\mathcal{F},\end{aligned}\quad (24)$$

$$\begin{aligned}\mathcal{M}[\mathcal{B}_c, P, \mathcal{B}_c^*] = & - \int \frac{d^4 p_1}{(2\pi)^4} g_{P\mathcal{B}_c \mathcal{B}_c^*} g_{P\mathcal{B}_c \mathcal{B}_c^*} \bar{u}(p_4, s_4) p_2^\mu p_3^\nu (\not{p}_k + m_k) \\ & \times \{-g_{\mu\nu} + \frac{\gamma_\mu \gamma_\nu}{3} + \frac{2p_{k\mu} p_{k\nu}}{3m_k^2} - \frac{p_{k\mu} \gamma_\nu - p_{k\nu} \gamma_\mu}{3m_k}\} (\not{p}_1 + m_1) \\ & \times (A_{SD} + B_{SD} \gamma_5) u(p, s) \mathcal{P}\mathcal{F},\end{aligned}\quad (25)$$

$$\begin{aligned}\mathcal{M}[\mathcal{B}_c, V, \mathcal{B}_c^*] = & \int \frac{d^4 p_1}{(2\pi)^4} [g_{V\mathcal{B}_c \mathcal{B}_c^*} \bar{u}(p_4, s_4) \gamma_5 \gamma_\nu (-p_2^\rho g^{\nu\sigma} + p_2^\nu g^{\rho\sigma})] \\ & g_{P\mathcal{B}_c \mathcal{B}_c^*} (\not{p}_k + m_k) \{-g_{\rho\mu} + \frac{\gamma_\rho \gamma_\mu}{3} + \frac{2p_{k\rho} p_{k\mu}}{3m_k^2} - \frac{p_{k\rho} \gamma_\mu - p_{k\mu} \gamma_\rho}{3m_k}\} p_{3\mu} \\ & \times (\not{p}_1 + m_1) (A_1 \gamma_\sigma \gamma_5 + A_2 \frac{p_{1\sigma}}{m_i} \gamma_5 + B_1 \gamma_\sigma + B_2 \frac{p_{1\sigma}}{m_i}) u(p, s) \mathcal{P}\mathcal{F}.\end{aligned}\quad (26)$$

where the note  $\mathcal{PF}$  represents the multiply of the propagators and form factor,

$$\mathcal{PF} = \frac{1}{(p_1^2 - m_1^2 + i\epsilon)(p_2^2 - m_2^2 + i\epsilon)(p_k^2 - m_k^2 + i\epsilon)} \left( \frac{\Lambda_k^2 - m_k^2}{\Lambda_k^2 - p_k^2} \right)^2. \quad (27)$$

In the given equation, strong coupling constants, such as  $g_{VPP}$ ,  $f_{1\mathcal{B}_c\mathcal{B}_cV}$ , and  $f_{2\mathcal{B}_c\mathcal{B}_cV}$  are calculated on-shell. The reliability of the strong coupling constants is compromised due to the exchange states  $V$  being generally off-shell. The form factor of the exchange particle  $F(p_j, m_j)$  are introduced to account for off-shell effects and self-consistency of the theoretical framework [115]. Furthermore, it is necessary to implement an appropriate regularization scheme to manage the inevitable divergence that occurs in the master integrals of the triangle diagram amplitude. The form factor introduced in Eq.(27) aligns with the Pauli-Villars regularization scheme.

$$F(p_k, m_k) = \left( \frac{\Lambda_k^2 - m_k^2}{\Lambda_k^2 - p_k^2} \right)^n. \quad (28)$$

The cutoff  $\Lambda_k$  can be given as

$$\Lambda_k = m_k + \eta\Lambda_{\text{QCD}}. \quad (29)$$

with  $\Lambda_{\text{QCD}} = 330\text{MeV}$  for the charm quark decays. The phenomenological parameter  $\eta$  is determined by experimental data which can not be derived from the first-principle method. In this work, multiple strong vertices require extensive experimental data for individual parameter calculation. In the next section, we will use the experimental data to determine the value of the parameter  $\eta$ . The form factor given by Eq. (28) typically exhibits monopole or dipole behavior, with the exponential factor  $n$  taking on values of 1 or 2. The branching ratios for  $B$  meson decays in Ref. [115] are similar for both choices, and then we select  $n = 2$ .

After gathering all the fragments, the amplitude of decay  $\mathcal{B}_{cc} \rightarrow \mathcal{B}_c P$  can be expressed as:

$$\begin{aligned} \mathcal{A}(\mathcal{B}_{cc} \rightarrow \mathcal{B}_c P) = & \mathcal{M}_{SD}(\mathcal{B}_{cc} \rightarrow \mathcal{B}_c P) + \mathcal{M}[P, \mathcal{B}_c; V] + \mathcal{M}[V, \mathcal{B}_c; P] + \mathcal{M}[V, \mathcal{B}_c; V] \\ & + \mathcal{M}[\mathcal{B}_c, P; \mathcal{B}_c] + \mathcal{M}[\mathcal{B}_c, V; \mathcal{B}_c] + \mathcal{M}[\mathcal{B}_c, P; \mathcal{B}_c^*] + \mathcal{M}[\mathcal{B}_c, V; \mathcal{B}_c^*], \end{aligned} \quad (30)$$

where  $\mathcal{M}_{SD}$  labels its short-distance contributions including the factorization contributions of  $T$  and  $C$  diagrams. The amplitudes for all channels can be found in Appendix A.

#### D. Decay asymmetry parameters and CP violation

As the amplitude for the two body nonleptonic weak decay of doubly heavy baryon  $\mathcal{B}_{cc} \rightarrow \mathcal{B}_c P$  can be deduced as

$$\mathcal{M}(\mathcal{B}_{cc} \rightarrow \mathcal{B}_c P) = i\bar{u}_{\mathcal{B}_c}(A + B\gamma_5)u_{\mathcal{B}_{cc}} = \mathcal{S} + \mathcal{P}\sigma \cdot \vec{p}_{\mathcal{B}_c} = i(H_{1/2} + H_{-1/2}), \quad (31)$$

here  $\vec{p}_{\mathcal{B}_c}$  is the three-momentum of singly charmed baryon  $\mathcal{B}_c$  in the rest frame of the mother particle  $\mathcal{B}_{cc}$ . In this decay process, two helicity amplitudes can be obtained in the Pauli-Dirac representation,

$$H_{\pm 1/2} = \sqrt{2m_{\mathcal{B}_{cc}}(E_{\mathcal{B}_c} + m_{\mathcal{B}_c})}A \mp \sqrt{2m_{\mathcal{B}_{cc}}(E_{\mathcal{B}_c} - m_{\mathcal{B}_c})}B, \quad (32)$$

here the subscript  $\pm 1/2$  denotes the helicity of doubly charmed baryons. The amplitudes  $\mathcal{S}$  and  $\mathcal{P}$  denote the parity-violating (PV) S-wave and parity-conserving (PC) P-wave amplitudes, respectively. In the above Eq. (31),  $A$  and  $B$  generally receive both factorizable short distance (SD) from Eq. (8) and non-factorizable long distance (LD) contributions

$$A = A_{SD} + A_{LD}, \quad B = B_{SD} + B_{LD}. \quad (33)$$

Then the decay width can be given as following,

$$\begin{aligned}\Gamma(\mathcal{B}_{cc} \rightarrow \mathcal{B}_c P) &= \frac{|\vec{p}_{\mathcal{B}_c}|}{8\pi} \left[ \frac{(m_{\mathcal{B}_{cc}} + m_{\mathcal{B}_c})^2 - m_P^2}{m_{\mathcal{B}_{cc}}^2} |A|^2 + \frac{(m_{\mathcal{B}_{cc}} - m_{\mathcal{B}_c})^2 - m_P^2}{m_{\mathcal{B}_{cc}}^2} |B|^2 \right] \\ &= 2|\vec{p}_{\mathcal{B}_c}|(|\mathcal{S}|^2 + |\mathcal{P}|^2) = \frac{|\vec{p}_{\mathcal{B}_c}|}{16\pi m_{\mathcal{B}_{cc}}^2} (|H_{1/2}|^2 + |H_{-1/2}|^2),\end{aligned}\quad (34)$$

where  $|\vec{p}_{\mathcal{B}_c}| = \sqrt{E_{\mathcal{B}_c}^2 - m_{\mathcal{B}_c}^2}$  is size of the final baryon  $\mathcal{B}_c$  momentum and the relations between  $|A|^2$ ,  $|B|^2$  and  $|\mathcal{S}|^2$ ,  $|\mathcal{P}|^2$  can be given as

$$|\mathcal{S}|^2 = \frac{(m_{\mathcal{B}_{cc}} + m_{\mathcal{B}_c})^2 - m_P^2}{16\pi m_{\mathcal{B}_{cc}}^2} |A|^2, \quad |\mathcal{P}|^2 = \frac{(m_{\mathcal{B}_{cc}} - m_{\mathcal{B}_c})^2 - m_P^2}{16\pi m_{\mathcal{B}_{cc}}^2} |B|^2, \quad (35)$$

$$|H_{1/2}|^2 + |H_{-1/2}|^2 = 2(|A|^2 + \kappa^2 |B|^2), \quad (36)$$

If the polarization of decay is measurable, there are additional experimental observables in the decay angular distribution. The asymmetry parameters can be used to understand the angular correlations and dynamics of strong interactions in this decay process  $\mathcal{B}_{cc} \rightarrow \mathcal{B}_c P$ , which can be defined as following [72, 129, 130]

$$\alpha = \frac{2\text{Re}(\mathcal{S}^*\mathcal{P})}{|\mathcal{S}|^2 + |\mathcal{P}|^2} = \frac{2\kappa\text{Re}(A^*B)}{|A|^2 + \kappa^2 |B|^2} = -\frac{|H_{1/2}|^2 - |H_{-1/2}|^2}{|H_{1/2}|^2 + |H_{-1/2}|^2}, \quad (37)$$

$$\beta = \frac{2\text{Im}(\mathcal{S}^*\mathcal{P})}{|\mathcal{S}|^2 + |\mathcal{P}|^2} = \frac{2\kappa\text{Im}(A^*B)}{|A|^2 + \kappa^2 |B|^2} = -\frac{2\text{Im}(H_{1/2}H_{-1/2}^*)}{|H_{1/2}|^2 + |H_{-1/2}|^2}, \quad (38)$$

$$\gamma = \frac{|\mathcal{S}|^2 - |\mathcal{P}|^2}{|\mathcal{S}|^2 + |\mathcal{P}|^2} = \frac{|A|^2 - \kappa^2 |B|^2}{|A|^2 + \kappa^2 |B|^2} = \frac{2\text{Re}(H_{1/2}H_{-1/2}^*)}{|H_{1/2}|^2 + |H_{-1/2}|^2}. \quad (39)$$

Here  $\kappa = |\vec{p}_{\mathcal{B}_c}|/(E_{\mathcal{B}_c} + m_{\mathcal{B}_c}) = \sqrt{(E_{\mathcal{B}_c} - m_{\mathcal{B}_c})/(E_{\mathcal{B}_c} + m_{\mathcal{B}_c})}$ . Only two of the variables are independent, subject to the constraint  $\alpha^2 + \beta^2 + \gamma^2 = 1$ . This constraint allows one to obtain

$$\beta = \sqrt{1 - \alpha^2} \sin \phi, \quad \gamma = \sqrt{1 - \alpha^2} \cos \phi, \quad \phi = \tan^{-1}(\beta/\gamma). \quad (40)$$

To experimentally measure the parameter  $\alpha$ , it is necessary to assess either the initial or final baryon polarization. While determining the initial polarization at LHCb might be challenging, the final baryon polarization can be ascertained from the decays of the final baryon. For measuring  $\beta$  and  $\gamma$ , information on both the initial and final baryon polarization is essential. In the following, we will mainly discuss  $\alpha$ , which is more likely to be measured.

As our calculation can give the strong phase of the decay amplitudes, the information of  $CP$  violation can be derived. The direct  $CP$  asymmetry is defined as:

$$\begin{aligned}A_{CP}^{\text{dir}}(\mathcal{B}_{cc} \rightarrow \mathcal{B}_c P) &= \frac{\Gamma(\mathcal{B}_{cc} \rightarrow \mathcal{B}_c P) - \bar{\Gamma}(\mathcal{B}_{cc} \rightarrow \mathcal{B}_c P)}{\Gamma(\mathcal{B}_{cc} \rightarrow \mathcal{B}_c P) + \bar{\Gamma}(\mathcal{B}_{cc} \rightarrow \mathcal{B}_c P)} \\ &= \frac{2r \sin \Delta\delta \sin \Delta\phi}{1 + r^2 + 2r \cos \Delta\delta \cos \Delta\phi},\end{aligned}\quad (41)$$

where  $r$  denotes the amplitude ratio. Furthermore,  $\Delta\delta$  and  $\Delta\phi$  symbolize the strong and weak phase differences respectively.

The violation of  $CP$  arises from the parameters associated with decay asymmetry.

$$\alpha_{CP} = \frac{\alpha - \bar{\alpha}}{\alpha + \bar{\alpha}}, \quad \beta_{CP} = \frac{\beta - \bar{\beta}}{\beta + \bar{\beta}}, \quad \gamma_{CP} = \frac{\gamma - \bar{\gamma}}{\gamma + \bar{\gamma}}. \quad (42)$$

### III. NUMERICAL RESULTS AND DISCUSSIONS

#### A. Input parameters

Calculation of this work requires inputs such as initial and final state masses, decay constants of pseudoscalar and vector mesons, strong couplings, transition form factors, and the lifetimes of the doubly charmed baryons, as  $\mathcal{BR}_i = \Gamma_i \cdot \tau$ . In the following, we will classify and discuss input parameter values in this work.

- The LHCb collaboration has successfully measured the mass and lifetime of  $\Xi_{cc}^{++}$ :  $m_{\Xi_{cc}^{++}} = 3.621$  MeV[6, 7],  $\tau_{\Xi_{cc}^{++}} = 256$  fs[133]. After these measurements, many theoretical works have studied the masses and lifetimes of doubly charmed baryons [53, 94, 134–137]. The measurement of  $\Xi_{cc}^{++}$  would benefit theoretical predictions on the other doubly charmed baryons. The results from Refs. [134, 137] are adopted in this work,  $m_{\Xi_{cc}^{++}} = 3.621$  MeV,  $m_{\Omega_{cc}^{++}} = 3.738$  MeV,  $\tau_{\Xi_{cc}^{++}} = 44$  fs and  $\tau_{\Omega_{cc}^{++}} = 206$  fs. The masses of the final states including singly heavy baryons, light pseudoscalar and vector mesons, can be easily found in Particle Data Group [94].
- The decay constants of pseudoscalar and vector mesons are obtained from the literature [1, 95, 96], and summarized in Tab. II. The form factors of the transition  $\mathcal{B}_{cc} \rightarrow \mathcal{B}_c$  have been calculated in many works [86]. In this work, we utilize the theoretical results of form factors within the light-front quark model, which have been successfully used to predict the discovery channel of  $\Xi_{cc}^{++}$  in Ref. [19].
- In addition, the non-perturbative strong coupling constants serve a pivotal role in our calculation. Most of them can be taken from theoretical works. In this work, we use theoretical results [113, 115, 118–123, 131, 132], which have been listed in Tab. II and combine SU(3) symmetry to obtain. For example, the strong couplings of singly heavy baryons and light mesons can be determined using the LCSRs method, as evidenced by  $g_{\Xi_c^+ \Xi_c^+ \pi^0} = 0.7$  [118]. The remaining couplings of this type can be inferred from SU(3) flavor symmetry.

#### B. The determination of $\eta$

In order to describe the off-shell effect of the exchanged particles, one form factor is introduced as given in Eq. (28). In this form factor, the parameter  $\eta$  is usually calculated from the experimental data as in [115]. In the case of doubly charmed baryon decays, using the experiment data [9]

$$\mathcal{RB} = \frac{\mathcal{B}(\Xi_{cc}^{++} \rightarrow \Xi_c'^+ \pi^+)}{\mathcal{B}(\Xi_{cc}^{++} \rightarrow \Xi_c^+ \pi^+)} = 1.41 \pm 0.17 \pm 0.10, \quad (43)$$

Table II: Decay constants (in units of MeV) of the light mesons [1, 95, 96] and strong couplings [115, 118–123, 131, 132] used in this work.

$f_\pi$	$f_{\eta_1}$	$f_\rho$	$f_\omega$	$f_{\eta_8}$	$f_\phi$	$f_K$	$f_{K^*}$
$130.2 \pm 1.2$	$151 \pm 2.6$	$216 \pm 5$	$195 \pm 3$	$169 \pm 2.6$	$233 \pm 4.6$	$155.7 \pm 3$	$217 \pm 7$
$g_{\rho\pi\pi}$	$g_{\Xi_c^+ \Xi_c^+ \pi^0}$	$g_{\Xi_c'^+ \Xi_c^+ \pi^0}$	$g_{\Sigma_c^+ \Sigma_c^0 \pi^+}$	$g_{\Sigma_c^{*0} \Lambda_c^+ \pi^-}$	$g_{\Sigma_c^{*+} \Sigma_c^0 \pi^+}$		
$6.05 \pm 0.02$	$0.70 \pm 0.22$	$3.1 \pm 1.1$	$8.0 \pm 2.8$	$3.9 \pm 0.6$	$4.3 \pm 0.4$		
$g_{\omega\rho\pi}$	$g_{\Sigma_c^{*+} \Lambda_c^+ \rho^0}$	$g_{\Sigma_c^{*0} \Sigma_c^+ \rho^-}$	$g_{\Xi_c^0 \Lambda_c^+ K^{*-}}$	$g_{\Sigma_c^0 \Lambda_c^+ \rho^-}$	$g_{\Sigma_c^+ \Sigma_c^0 \rho^+}$		
$-10 \pm 1$	$10 \pm 1.8$	$5.77 \pm 0.5$	$\{4.6 \pm 1.5, 6 \pm 2\}$	$\{2.6 \pm 0.9, 16 \pm 5.3\}$	$\{4 \pm 1.3, 27 \pm 9\}$		

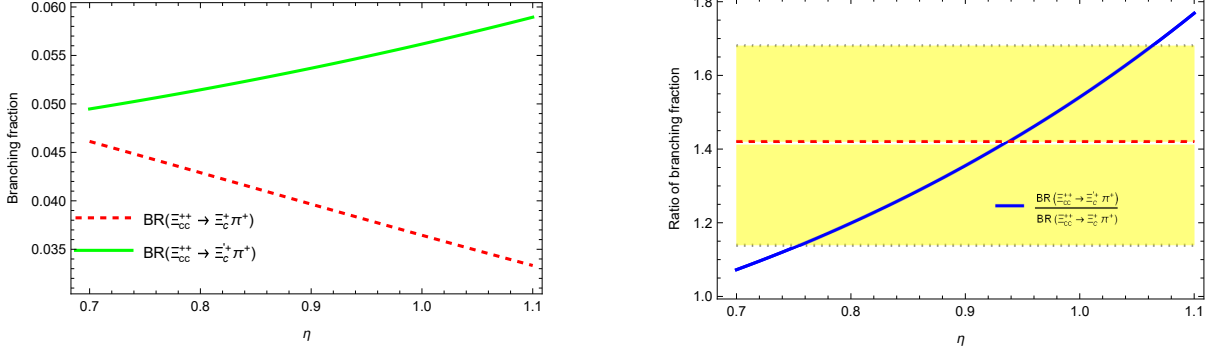


Figure 4: (a): The theoretical predictions for the branching fractions of  $\Xi_{cc}^{++} \rightarrow \Xi_c^+ \pi^+$  and  $\Xi_{cc}^{++} \rightarrow \Xi_c'^+ \pi^+$  in logarithmic coordinates; (b): Ratio of branching fractions with  $\eta \sim [0.7, 1.1]$ .

this parameter can be determined as  $\eta = 0.9 \pm 0.2$ . With  $\eta \sim [0.7, 1.1]$ , the dependence of the branching fractions for  $\Xi_{cc}^{++} \rightarrow \Xi_c^+ \pi^+$  and  $\Xi_{cc}^{++} \rightarrow \Xi_c'^+ \pi^+$  can be shown as Fig. 4 (a). The long-distance contributions, primarily stemming from Fig. 3 (a) and (c), coupled with the different form factors of the two processes, lead to an interesting outcome. In process  $\Xi_{cc}^{++} \rightarrow \Xi_c'^+ \pi^+$ , the contributions from Fig. 3 (a) and (c) synergistically reinforce one another. Conversely, in process  $\Xi_{cc}^{++} \rightarrow \Xi_c^+ \pi^+$ , these contributions negate each other. Consequently, as  $\eta$  increases, there is a corresponding decrease in the branching ratio of process  $\Xi_{cc}^{++} \rightarrow \Xi_c^+ \pi^+$ . It is said that the branching fractions are highly dependent on the value of the parameter  $\eta$ , the branching fractions could change about 20% of magnitude. While as depicted in Fig. 4 (b), the ratio of the two branching fractions can also be given as,

$$\mathcal{RB} = \frac{\mathcal{B}(\Xi_{cc}^{++} \rightarrow \Xi_c'^+ \pi^+)}{\mathcal{B}(\Xi_{cc}^{++} \rightarrow \Xi_c^+ \pi^+)} = 1.35_{-0.66}^{+0.81}. \quad (44)$$

the uncertainty of the ratio is 60% from the parameter  $\eta$ . The lack of more experimental data for the calculation of  $\eta$  will lead to large uncertainties in the theoretical predictions of the branching fractions. This is a well-known issue with final state interaction effects, which have large theoretical uncertainties. Nonetheless, the theoretical prediction using this value of  $\eta$  remains highly reliable. In this work, we will present the numerical predictions of physical observation with  $\eta = 0.9 \pm 0.2$ , to show the absolute uncertainty of each mode.

### C. Ratios of amplitudes and decay widths

Upon determining  $\eta$ , the modulus of amplitude including  $A$ ,  $B$ , and helicity amplitudes can be numerically computed using the amplitude for each nonleptonic decay mode, as detailed in Appendix A. Due to the limitations on the length of the article, we have not provided modulus of amplitude and widths for all processes. Instead, we have only presented results for processes that are short-distance contributions dominated in the upper part of Tab. III, as well as those that are long-distance contributions dominated and Cabibbo-favored processes in the lower part. In addition to the error introduced by the parameter  $\eta$ , we also discuss errors arising from other input parameters. As illustrated in Tab. III, we present two distinct errors for each amplitude. The first source of uncertainty stems from the input parameters including decay constants and strong couplings. The second uncertainty is derived from the parameter  $\eta = 0.9 \pm 0.2$ . And since the amplitudes  $A_{SD}$  and  $B_{SD}$  not involving strong couplings and  $\eta$ , there is only uncertainty from decay constants. Then we can found that the uncertainty from decay constants is much smaller than that

from the strong coupling constants and  $\eta$ . This is because almost of these decay constants have been precisely determined using experimental data [1]. Nevertheless, there is a significant lack of experimental data available for determining the parameters: strong couplings and  $\eta$ . In Tab. IV, we conduct a comparative analysis with other theoretical works. In contrast to other studies, our work incorporates both real and imaginary contributions within the amplitudes, which will provide the strong phases naturally to understand the  $CP$  asymmetries and decay asymmetries. From Tab. III, it is evident that the imaginary component of the long-distance contribution closely approximates its real counterpart.

Besides, the topological diagrams have the relations of  $\frac{|C|}{|T|} \sim \frac{|C'|}{|C|} \sim \frac{|E_1|}{|C|} \sim \frac{|E_2|}{|C|} \sim O(\frac{\Lambda_{QCD}^h}{m_c})$  in the heavy baryon decays, manifested by the soft-collinear effective theory [141, 142]. These relations are important in the phenomenological studies on the searches for the double-heavy-flavor baryons, and give us more hints on the dynamics of heavy baryon decays. From the above relations, all the tree-level topological diagrams are at the same order in charmed baryon decays due to  $\Lambda_{QCD}^h/m_c \sim 1$ . It would be very useful to numerically test these relations in our framework.

Based on the topological analysis in Tab. I,  $\mathcal{A}(\Xi_{cc}^{++} \rightarrow \Sigma_c^{++} \bar{K}^0) \sim \tilde{C}$  and  $\mathcal{A}(\Xi_{cc}^{++} \rightarrow \Xi_c'^+ \pi^+) \sim (\tilde{T} + \tilde{C}')/\sqrt{2}$ , we obtain the ratios  $\tilde{C}_{LD}/\tilde{T}_{SD}$  and  $\tilde{C}'_{LD}/\tilde{C}_{LD}$  as,

$$\frac{|\tilde{C}_{LD}|}{|\tilde{T}_{SD}|} = \frac{|\mathcal{A}(\Xi_{cc}^{++} \rightarrow \Sigma_c^{++} \bar{K}^0)|_{LD}}{\sqrt{2}|\mathcal{A}(\Xi_{cc}^{++} \rightarrow \Xi_c'^+ \pi^+)|_{SD}} = 0.14 \sim 0.30, \quad (45)$$

$$\frac{|\tilde{C}'_{LD}|}{|\tilde{C}_{LD}|} = \frac{\sqrt{2}|\mathcal{A}(\Xi_{cc}^{++} \rightarrow \Xi_c'^+ \pi^+)|_{LD}}{|\mathcal{A}(\Xi_{cc}^{++} \rightarrow \Sigma_c^{++} \bar{K}^0)|_{LD}} = 1.02 \sim 1.06. \quad (46)$$

In the following to consider the relations between  $C$ ,  $E_1$  and  $E_2$ , it would be more convenient to study the processes with a pure topological diagram. The advantage of avoiding interference between diagrams is that they could be directly determined by the experimental data in the future. With the help of  $\mathcal{A}(\Xi_{cc}^+ \rightarrow \Sigma_c^{++} K^-) \sim \tilde{E}_1$ ,  $\mathcal{A}(\Xi_{cc}^+ \rightarrow \Omega_c^0 K^+) \sim \tilde{E}_2$  and  $\mathcal{A}(\Xi_{cc}^{++} \rightarrow \Sigma_c^{++} \bar{K}^0) \sim \tilde{C}$ , the ratios  $\tilde{E}_{1LD}/\tilde{C}_{LD}$  and  $\tilde{E}_{2LD}/\tilde{C}_{LD}$  can be easily carried out,

$$\frac{|\tilde{E}_{1LD}|}{|\tilde{C}_{LD}|} = \frac{|\mathcal{A}(\Xi_{cc}^+ \rightarrow \Sigma_c^{++} K^-)|_{LD}}{|\mathcal{A}(\Xi_{cc}^{++} \rightarrow \Sigma_c^{++} \bar{K}^0)|_{LD}} = 0.48 \sim 0.52, \quad (47)$$

$$\frac{|\tilde{E}_{2LD}|}{|\tilde{C}_{LD}|} = \frac{|\mathcal{A}(\Xi_{cc}^+ \rightarrow \Omega_c^0 K^+)|_{LD}}{|\mathcal{A}(\Xi_{cc}^{++} \rightarrow \Sigma_c^{++} \bar{K}^0)|_{LD}} = 0.70 \sim 0.77. \quad (48)$$

From Eqs. (45-48), considering the relatively large parameter uncertainty, all these results are consistent with the relations found in [141, 142],

$$\frac{|C|}{|T|} \sim \frac{|C'|}{|C|} \sim \frac{|E_1|}{|C|} \sim \frac{|E_2|}{|C|} \sim \mathcal{O}\left(\frac{\Lambda_{QCD}^h}{m_c}\right) \sim \mathcal{O}(1). \quad (49)$$

The results shown with Eqs. (45-48) are different with each other. This can be understood by the flavor  $SU(3)$  breaking effects. The flavor  $SU(3)$  symmetry is of great significance in the weak decays of heavy hadrons. In terms of a few  $SU(3)$  irreducible amplitudes, several relations between the widths of doubly charmed baryon decays are obtained [68]. It is important to numerically test the flavor  $SU(3)$  symmetry and its breaking effects.

In the following, we show our numerical results on the ratios of decay widths. In the  $SU(3)$

Table III: The amplitudes of  $\mathcal{B}_{cc} \rightarrow \mathcal{B}_c P$  are in unit  $10^{-2} G_F \text{GeV}^2$ . The processes shown in the upper part of this table are dominated by short-distance contributions, while those in the lower part are dominated by long-distance contributions and Cabibbo-favored. The first uncertainty comes from input parameters: decay constants and strong couplings, which have been listed in Tab. II. The second uncertainty is due to the variation of the phenomenological parameter  $\eta = 0.9 \pm 0.2$ . While for the amplitudes  $A_{SD}$  and  $B_{SD}$ , there is only uncertainty from decay constants.

channels	$A_{SD}$	$B_{SD}$	$A_{LD}$	$B_{LD}$	$A_{tot}$	$B_{tot}$
$\Xi_{cc}^+ \rightarrow \Xi_c^+ \pi^+$	$9.92^{+0.09}_{-0.09}$	$14.80^{+0.14}_{-0.14}$	$-1.82^{+0.32+0.61}_{-0.33-0.67} + 0.21^{+0.02+0.16}_{-0.04-0.11} i$	$-5.10^{+1.01+1.69}_{-1.13-1.81} + 3.26^{+1.11+1.37}_{-0.91-1.18} i$	$8.10^{+0.28+0.61}_{-0.29-0.67} + 0.21^{+0.02+0.16}_{-0.04-0.11} i$	$9.66^{+0.94+1.69}_{-1.06-1.81} + 3.26^{+1.11+1.37}_{-0.91-1.18} i$
$\Xi_{cc}^+ \rightarrow \Xi_c^+ \pi^0$	$-5.27^{+0.05}_{-0.05}$	$-42.30^{+0.39}_{-0.39}$	$-1.02^{+0.28+0.33}_{-0.40-0.36} + 1.58^{+0.65+0.67}_{-0.46-0.58} i$	$-2.61^{+0.52+0.80}_{-0.56-0.85} + 2.48^{+1.28+1.32}_{-0.94-1.02} i$	$-6.29^{+0.31+0.33}_{-0.42-0.36} + 1.58^{+0.65+0.67}_{-0.46-0.58} i$	$-44.90^{+0.72+0.80}_{-0.75-0.85} + 2.48^{+1.28+1.32}_{-0.94-1.02} i$
$\Xi_{cc}^+ \rightarrow \Sigma_c^+ \pi^+$	$1.18^{+0.01}_{-0.01}$	$8.22^{+0.08}_{-0.08}$	$-0.18^{+0.03+0.05}_{-0.00-0.05} - 0.44^{+0.12+0.16}_{-0.18-0.18} i$	$-2.50^{+0.40+0.74}_{-0.40-0.80} + 0.66^{+0.03+0.04}_{-0.14-0.08} i$	$1.01^{+0.04+0.05}_{-0.01-0.05} - 0.44^{+0.12+0.16}_{-0.18-0.18} i$	$5.72^{+0.36+0.74}_{-0.36-0.80} + 0.65^{+0.03+0.04}_{-0.14-0.08} i$
$\Xi_{cc}^+ \rightarrow \Lambda_c^+ \pi^+$	$-2.29^{+0.02}_{-0.02}$	$-2.87^{+0.03}_{-0.03}$	$-0.24^{+0.03+0.08}_{-0.03-0.08} + 0.36^{+0.10+0.14}_{-0.07-0.13} i$	$1.24^{+0.29+0.49}_{-0.26-0.43} - 0.87^{+0.22+0.34}_{-0.25-0.41} i$	$-2.54^{+0.04+0.08}_{-0.04-0.08} + 0.36^{+0.10+0.14}_{-0.07-0.13} i$	$-1.63^{+0.28+0.49}_{-0.25-0.43} - 0.87^{+0.22+0.34}_{-0.25-0.41} i$
$\Xi_{cc}^+ \rightarrow \Xi_c^0 K^+$	$-1.54^{+0.03}_{-0.03}$	$-12.30^{+0.24}_{-0.24}$	$-0.02^{+0.01+0.02}_{-0.01-0.02} - 0.06^{+0.03+0.02}_{-0.13-0.16} i$	$-1.46^{+0.28+0.46}_{-0.28+0.46} + 0.58^{+0.20+0.08}_{-0.17-0.09} i$	$-1.56^{+0.02+0.02}_{-0.03-0.03} - 0.06^{+0.03+0.02}_{-0.13-0.16} i$	$-13.70^{+0.40+0.46}_{-0.45-0.48} + 0.58^{+0.20+0.08}_{-0.17-0.09} i$
$\Xi_{cc}^+ \rightarrow \Xi_c^0 K^0$	$2.96^{+0.06}_{-0.06}$	$4.27^{+0.08}_{-0.08}$	$-0.23^{+0.02+0.03}_{-0.01-0.04} - 0.34^{+0.07+0.13}_{-0.09-0.16} i$	$-1.84^{+0.30+0.58}_{-0.29-0.61} - 0.94^{+0.17+0.31}_{-0.25-0.33} i$	$2.73^{+0.03+0.05}_{-0.01-0.04} - 0.34^{+0.07+0.13}_{-0.09-0.16} i$	$2.43^{+0.26+0.58}_{-0.25-0.61} - 0.94^{+0.17+0.31}_{-0.25-0.33} i$
$\Xi_{cc}^+ \rightarrow \Lambda_c^+ K^+$	$-0.69^{+0.01}_{-0.01}$	$-0.84^{+0.02}_{-0.02}$	$0.10^{+0.01+0.03}_{-0.01-0.03} + 0.07^{+0.02+0.02}_{-0.01-0.02} i$	$0.18^{+0.02+0.04}_{-0.03-0.05} + 0.20^{+0.05+0.10}_{-0.04-0.08} i$	$-0.60^{+0.00+0.03}_{-0.01-0.03} + 0.07^{+0.02+0.02}_{-0.01-0.02} i$	$-0.65^{+0.01+0.04}_{-0.02-0.05} + 0.20^{+0.05+0.10}_{-0.04-0.08} i$
$\Xi_{cc}^+ \rightarrow \Sigma_c^+ K^+$	$0.35^{+0.01}_{-0.01}$	$2.40^{+0.05}_{-0.05}$	$-0.09^{+0.02+0.02}_{-0.02-0.04} + 0.04^{+0.00+0.02}_{-0.00-0.02} i$	$0.46^{+0.06+0.12}_{-0.09-0.13} - 0.28^{+0.05+0.09}_{-0.09-0.09} i$	$0.26^{+0.01+0.04}_{-0.01-0.04} + 0.04^{+0.00+0.02}_{-0.00-0.02} i$	$2.86^{+0.11+0.13}_{-0.11-0.13} - 0.28^{+0.09+0.09}_{-0.09-0.09} i$
$\Xi_{cc}^0 \rightarrow \Xi_c^0 \pi^+$	$9.89^{+0.09}_{-0.09}$	$14.80^{+0.14}_{-0.14}$	$2.07^{+0.41+0.73}_{-0.38-0.68} + 0.81^{+0.16+0.33}_{-0.19-0.42} i$	$5.55^{+1.11+2.01}_{-1.01-1.85} - 5.18^{+1.01+2.03}_{-1.16-2.49} i$	$12.00^{+0.46+0.73}_{-0.42-0.68} - 0.81^{+0.16+0.33}_{-0.19-0.42} i$	$20.30^{+1.17+2.01}_{-1.08-1.85} - 5.18^{+1.01+2.03}_{-1.16-2.49} i$
$\Xi_{cc}^0 \rightarrow \Xi_c^0 \pi^0$	$-5.27^{+0.05}_{-0.05}$	$-42.30^{+0.39}_{-0.39}$	$0.54^{+0.14+0.20}_{-0.11-0.18} - 0.62^{+0.13+0.23}_{-0.16-0.26} i$	$3.08^{+0.52+1.00}_{-0.51-0.95} - 2.25^{+0.40+0.94}_{-0.44-1.20} i$	$-4.73^{+0.12+0.20}_{-0.12+0.20} - 0.62^{+0.13+0.23}_{-0.16-0.26} i$	$-39.30^{+0.32+1.00}_{-0.31-0.95} - 2.25^{+0.40+0.94}_{-0.44-1.20} i$
$\Xi_{cc}^0 \rightarrow \Sigma_c^0 \pi^+$	$1.67^{+0.02}_{-0.02}$	$11.60^{+0.11}_{-0.11}$	$-0.76^{+0.13+0.25}_{-0.14-0.27} - 0.01^{+0.02+0.03}_{-0.03-0.01} i$	$-4.51^{+0.77+1.50}_{-0.80-1.63} + 1.66^{+0.20+0.78}_{-0.22-0.64} i$	$0.92^{+0.12+0.25}_{-0.13-0.27} - 0.01^{+0.02+0.03}_{-0.03-0.01} i$	$7.12^{+0.72+1.50}_{-0.74-1.63} + 1.66^{+0.17+0.78}_{-0.22-0.64} i$
$\Xi_{cc}^0 \rightarrow \Xi_c^0 K^+$	$1.54^{+0.03}_{-0.03}$	$12.30^{+0.24}_{-0.24}$	$-0.69^{+0.14+0.24}_{-0.16-0.27} + 0.39^{+0.07+0.20}_{-0.07-0.16} i$	$1.26^{+0.14+0.44}_{-0.18-0.41} - 0.44^{+0.09+0.25}_{-0.11-0.37} i$	$0.85^{+0.12+0.24}_{-0.14-0.27} + 0.39^{+0.07+0.20}_{-0.07-0.16} i$	$13.50^{+0.26+0.44}_{-0.30-0.41} + 0.45^{+0.09+0.25}_{-0.11-0.37} i$
$\Xi_{cc}^0 \rightarrow \Xi_c^0 K^0$	$-2.96^{+0.06}_{-0.06}$	$-4.28^{+0.08}_{-0.08}$	$-0.00^{+0.03+0.03}_{-0.02-0.01} - 0.23^{+0.07+0.16}_{-0.05-0.11} i$	$-0.92^{+0.12+0.29}_{-0.08-0.30} - 0.36^{+0.10+0.07}_{-0.16-0.03} i$	$-2.96^{+0.00-0.01}_{-0.01-0.03} - 0.23^{+0.05+0.09}_{-0.05-0.11} i$	$-5.20^{+0.17+0.29}_{-0.13-0.30} - 0.36^{+0.10+0.07}_{-0.16-0.03} i$
$\Xi_{cc}^0 \rightarrow \Sigma_c^0 K^+$	$2.14^{+0.04}_{-0.04}$	$14.70^{+0.28}_{-0.28}$	—	—	$2.14^{+0.04}_{-0.04}$	$14.70^{+0.28}_{-0.28}$
$\Omega_{cc}^+ \rightarrow \Omega_c^+ \pi^+$	$-7.39^{+0.07}_{-0.07}$	$-61.60^{+0.57}_{-0.57}$	—	—	$-7.39^{+0.07}_{-0.07}$	$-61.60^{+0.57}_{-0.57}$
$\Omega_{cc}^+ \rightarrow \Xi_c^+ \pi^+$	$2.16^{+0.02}_{-0.02}$	$2.99^{+0.03}_{-0.03}$	$0.26^{+0.06+0.10}_{-0.05-0.09} - 0.30^{+0.07+0.11}_{-0.09-0.13} i$	$-0.88^{+0.14+0.28}_{-0.13-0.28} + 0.03^{+0.05+0.04}_{-0.12-0.09} i$	$2.42^{+0.07+0.10}_{-0.06-0.09} - 0.30^{+0.07+0.11}_{-0.09-0.13} i$	$2.12^{+0.13+0.28}_{-0.11-0.28} + 0.02^{+0.05+0.04}_{-0.12-0.09} i$
$\Omega_{cc}^+ \rightarrow \Xi_c^0 \pi^+$	$1.16^{+0.01}_{-0.01}$	$8.47^{+0.08}_{-0.08}$	$-0.16^{+0.01+0.05}_{-0.00-0.04} - 0.42^{+0.10+0.15}_{-0.13-0.16} i$	$-3.61^{+0.63+1.21}_{-0.66-1.31} + 1.63^{+0.16+0.63}_{-0.22-0.56} i$	$1.00^{+0.01+0.05}_{-0.01-0.04} - 0.42^{+0.10+0.15}_{-0.13-0.16} i$	$4.86^{+0.59+1.21}_{-0.62-1.31} + 1.63^{+0.16+0.63}_{-0.22-0.56} i$
$\Omega_{cc}^+ \rightarrow \Omega_c^0 K^+$	$-2.17^{+0.04}_{-0.04}$	$-17.90^{+0.34}_{-0.34}$	$-0.13^{+0.02+0.05}_{-0.02-0.06} - 0.16^{+0.05+0.05}_{-0.08-0.04} i$	$-1.22^{+0.26+0.39}_{-0.33-0.40} + 0.29^{+0.02+0.00}_{-0.09-0.10} i$	$-2.29^{+0.04+0.05}_{-0.04-0.06} - 0.16^{+0.05+0.05}_{-0.08-0.04} i$	$-19.10^{+0.43+0.39}_{-0.50-0.40} + 0.29^{+0.02+0.00}_{-0.09-0.10} i$
$\Omega_{cc}^+ \rightarrow \Xi_c^0 K^0$	$0.65^{+0.01}_{-0.01}$	$0.87^{+0.02}_{-0.02}$	$-0.07^{+0.01+0.02}_{-0.01-0.02} - 0.00^{+0.00+0.00}_{-0.00-0.00} i$	$-0.04^{+0.01+0.01}_{-0.00-0.00} - 0.21^{+0.05+0.08}_{-0.07-0.10} i$	$0.59^{+0.00+0.02}_{-0.00-0.02} - 0.00^{+0.00+0.00}_{-0.00-0.00} i$	$0.83^{+0.02+0.01}_{-0.01-0.00} - 0.21^{+0.05+0.08}_{-0.07-0.10} i$
$\Omega_{cc}^+ \rightarrow \Xi_c^+ K^+$	$0.34^{+0.01}_{-0.01}$	$2.48^{+0.05}_{-0.05}$	$-0.06^{+0.01+0.02}_{-0.02-0.02} + 0.06^{+0.02+0.03}_{-0.01-0.02} i$	$0.32^{+0.06+0.12}_{-0.06-0.11} - 0.28^{+0.05+0.11}_{-0.05-0.13} i$	$0.28^{+0.01+0.02}_{-0.01-0.02} + 0.06^{+0.02+0.03}_{-0.01-0.02} i$	$2.80^{+0.09+0.12}_{-0.08-0.11} - 0.28^{+0.05+0.11}_{-0.05-0.13} i$
$\Xi_{cc}^+ \rightarrow \Sigma_c^+ \pi^+ \bar{K}^0$	$-0.15^{+0.00}_{-0.00}$	$-0.23^{+0.00}_{-0.00}$	$-0.20^{+0.32+0.11}_{-0.38-0.03} - 1.37^{+0.20+0.46}_{-0.00-0.54} i$	$-2.58^{+0.30+0.85}_{-0.19-0.92} + 13.40^{+2.43+4.66}_{-3.31-5.24} i$	$-0.35^{+0.22+0.11}_{-0.38-0.03} - 1.37^{+0.20+0.46}_{-0.00-0.54} i$	$-2.81^{+0.30+0.85}_{-0.19-0.92} + 13.40^{+2.43+4.66}_{-3.31-5.24} i$
$\Xi_{cc}^+ \rightarrow \Omega_c^0 K^+$	—	—	$2.20^{+0.52+0.82}_{-0.45-0.75} - 2.18^{+0.44+0.84}_{-0.52-1.02} i$	$-7.29^{+1.19+2.29}_{-0.45-0.75} + 1.80^{+0.07+1.05}_{-0.19-0.82} i$	$2.20^{+0.52+0.82}_{-0.45-0.75} - 2.18^{+0.44+0.84}_{-0.52-1.02} i$	$-7.29^{+1.19+2.29}_{-0.45-0.75} + 1.80^{+0.07+1.05}_{-0.19-0.82} i$
$\Xi_{cc}^+ \rightarrow \Sigma_c^+ \bar{K}^0$	$-0.11^{+0.00}_{-0.00}$	$-0.16^{+0.00}_{-0.00}$	$-0.50^{+0.29+0.10}_{-0.48-0.06} - 0.54^{+0.41+0.17}_{-0.18-0.19} i$	$-0.58^{+0.49+0.19}_{-0.08-0.21} - 13.00^{+2.26+4.58}_{-3.07-5.20} i$	$-0.66^{+0.29+0.10}_{-0.48-0.06} - 0.54^{+0.41+0.17}_{-0.18-0.19} i$	$-0.81^{+0.49+0.19}_{-0.07-0.21} - 13.00^{+2.26+4.58}_{-3.07-5.20} i$
$\Xi_{cc}^+ \rightarrow \Lambda_c^+ \bar{K}^0$	$-0.15^{+0.00}_{-0.00}$	$-0.23^{+0.00}_{-0.00}$	$2.23^{+0.13+0.83}_{-0.23-0.76} + 1.41^{+0.10+0.55}_{-0.03-0.68} i$	$1.93^{+0.46+0.63}_{-0.29-0.61} - 14.10^{+2.16+5.22}_{-2.74-6.19} i$	$2.07^{+0.13+0.83}_{-0.23-0.76} + 1.41^{+0.10+0.55}_{-0.03-0.68} i$	$1.70^{+0.45+0.63}_{-0.29-0.61} - 14.10^{+2.16+5.22}_{-2.74-6.19} i$
$\Xi_{cc}^+ \rightarrow \Sigma_c^+ K^0$	—	—	$-0.49^{+0.30+0.18}_{-0.09+0.23} + 0.48^{+0.24+0.19}_{-0.24-0.19} i$	$3.35^{+0.50+1.11}_{-0.49+0.19} - 9.70^{+1.36+3.61}_{-1.73-4.28} i$	$-0.49^{+0.30+0.18}_{-0.09+0.23} + 0.48^{+0.24+0.19}_{-0.24-0.19} i$	$3.35^{+0.50+1.11}_{-0.49+0.19} - 9.70^{+1.36+3.61}_{-1.73-4.28} i$
$\Xi_{cc}^+ \rightarrow \Xi_c^+ K^0$	—	—	$-0.67^{+0.09+0.23}_{-0.08-0.25} + 0.13^{+0.06+0.09}_{-0.13-0.06} i$	$3.42^{+0.68+1.27}_{-0.64-1.18} - 2.00^{+0.66+0.69}_{-0.84-0.76} i$	$-0.67^{+0.09+0.23}_{-0.08-0.25} + 0.13^{+0.06+0.09}_{-0.13-0.06} i$	$3.42^{+0.68+1.27}_{-0.64-1.18} - 2.00^{+0.66+0.69}_{-0.84-0.76} i$
$\Xi_{cc}^+ \rightarrow \Xi_c^+ \eta_1$	—	—	$-0.52^{+0.19+0.17}_{-0.28-0.18} + 0.78^{+0.43+0.34}_{-0.29-0.29} i$	$1.64^{+0.24+0.57}_{-0.20-0.54} - 3.79^{+0.37+0.23}_{-0.20-1.67} i$	$-0.52^{+0.19+0.17}_{-0.28-0.18} + 0.78^{+0.43+0.34}_{-0.29-0.29} i$	$1.64^{+0.24+0.57}_{-0.20-0.54} - 3.79^{+0.37+0.23}_{-0.20-1.67} i$
$\Xi_{cc}^+ \rightarrow \Xi_c^+ \eta_8$	—	—	$-0.12^{+0.04+0.04}_{-0.02-0.03} + 0.43^{+0.03+0.17}_{-0.03-0.15} i$	$-3.40^{+0.46+1.13}_{-0.58-1.22} + 10.50^{+1.85+4.69}_{-1.46-3.94} i$	$-0.12^{+0.04+0.04}_{-0.02-0.03} + 0.43^{+0.03+0.17}_{-0.03-0.15} i$	$-3.40^{+0.46+1.13}_{-0.58-1.22} + 10.50^{+1.85+4.69}_{-1.46-3.94} i$
$\Xi_{cc}^+ \rightarrow \Xi_c^+ \pi^0$	—	—	$0.74^{+0.02+0.20}_{-0.08-0.21} + 1.04^{+0.30+0.38}_{-0.23-0.35} i$	$2.39^{+0.31+0.61}_{-0.37-0.66} + 3.35^{+0.75+1.54}_{-0.95-1.27} i$	$0.74^{+0.02+0.20}_{-0.08-0.21} + 1.04^{+0.30+0.38}_{-0.23-0.35} i$	$2.39^{+0.31+0.61}_{-0.37-0.66} + 3.35^{+0.75+1.54}_{-0.95-1.27} i$
$\Xi_{cc}^+ \rightarrow \Xi_c^+ \eta_1$	—	—	$-0.13^{+0.09+0.04}_{-0.15-0.04} + 0.14^{+0.23+0.07}_{-0.14-0.06} i$	$1.85^{+0.38+0.67}_{-0.30-0.61} - 6.49^{+0.92+2.42}_{-1.10-2.86} i$	$-0.13^{+0.09+0.04}_{-0.15-0.04} + 0.14^{+0.23+0.07}_{-0.14-0.06} i$	$1.85^{+0.38+0.67}_{-0.30-0.61} - 6.49^{+0.92+2.42}_{-1.10-2.86} i$
$\Xi_{cc}^+ \rightarrow \Xi_c^+ \eta_8$	—	—	$-0.42^{+0.34+0.15}_{-0.21-0.14} - 0.53^{+0.30+0.21}_{-0.48-0.25} i$	$-3.79^{+0.66+1.27}_{-0.85-1.38} + 12.80^{+2.40+5.62}_{-1.96-4.74} i$	$-0.42^{+0.34+0.15}_{-0.21-0.14} - 0.53^{+0.30+0.21}_{-0.48-0.25} i$	$-3.79^{+0.66+1.27}_{-0.85-1.38} + 12.80^{+2.40+5.62}_{-1.96-4.74} i$
$\Omega_{cc}^+ \rightarrow \Xi_c^+ \bar{K}^0$	$0.08^{+0.00}_{-0.00}$	$0.68^{+0.01}_{-0.01}$	$0.99^{+0.02+0.53}_{-0.12-0.42} + 1.63^{+0.01+0.73}_{-0.01-0.73} i$	$-5.86^{+0.90+1.87}_{-0.60-1.96} - 8.35^{+1.06+2.81}_{-1.44-3.07} i$	$1.10^{+0.02+0.53}_{-0.12-0.42} - 1.63^{+0.01+0.73}_{-0.01-0.73} i$	$-4.90^{+0.90+2.81}_{-0.60-1.96} - 8.35^{+1.06+2.81}_{-1.44-3.07} i$
$\Omega_{cc}^+ \rightarrow \Xi_c^+ \bar{K}^0$	$0.12^{+0.00}_{-0.00}$	$0.96^{+0.01}_{-0.01}$	$2.41^{+0.56+0.98}_{-0.46-0.86} - 4.31^{+0.83+1.59}_{-1.02-1.88} i$	$-3.36^{+0.64+1.06}_{-0.55-1.10} - 11.10^{+1.71+4.04}_{-2.20-4.72} i$	$2.53^{+0.56+0.98}_{-0.46-0.86} - 4.31^{+0.83+1.59}_{-1.02-1.88} i$	$-2.40^{+0.64+1.06}_{-0.55-1.10} - 11.10^{+1.71+4.04}_{-2.20-4.72} i$

Table IV: Comparison of the decay amplitudes of  $\Xi_{cc}^{++} \rightarrow \Xi_c^{(\prime)+} \pi^+$  from this work with those from the literature. All the amplitudes below are in unit  $10^{-2} G_F \text{GeV}^2$ . In this table, we list the theoretical prediction from the pole approximation (PA) in tandem with the SU(3)F symmetry [138], the non-relativistic quark model (NRQM) [139], the pole model (PM) with current algebra (CA) [72], the Ab initio three-loop calculation (AITLC) [73], the heavy quark effective theory (HQET) with pole model (PM) [70], light-cone sum rules (LCSR) with HQET [75], and the bag model [140].

$\Xi_{cc}^{++} \rightarrow \Xi_c^+ \pi^+$	$A_{SD}$	$A_{LD}$	$A_{tot}$	$B_{SD}$	$B_{LD}$	$B_{tot}$
This work	9.92	$-1.82 + 0.21i$	$8.10 + 0.21i$	14.80	$-5.11 + 3.26i$	$9.66 + 3.26i$
PA+SU(3) [138]	5.36	-1.12	-	7.59	-1.43	-
NRQM [139]	7.4	-12.4	-5.0	-13	21.8	8.8
PM+CA [72]	7.40	-10.79	-3.38	-15.06	18.91	3.85
AITLC [73]	-8.1	11.5	3.4	13.0	-18.5	-5.6
HQET+PM [70]	9.52	0	9.52	-19.45	-24.95	-44.40
LCSR+HQET [75]	9.52	-16.67	-7.18	-19.45	-20.47	-39.92
Bag Model [140]	4.83	-9.99	-5.16	5.16	13.6	18.8
$\Xi_{cc}^{++} \rightarrow \Xi_c'^+ \pi^+$	$A_{SD}$	$A_{LD}$	$A_{tot}$	$B_{SD}$	$B_{LD}$	$B_{tot}$
This work	-5.28	$-1.02 + 1.58i$	$-6.30 + 1.58i$	-42.40	$-2.61 + 2.48i$	$-45.00 + 2.48i$
PA+SU(3) [138]	-2.80	0		-22.31	0	
NRQM [139]	3.7	0	3.7	-37.1	0	-31.0
PM+CA [72]	4.5	-0.04	4.5	-48.5	-0.06	-48.4
AITLC [73]	-4.3	-0.1	-4.4	37.6	1.4	39.0
HQET+PM [70]	5.10	0	5.10	-62.37	0	-62.37
LCSR+HQET [75]	5.10	-0.83	4.27	-62.37	-8.86	-71.23
Bag Model [140]	7.38	-4.82	2.56	-51.0	7.26	-43.7



limit, they should be unity. Any deviation would indicate the  $SU(3)$  breaking effects.

$$\frac{\Gamma(\Xi_{cc}^{++} \rightarrow \Lambda_c^+ \pi^+)}{\Gamma(\Xi_{cc}^{++} \rightarrow \Xi_c^+ K^+)} = \frac{|\lambda_d(T + C')|^2}{|\lambda_s(T + C')|^2} = 1.01 \sim 1.13, \quad (50)$$

$$\frac{\Gamma(\Xi_{cc}^+ \rightarrow \Xi_c^+ K^0)}{\Gamma(\Omega_{cc}^+ \rightarrow \Lambda_c^+ \bar{K}^0)} = \frac{|\lambda_s C' + \lambda_d E_1|^2}{|\lambda_d C' + \lambda_s E_1|^2} = 0.53 \sim 0.56, \quad (51)$$

$$\frac{\Gamma(\Xi_{cc}^+ \rightarrow \Xi_c^0 K^+)}{\Gamma(\Omega_{cc}^+ \rightarrow \Xi_c^0 \pi^+)} = \frac{|\lambda_s T + \lambda_d E_2|^2}{|-\lambda_d T - \lambda_s E_2|^2} = 1.02 \sim 1.19, \quad (52)$$

$$\frac{\Gamma(\Xi_{cc}^{++} \rightarrow \Sigma_c^{++} \pi^0)}{\frac{1}{3}\Gamma(\Xi_{cc}^{++} \rightarrow \Sigma_c^{++} \eta_8)} = \frac{|-\frac{1}{\sqrt{2}}\tilde{C}|^2}{|-\frac{1}{\sqrt{6}}(\lambda_d - 2\lambda_s)\tilde{C}|^2} = 1.24 \sim 1.50, \quad (53)$$

$$\frac{\Gamma(\Xi_{cc}^{++} \rightarrow \Sigma_c^+ \pi^+)}{\Gamma(\Xi_{cc}^{++} \rightarrow \Xi_c'^+ K^+)} = \frac{|\frac{1}{\sqrt{2}}\lambda_d(\tilde{T} + \tilde{C}')|^2}{|\frac{1}{\sqrt{2}}\lambda_s(\tilde{T} + \tilde{C}')|^2} = 0.44 \sim 0.45, \quad (54)$$

$$\frac{\Gamma(\Xi_{cc}^+ \rightarrow \Sigma_c^{++} \pi^-)}{\Gamma(\Omega_{cc}^+ \rightarrow \Sigma_c^{++} K^-)} = \frac{|\lambda_d \tilde{E}_1|^2}{|\lambda_s \tilde{E}_1|^2} = 0.49 \sim 0.62, \quad (55)$$

$$\frac{\Gamma(\Omega_{cc}^+ \rightarrow \Omega_c^0 K^+)}{\Gamma(\Xi_{cc}^+ \rightarrow \Sigma_c^0 \pi^+)} = \frac{|\lambda_s(\tilde{T} + \tilde{E}_2)|^2}{|\lambda_d(\tilde{T} + \tilde{E}_2)|^2} = 3.54 \sim 6.36, \quad (56)$$

$$\frac{\Gamma(\Xi_{cc}^+ \rightarrow \Xi_c'^+ K^0)}{\Gamma(\Omega_{cc}^+ \rightarrow \Sigma_c^+ \bar{K}^0)} = \frac{|\frac{1}{\sqrt{2}}(\lambda_s \tilde{C}' + \lambda_d \tilde{E}_1)|^2}{|\frac{1}{\sqrt{2}}(\lambda_d \tilde{C}' + \lambda_s \tilde{E}_1)|^2} = 0.69 \sim 0.72, \quad (57)$$

$$\frac{\Gamma(\Omega_{cc}^+ \rightarrow \Xi_c'^0 \pi^+)}{\Gamma(\Xi_{cc}^+ \rightarrow \Xi_c'^0 K^+)} = \frac{|\frac{1}{\sqrt{2}}(\lambda_d \tilde{T}' + \lambda_s \tilde{E}_2)|^2}{|\frac{1}{\sqrt{2}}(\lambda_s \tilde{T}' + \lambda_d \tilde{E}_2)|^2} = 0.50 \sim 0.51. \quad (58)$$

The numerical results presented above indicate that long-distance final-state interactions can significantly contribute to  $SU(3)$  symmetry breaking. This effect originates from several factors, including the exchanged particles, hadronic strong coupling constants, transition form factors, and decay constants. The interference between distinct diagrams is also considered.

In our calculation of Eqs. (50)-(58), the large values mainly stem from the strong coupling constants. Taking  $\Gamma(\Omega_{cc}^+ \rightarrow \Omega_c^0 K^+)/\Gamma(\Xi_{cc}^+ \rightarrow \Sigma_c^0 \pi^+) = 3.54 \sim 6.36$  as an example, the two decay modes are both dominated by the triangle diagram  $\mathcal{M}(V, B; V)$  contribution, including  $\mathcal{M}(K^{*+}, \Omega_c^0; \phi)$ ,  $\mathcal{M}(\rho^+, \Xi_c^{(j)0}; \bar{K}^{*0})$  for  $\Omega_{cc}^+ \rightarrow \Omega_c^0 K^+$  and  $\mathcal{M}(\rho^+, \Sigma_c^0; \rho^0)$ ,  $\mathcal{M}(K^{*+}, \Xi_c^{(j)0}; K^{*0})$  for  $\Xi_{cc}^+ \rightarrow \Sigma_c^0 \pi^+$ . Due to  $g_{K^{*+}\phi K^+}/g_{\rho^+\rho^0\pi^+} = g_{\Omega_c^0\Omega_c^0\phi}/g_{\Sigma_c^0\Sigma_c^0\rho^0} = \sqrt{2}$ , the ratio  $\mathcal{M}(K^{*+}, \Omega_c^0; \phi)/\mathcal{M}(\rho^+, \Sigma_c^0; \rho^0)$  will be 2. While the ratios of other two amplitudes  $\mathcal{M}(\rho^+, \Xi_c^{(j)0}; \bar{K}^{*0})/\mathcal{M}(K^{*+}, \Xi_c^{(j)0}; K^{*0})$  will be 1, for  $g_{\rho^+\bar{K}^{*0}K^+}/g_{K^{*+}K^{*0}\pi^+} = g_{\Omega_c^0\Xi_c^{(j)0}K^{*0}}/g_{\Sigma_c^0\Xi_c^{(j)0}K^{*0}} = 1$ . Therefore,  $\Gamma(\Omega_{cc}^+ \rightarrow \Omega_c^0 K^+)$  is slightly larger than  $\Gamma(\Xi_{cc}^+ \rightarrow \Sigma_c^0 \pi^+)$ , combining the effects from other input parameters.

All strong couplings utilized in this study are sourced from existing literature and align with  $SU(3)$  flavor symmetry. These non-perturbative values carry significant theoretical uncertainties, warranting a comprehensive and meticulous examination in future research.

#### D. Branching ratio and Decay asymmetry parameters

The branching ratio and three asymmetry parameters ( $\alpha$ ,  $\beta$ ,  $\gamma$ ) of each nonleptonic decay  $\mathcal{B}_{cc} \rightarrow \mathcal{B}_c P$  can be predicted. The branching ratios and decay symmetry parameters of the short-distance contribution dominated channels (with  $T$  topology) are listed into Tab. V. For the long-

Table V: Branching ratios and decay asymmetry parameters for the short-distance dynamics dominated modes. The “CF”, “SCS” and “DCS” represent CKM favored, singly CKM suppressed and doubly CKM suppressed processes, respectively. And  $\mathcal{B}_{SD}$ ,  $\mathcal{B}_{LD}$  and  $\mathcal{B}_{tot}$  denote the branching ratio of short-distance contribution, long-distance contribution and total one respectively. The first uncertainty comes from input parameters: decay constants and strong couplings, which have been listed in Tab. II. The second uncertainty is due to the variation of the phenomenological parameter  $\eta = 0.9 \pm 0.2$ . While for the branching ratio  $\mathcal{B}_{SD}$ , there is only uncertainty from decay constants.

channels	CKM	$\mathcal{B}_{SD}[10^{-3}]$	$\mathcal{B}_{LD}[10^{-3}]$	$\mathcal{B}_{tot}[10^{-3}]$	$\alpha$	$\beta$	$\gamma$
$\Xi_{cc}^{++} \rightarrow \Xi_c^{+} \pi^{+}$	CF	$60.70^{+1.12}_{-1.11}$	$2.67^{+1.30+2.37}_{-0.82-1.50}$	$39.70^{+2.97+6.47}_{-2.73-6.33}$	$-0.43^{+0.03+0.04}_{-0.02-0.03}$	$0.13^{+0.06+0.07}_{-0.04-0.05}$	$-0.89^{+0.01+0.01}_{-0.00-0.01}$
$\Xi_{cc}^{++} \rightarrow \Xi_c^{\prime+} \pi^{+}$	CF	$42.30^{+0.78}_{-0.78}$	$2.13^{+2.40+2.09}_{-0.87-1.24}$	$53.70^{+5.86+5.26}_{-3.58-4.20}$	$-0.97^{+0.00+0.00}_{-0.00-0.00}$	$0.19^{+0.04+0.05}_{-0.04-0.06}$	$0.14^{+0.04+0.05}_{-0.07-0.06}$
$\Xi_{cc}^{++} \rightarrow \Sigma_c^{+} \pi^{+}$	SCS	$2.23^{+0.04}_{-0.04}$	$0.27^{+0.17+0.21}_{-0.08-0.14}$	$1.39^{+0.09+0.18}_{-0.04-0.12}$	$-0.87^{+0.07+0.12}_{-0.04-0.07}$	$0.50^{+0.06+0.14}_{-0.11-0.16}$	$0.00^{+0.10+0.12}_{-0.17-0.18}$
$\Xi_{cc}^{++} \rightarrow \Lambda_c^{+} \pi^{+}$	SCS	$3.44^{+0.06}_{-0.06}$	$0.18^{+0.11+0.17}_{-0.06-0.11}$	$4.08^{+0.17+0.32}_{-0.13-0.25}$	$-0.26^{+0.06+0.11}_{-0.05-0.10}$	$0.19^{+0.04+0.06}_{-0.04-0.06}$	$-0.95^{+0.01+0.02}_{-0.00-0.01}$
$\Xi_{cc}^{++} \rightarrow \Xi_c^{\prime+} K^{+}$	SCS	$2.74^{+0.11}_{-0.10}$	$0.03^{+0.02+0.02}_{-0.01-0.01}$	$3.18^{+0.19+0.18}_{-0.15-0.16}$	$-0.96^{+0.00+0.01}_{-0.00-0.01}$	$-0.08^{+0.01+0.02}_{-0.02-0.01}$	$0.26^{+0.01+0.02}_{-0.01-0.02}$
$\Xi_{cc}^{++} \rightarrow \Xi_c^{+} K^{+}$	SCS	$4.82^{+0.19}_{-0.18}$	$0.15^{+0.07+0.13}_{-0.04-0.08}$	$4.02^{+0.13+0.16}_{-0.04-0.08}$	$-0.31^{+0.03+0.06}_{-0.03-0.05}$	$-0.08^{+0.01+0.02}_{-0.02-0.04}$	$-0.95^{+0.01+0.02}_{-0.01-0.01}$
$\Xi_{cc}^{++} \rightarrow \Lambda_c^{+} K^{+}$	DCS	$0.29^{+0.01}_{-0.01}$	$0.01^{+0.00+0.01}_{-0.00-0.00}$	$0.21^{+0.00+0.02}_{-0.00-0.02}$	$-0.44^{+0.00+0.01}_{-0.01-0.01}$	$-0.09^{+0.01+0.04}_{-0.02-0.06}$	$-0.89^{+0.00+0.01}_{-0.00-0.00}$
$\Xi_{cc}^{++} \rightarrow \Sigma_c^{+} K^{+}$	DCS	$0.16^{+0.01}_{-0.01}$	$0.01^{+0.00+0.01}_{-0.00-0.01}$	$0.17^{+0.01+0.01}_{-0.01-0.00}$	$-0.79^{+0.05+0.12}_{-0.04-0.09}$	$-0.21^{+0.02+0.08}_{-0.00-0.09}$	$0.58^{+0.06+0.11}_{-0.06-0.12}$
$\Xi_{cc}^{+} \rightarrow \Xi_c^0 \pi^{+}$	CF	$10.40^{+0.19}_{-0.19}$	$0.68^{+0.34+0.63}_{-0.21-0.39}$	$15.60^{+1.38+2.26}_{-1.15-1.90}$	$-0.58^{+0.01+0.02}_{-0.01-0.02}$	$-0.11^{+0.02+0.04}_{-0.02-0.04}$	$-0.81^{+0.01+0.02}_{-0.01-0.02}$
$\Xi_{cc}^{+} \rightarrow \Xi_c^0 \pi^{+}$	CF	$7.26^{+0.13}_{-0.13}$	$0.10^{+0.06+0.10}_{-0.03-0.06}$	$6.15^{+0.13+0.33}_{-0.14-0.32}$	$-0.95^{+0.01+0.01}_{-0.00-0.00}$	$-0.07^{+0.02+0.02}_{-0.02-0.03}$	$0.31^{+0.01+0.01}_{-0.01-0.01}$
$\Xi_{cc}^{+} \rightarrow \Sigma_c^0 \pi^{+}$	SCS	$0.76^{+0.01}_{-0.01}$	$0.14^{+0.06+0.12}_{-0.04-0.08}$	$0.28^{+0.06+0.13}_{-0.05-0.10}$	$-0.89^{+0.06+0.10}_{-0.02-0.04}$	$0.22^{+0.08+0.11}_{-0.05-0.09}$	$0.40^{+0.05+0.12}_{-0.03-0.06}$
$\Xi_{cc}^{+} \rightarrow \Xi_c^0 K^{+}$	SCS	$0.47^{+0.02}_{-0.02}$	$0.05^{+0.03+0.06}_{-0.02-0.03}$	$0.41^{+0.00+0.01}_{-0.00-0.01}$	$-0.69^{+0.12+0.23}_{-0.07-0.18}$	$-0.34^{+0.07+0.15}_{-0.08-0.14}$	$0.64^{+0.06+0.08}_{-0.08-0.14}$
$\Xi_{cc}^{+} \rightarrow \Xi_c^0 K^{+}$	SCS	$0.82^{+0.03}_{-0.03}$	$0.01^{+0.00+0.01}_{-0.00-0.00}$	$0.85^{+0.01+0.00}_{-0.01-0.00}$	$-0.55^{+0.01+0.03}_{-0.01-0.03}$	$-0.00^{+0.00+0.01}_{-0.00-0.02}$	$-0.83^{+0.01+0.02}_{-0.01-0.02}$
$\Xi_{cc}^{+} \rightarrow \Sigma_c^0 K^{+}$	DCS	$1.00^{+0.04}_{-0.04}$	—	$1.00^{+0.04}_{-0.04}$	—0.98	—	0.18
$\Omega_{cc}^{+} \rightarrow \Omega_c^0 \pi^{+}$	CF	$68.10^{+1.26}_{-1.25}$	—	$68.10^{+1.26}_{-1.25}$	—0.96	—	0.28
$\Omega_{cc}^{+} \rightarrow \Xi_c^0 \pi^{+}$	SCS	$2.46^{+0.05}_{-0.05}$	$0.09^{+0.06+0.09}_{-0.03-0.05}$	$2.99^{+0.21+0.27}_{-0.15-0.21}$	$-0.34^{+0.03+0.06}_{-0.03-0.06}$	$0.05^{+0.00+0.00}_{-0.01-0.01}$	$-0.94^{+0.01+0.02}_{-0.01-0.02}$
$\Omega_{cc}^{+} \rightarrow \Xi_c^0 \pi^{+}$	SCS	$1.75^{+0.03}_{-0.03}$	$0.34^{+0.17+0.30}_{-0.10-0.19}$	$0.96^{+0.07+0.18}_{-0.00-0.10}$	$-0.74^{+0.17+0.33}_{-0.09-0.17}$	$0.66^{+0.07+0.18}_{-0.13-0.24}$	$-0.15^{+0.11+0.19}_{-0.15-0.21}$
$\Omega_{cc}^{+} \rightarrow \Omega_c^0 K^{+}$	SCS	$4.43^{+0.17}_{-0.17}$	$0.03^{+0.02+0.02}_{-0.01-0.02}$	$5.03^{+0.24+0.25}_{-0.20-0.21}$	$-0.98^{+0.00+0.00}_{-0.00-0.00}$	$-0.08^{+0.02+0.02}_{-0.03-0.01}$	$0.17^{+0.01+0.00}_{-0.00-0.01}$
$\Omega_{cc}^{+} \rightarrow \Xi_c^0 K^{+}$	DCS	$0.20^{+0.01}_{-0.01}$	$0.00^{+0.00+0.00}_{-0.00-0.00}$	$0.17^{+0.00+0.01}_{-0.00-0.01}$	$-0.50^{+0.01+0.01}_{-0.01-0.01}$	$-0.13^{+0.03+0.05}_{-0.04-0.06}$	$-0.86^{+0.01+0.02}_{-0.01-0.01}$
$\Omega_{cc}^{+} \rightarrow \Xi_c^0 K^{+}$	DCS	$0.12^{+0.00}_{-0.00}$	$0.01^{+0.00+0.01}_{-0.00-0.00}$	$0.13^{+0.00+0.01}_{-0.00-0.00}$	$-0.85^{+0.05+0.09}_{-0.04-0.07}$	$-0.28^{+0.05+0.10}_{-0.06-0.11}$	$0.45^{+0.04+0.08}_{-0.05-0.08}$

Table VI: Branching ratios and decay asymmetry parameters for the long-distance dominated Cabibbo-favored ( $\lambda_{sd}$ ) modes. The first uncertainty comes from input parameters: decay constants and strong couplings, which have been listed in Tab. II. The second uncertainty is due to the variation of the phenomenological parameter  $\eta = 0.9 \pm 0.2$ . While for the branching ratio  $\mathcal{B}_{SD}$ , there is only uncertainty from decay constants.

channels	$\mathcal{B}_{SD}[10^{-5}]$	$\mathcal{B}_{LD}[10^{-3}]$	$\mathcal{B}_{tot}[10^{-3}]$	$\alpha$	$\beta$	$\gamma$
$\Xi_{cc}^{++} \rightarrow \Sigma_c^{++} K^0$	$1.32^{+0.02}_{-0.02}$	$3.92^{+1.71+3.63}_{-0.86-2.22}$	$3.98^{+1.77+3.62}_{-0.89-2.22}$	$-0.88^{+0.17+0.01}_{-0.03-0.01}$	$0.04^{+0.22+0.12}_{-0.18-0.10}$	$0.48^{+0.11+0.02}_{-0.18-0.05}$
$\Xi_{cc}^{+} \rightarrow \Omega_c^0 K^{+}$	—	$0.78^{+0.45+0.78}_{-0.25-0.46}$	$0.78^{+0.45+0.78}_{-0.25-0.46}$	$0.47^{+0.03+0.02}_{-0.03-0.02}$	$-0.28^{+0.00+0.02}_{-0.01-0.02}$	$-0.83^{+0.02+0.02}_{-0.02-0.02}$
$\Xi_{cc}^{+} \rightarrow \Sigma_c^{+} \bar{K}^0$	$0.11^{+0.00}_{-0.00}$	$0.51^{+0.34+0.47}_{-0.12-0.29}$	$0.52^{+0.36+0.47}_{-0.13-0.29}$	$-0.45^{+0.30+0.01}_{-0.22-0.02}$	$0.48^{+0.15+0.11}_{-0.25-0.10}$	$0.75^{+0.07+0.06}_{-0.14-0.10}$
$\Xi_{cc}^{+} \rightarrow \Lambda_c^{+} \bar{K}^0$	$0.25^{+0.00}_{-0.00}$	$1.53^{+0.44+1.57}_{-0.32-0.91}$	$1.46^{+0.43+1.55}_{-0.31-0.89}$	$-0.65^{+0.04+0.01}_{-0.04-0.01}$	$-0.74^{+0.03+0.02}_{-0.00-0.01}$	$0.17^{+0.13+0.01}_{-0.09-0.00}$
$\Xi_{cc}^{+} \rightarrow \Sigma_c^{+} K^{-}$	—	$0.33^{+0.22+0.35}_{-0.09-0.20}$	$0.33^{+0.22+0.35}_{-0.09-0.20}$	$0.60^{+0.13+0.00}_{-0.28-0.00}$	$0.30^{+0.03+0.01}_{-0.08-0.01}$	$0.74^{+0.12+0.00}_{-0.18-0.00}$
$\Xi_{cc}^{+} \rightarrow \Xi_c^{\prime+} \pi^0$	—	$0.08^{+0.04+0.08}_{-0.02-0.05}$	$0.08^{+0.04+0.08}_{-0.02-0.05}$	$0.94^{+0.01+0.01}_{-0.14-0.02}$	$0.34^{+0.19+0.04}_{-0.25-0.03}$	$-0.03^{+0.11+0.00}_{-0.16-0.01}$
$\Xi_{cc}^{+} \rightarrow \Xi_c^{\prime+} \eta_1$	—	$0.10^{+0.12+0.10}_{-0.04-0.06}$	$0.10^{+0.12+0.10}_{-0.04-0.06}$	$0.89^{+0.07+0.00}_{-0.14-0.01}$	$0.16^{+0.02+0.01}_{-0.05-0.01}$	$-0.43^{+0.53+0.01}_{-0.18-0.01}$
$\Xi_{cc}^{+} \rightarrow \Xi_c^{\prime+} \eta_8$	—	$0.03^{+0.01+0.03}_{-0.01-0.02}$	$0.03^{+0.01+0.03}_{-0.01-0.02}$	$-0.89^{+0.06+0.02}_{-0.04-0.02}$	$0.03^{+0.08+0.00}_{-0.07-0.00}$	$0.46^{+0.07+0.03}_{-0.10-0.04}$
$\Xi_{cc}^{+} \rightarrow \Xi_c^{+} \pi^0$	—	$0.22^{+0.11+0.18}_{-0.06-0.12}$	$0.22^{+0.11+0.18}_{-0.06-0.12}$	$-0.89^{+0.01+0.02}_{-0.05-0.02}$	$-0.00^{+0.06+0.03}_{-0.06-0.04}$	$-0.46^{+0.01+0.04}_{-0.01-0.03}$
$\Xi_{cc}^{+} \rightarrow \Xi_c^{+} \eta_1$	—	$0.11^{+0.07+0.12}_{-0.03-0.07}$	$0.11^{+0.07+0.12}_{-0.03-0.07}$	$0.29^{+0.23+0.01}_{-0.33-0.01}$	$0.15^{+0.05+0.01}_{-0.10-0.01}$	$0.95^{+0.01+0.00}_{-0.16-0.00}$
$\Xi_{cc}^{+} \rightarrow \Xi_c^{+} \eta_8$	—	$0.13^{+0.13+0.14}_{-0.04-0.08}$	$0.13^{+0.13+0.14}_{-0.04-0.08}$	$0.72^{+0.11+0.01}_{-0.44-0.01}$	$0.29^{+0.02+0.03}_{-0.13-0.02}$	$0.63^{+0.18+0.00}_{-0.29-0.00}$
$\Omega_{cc}^{+} \rightarrow \Xi_c^{\prime+} \bar{K}^0$	$0.82^{+0.02}_{-0.02}$	$2.76^{+0.07+2.82}_{-0.31-1.63}$	$2.74^{+0.05+2.83}_{-0.30-1.63}$	$-0.42^{+0.01+0.02}_{-0.01-0.04}$	$-0.88^{+0.06+0.01}_{-0.02-0.00}$	$-0.20^{+0.28+0.04}_{-0.14-0.05}$
$\Omega_{cc}^{+} \rightarrow \Xi_c^{+} \bar{K}^0$	$2.07^{+0.04}_{-0.04}$	$13.10^{+7.37+13.60}_{-3.97-7.83}$	$13.30^{+7.42+13.70}_{-4.00-7.89}$	$-0.54^{+0.01+0.00}_{-0.03-0.00}$	$-0.49^{+0.01+0.01}_{-0.00-0.01}$	$-0.69^{+0.03+0.00}_{-0.01-0.00}$

Table VII: Same as Table.VI but for the long-distance dominated singly Cabibbo-suppressed modes.

channels	$\mathcal{B}_{SD}[10^{-7}]$	$\mathcal{B}_{LD}[10^{-4}]$	$\mathcal{B}_{tot}[10^{-4}]$	$\alpha$	$\beta$	$\gamma$
$\Xi_{cc}^{++} \rightarrow \Sigma_c^{++} \pi^0$	$3.89^{+0.07}_{-0.07}$	$4.05^{+2.95+3.73}_{-1.31-2.25}$	$3.92^{+2.90+3.70}_{-1.27-2.21}$	$-0.47^{+0.15+0.07}_{-0.15-0.06}$	$0.58^{+0.07+0.01}_{-0.16-0.03}$	$0.66^{+0.01+0.07}_{-0.04-0.06}$
$\Xi_{cc}^{++} \rightarrow \Sigma_c^{++} \eta_1$	$3.81^{+0.15}_{-0.15}$	$0.09^{+0.11+0.07}_{-0.03-0.05}$	$0.09^{+0.10+0.07}_{-0.03-0.04}$	$0.57^{+0.05+0.13}_{-0.46-0.25}$	$0.82^{+0.01+0.13}_{-0.11-0.11}$	$0.04^{+0.23+0.02}_{-0.25-0.05}$
$\Xi_{cc}^{++} \rightarrow \Sigma_c^{++} \eta_8$	$1.16^{+0.05}_{-0.05}$	$8.22^{+7.84+7.78}_{-3.13-4.74}$	$7.84^{+7.71+7.65}_{-3.04-4.61}$	$-0.50^{+0.04+0.01}_{-0.06-0.01}$	$0.20^{+0.03+0.01}_{-0.01-0.01}$	$-0.84^{+0.05+0.01}_{-0.03-0.01}$
$\Xi_{cc}^{+} \rightarrow \Sigma_c^{+} \pi^0$	$0.47^{+0.01}_{-0.01}$	$0.27^{+0.11+0.29}_{-0.06-0.16}$	$0.28^{+0.12+0.29}_{-0.06-0.16}$	$-0.56^{+0.13+0.05}_{-0.06-0.06}$	$-0.12^{+0.21+0.07}_{-0.18-0.06}$	$0.82^{+0.05+0.02}_{-0.13-0.04}$
$\Xi_{cc}^{+} \rightarrow \Sigma_c^{+} \eta_1$	$0.33^{+0.01}_{-0.01}$	$0.04^{+0.05+0.04}_{-0.01-0.03}$	$0.04^{+0.04+0.04}_{-0.01-0.02}$	$0.98^{+0.06+0.01}_{-0.42-0.06}$	$-0.11^{+0.01+0.04}_{-0.13-0.10}$	$0.14^{+0.39+0.20}_{-0.32-0.11}$
$\Xi_{cc}^{+} \rightarrow \Sigma_c^{+} \eta_8$	$0.10^{+0.00}_{-0.00}$	$0.74^{+0.83+0.70}_{-0.30-0.43}$	$0.70^{+0.81+0.68}_{-0.28-0.41}$	$-0.21^{+0.01+0.02}_{-0.01-0.02}$	$0.40^{+0.15+0.01}_{-0.06-0.01}$	$-0.89^{+0.10+0.01}_{-0.03-0.01}$
$\Xi_{cc}^{+} \rightarrow \Lambda_c^{+} \pi^0$	$1.22^{+0.02}_{-0.02}$	$0.96^{+0.38+1.01}_{-0.24-0.58}$	$0.93^{+0.38+1.00}_{-0.24-0.56}$	$-0.62^{+0.01+0.06}_{-0.02-0.05}$	$-0.69^{+0.01+0.03}_{-0.01-0.04}$	$-0.38^{+0.02+0.04}_{-0.00-0.03}$
$\Xi_{cc}^{+} \rightarrow \Lambda_c^{+} \eta_1$	$0.73^{+0.03}_{-0.03}$	$0.06^{+0.03+0.07}_{-0.02-0.04}$	$0.07^{+0.03+0.07}_{-0.01-0.04}$	$0.07^{+0.24+0.08}_{-0.27-0.14}$	$-0.35^{+0.10+0.07}_{-0.09-0.12}$	$0.93^{+0.06+0.01}_{-0.11-0.05}$
$\Xi_{cc}^{+} \rightarrow \Lambda_c^{+} \eta_8$	$0.26^{+0.01}_{-0.01}$	$0.65^{+0.20+0.68}_{-0.14-0.39}$	$0.69^{+0.20+0.69}_{-0.15-0.40}$	$-0.71^{+0.00+0.03}_{-0.10-0.04}$	$-0.70^{+0.01+0.04}_{-0.00-0.04}$	$-0.01^{+0.07+0.04}_{-0.05-0.06}$
$\Xi_{cc}^{+} \rightarrow \Sigma_c^{+} \pi^{-}$	—	$0.18^{+0.11+0.18}_{-0.05-0.10}$	$0.18^{+0.10+0.18}_{-0.05-0.10}$	$0.73^{+0.10+0.01}_{-0.24-0.00}$	$0.13^{+0.05+0.00}_{-0.09-0.01}$	$0.67^{+0.15+0.00}_{-0.18-0.00}$
$\Xi_{cc}^{+} \rightarrow \Xi_c^{+} K^0$	—	$0.32^{+0.18+0.30}_{-0.10-0.18}$	$0.32^{+0.18+0.30}_{-0.10-0.18}$	$0.96^{+0.01+0.00}_{-0.02-0.01}$	$0.23^{+0.07+0.03}_{-0.09-0.02}$	$0.13^{+0.03+0.00}_{-0.01-0.01}$
$\Xi_{cc}^{+} \rightarrow \Xi_c^{+} K^0$	—	$0.44^{+0.29+0.37}_{-0.13-0.24}$	$0.44^{+0.29+0.37}_{-0.13-0.24}$	$-0.19^{+0.13+0.05}_{-0.15-0.05}$	$-0.90^{+0.03+0.02}_{-0.030.00}$	$-0.40^{+0.02+0.02}_{-0.06-0.02}$
$\Omega_{cc}^{+} \rightarrow \Sigma_c^{+} \bar{K}^0$	—	$2.09^{+1.15+2.14}_{-0.62-1.24}$	$2.09^{+1.15+2.14}_{-0.62-1.24}$	$-0.37^{+0.03+0.03}_{-0.07-0.03}$	$-0.79^{+0.03+0.02}_{-0.02-0.02}$	$-0.49^{+0.12+0.01}_{-0.06-0.01}$
$\Omega_{cc}^{+} \rightarrow \Lambda_c^{+} \bar{K}^0$	—	$3.93^{+2.33+3.95}_{-1.12-2.31}$	$3.93^{+2.33+3.95}_{-1.12-2.31}$	$0.34^{+0.15+0.03}_{-0.20-0.04}$	$0.67^{+0.00+0.06}_{-0.04-0.06}$	$0.67^{+0.04+0.04}_{-0.08-0.05}$
$\Omega_{cc}^{+} \rightarrow \Sigma_c^{+} K^{-}$	—	$1.67^{+0.71+1.77}_{-0.35-1.01}$	$1.67^{+0.71+1.77}_{-0.35-1.01}$	$0.33^{+0.03+0.02}_{-0.24-0.01}$	$0.32^{+0.03+0.02}_{-0.07-0.02}$	$0.89^{+0.04+0.00}_{-0.14-0.00}$
$\Omega_{cc}^{+} \rightarrow \Xi_c^{+} \pi^0$	—	$3.01^{+2.15+3.03}_{-1.01-1.78}$	$3.01^{+2.15+3.03}_{-1.01-1.78}$	$-0.24^{+0.00+0.07}_{-0.02-0.07}$	$-0.76^{+0.04+0.04}_{-0.04-0.05}$	$-0.60^{+0.05+0.04}_{-0.03-0.02}$
$\Omega_{cc}^{+} \rightarrow \Xi_c^{+} \eta_1$	—	$0.48^{+0.55+0.49}_{-0.15-0.28}$	$0.48^{+0.55+0.49}_{-0.15-0.28}$	$0.96^{+0.12+0.00}_{-0.25-0.00}$	$0.24^{+0.03+0.00}_{-0.04-0.01}$	$-0.11^{+0.49+0.02}_{-0.28-0.03}$
$\Omega_{cc}^{+} \rightarrow \Xi_c^{+} \eta_8$	—	$8.95^{+8.17+8.72}_{-3.31-5.22}$	$8.95^{+8.17+8.72}_{-3.31-5.22}$	$-0.62^{+0.05+0.00}_{-0.06-0.00}$	$0.11^{+0.00+0.01}_{-0.01-0.01}$	$-0.78^{+0.06+0.00}_{-0.03-0.00}$
$\Omega_{cc}^{+} \rightarrow \Xi_c^{+} \pi^0$	—	$2.65^{+1.53+2.62}_{-0.82-1.55}$	$2.65^{+1.53+2.62}_{-0.82-1.55}$	$0.28^{+0.01+0.08}_{-0.02-0.07}$	$-0.50^{+0.00+0.04}_{-0.01-0.03}$	$-0.82^{+0.00+0.01}_{-0.00-0.00}$
$\Omega_{cc}^{+} \rightarrow \Xi_c^{+} \eta_1$	—	$0.72^{+0.29+0.78}_{-0.15-0.44}$	$0.72^{+0.29+0.78}_{-0.15-0.44}$	$-0.04^{+0.24+0.00}_{-0.24-0.00}$	$0.12^{+0.05+0.01}_{-0.06-0.01}$	$0.99^{+0.06+0.00}_{-0.07-0.00}$
$\Omega_{cc}^{+} \rightarrow \Xi_c^{+} \eta_8$	—	$2.55^{+1.98+2.42}_{-0.89-1.47}$	$2.55^{+1.98+2.42}_{-0.89-1.47}$	$-0.80^{+0.04+0.00}_{-0.04-0.00}$	$0.15^{+0.00+0.02}_{-0.00-0.01}$	$-0.58^{+0.06+0.01}_{-0.05-0.01}$

Table VIII: Same as Tab. VI but for the long-distance dominated doubly Cabibbo-suppressed modes.

channels	$\mathcal{B}_{SD}[10^{-8}]$	$\mathcal{B}_{LD}[10^{-5}]$	$\mathcal{B}_{tot}[10^{-5}]$	$\alpha$	$\beta$	$\gamma$
$\Xi_{cc}^{++} \rightarrow \Sigma_c^{++} K^0$	$6.32^{+0.25}_{-0.24}$	$1.59^{+1.09+1.41}_{-0.48-0.86}$	$1.68^{+1.12+1.43}_{-0.50-0.89}$	$-0.09^{+0.19+0.08}_{-0.22-0.07}$	$0.85^{+0.00+0.04}_{-0.09-0.05}$	$0.51^{+0.00+0.09}_{-0.04-0.10}$
$\Xi_{cc}^{+} \rightarrow \Sigma_c^{+} K^0$	$0.64^{+0.03}_{-0.02}$	$0.10^{+0.04+0.08}_{-0.02-0.05}$	$0.09^{+0.03+0.08}_{-0.01-0.05}$	$0.05^{+0.19+0.04}_{-0.15-0.02}$	$-0.50^{+0.40+0.03}_{-0.21-0.03}$	$0.87^{+0.00+0.01}_{-0.28-0.02}$
$\Xi_{cc}^{+} \rightarrow \Lambda_c^{+} K^0$	$1.76^{+0.07}_{-0.07}$	$0.49^{+0.30+0.53}_{-0.15-0.30}$	$0.50^{+0.30+0.53}_{-0.15-0.30}$	$-0.55^{+0.01+0.05}_{-0.03-0.05}$	$-0.66^{+0.01+0.02}_{-0.00-0.01}$	$-0.51^{+0.04+0.03}_{-0.02-0.04}$
$\Omega_{cc}^{+} \rightarrow \Sigma_c^{+} \pi^0$	—	$0.88^{+0.54+0.90}_{-0.27-0.52}$	$0.88^{+0.54+0.90}_{-0.27-0.52}$	$0.93^{+0.02+0.00}_{-0.09-0.00}$	$0.26^{+0.01+0.00}_{-0.03-0.00}$	$0.27^{+0.16+0.01}_{-0.12-0.01}$
$\Omega_{cc}^{+} \rightarrow \Sigma_c^{+} \eta_1$	—	$0.15^{+0.05+0.09}_{-0.04-0.06}$	$0.15^{+0.05+0.09}_{-0.04-0.06}$	$0.96^{+0.07+0.00}_{-0.25-0.00}$	$0.27^{+0.03+0.01}_{-0.05-0.01}$	$-0.04^{+0.45+0.01}_{-0.25-0.02}$
$\Omega_{cc}^{+} \rightarrow \Sigma_c^{+} \eta_8$	—	$0.10^{+0.12+0.09}_{-0.04-0.06}$	$0.10^{+0.12+0.09}_{-0.04-0.06}$	$-0.77^{+0.12+0.02}_{-0.02-0.02}$	$0.62^{+0.00+0.03}_{-0.07-0.03}$	$-0.16^{+0.38+0.02}_{-0.16-0.01}$
$\Omega_{cc}^{+} \rightarrow \Lambda_c^{+} \pi^0$	—	$0.43^{+0.23+0.40}_{-0.10-0.25}$	$0.43^{+0.23+0.40}_{-0.10-0.25}$	$0.17^{+0.25+0.07}_{-0.29-0.08}$	$-0.85^{+0.07+0.03}_{-0.03-0.03}$	$0.50^{+0.02+0.02}_{-0.14-0.03}$
$\Omega_{cc}^{+} \rightarrow \Lambda_c^{+} \eta_1$	—	$0.17^{+0.09+0.19}_{-0.04-0.11}$	$0.17^{+0.09+0.19}_{-0.04-0.11}$	$-0.05^{+0.27+0.00}_{-0.28-0.00}$	$0.06^{+0.07+0.01}_{-0.09-0.01}$	$1.00^{+0.08+0.00}_{-0.11-0.00}$
$\Omega_{cc}^{+} \rightarrow \Lambda_c^{+} \eta_8$	—	$1.21^{+0.62+1.02}_{-0.37-0.67}$	$1.21^{+0.62+1.02}_{-0.37-0.67}$	$-0.41^{+0.07+0.03}_{-0.05-0.02}$	$-0.90^{+0.04+0.02}_{-0.03-0.02}$	$-0.15^{+0.03+0.05}_{-0.05-0.05}$
$\Omega_{cc}^{+} \rightarrow \Sigma_c^0 \pi^{+}$	—	$1.34^{+0.79+1.33}_{-0.43-0.79}$	$1.34^{+0.79+1.33}_{-0.43-0.79}$	$0.99^{+0.01+0.00}_{-0.01-0.00}$	$0.01^{+0.00+0.00}_{-0.01-0.00}$	$-0.16^{+0.06+0.01}_{-0.05-0.00}$
$\Omega_{cc}^{+} \rightarrow \Sigma_c^{+} \pi^{-}$	—	$0.69^{+0.37+0.74}_{-0.17-0.42}$	$0.69^{+0.37+0.74}_{-0.17-0.42}$	$0.49^{+0.15+0.00}_{-0.24-0.00}$	$0.26^{+0.04+0.01}_{-0.08-0.01}$	$0.83^{+0.08+0.00}_{-0.15-0.00}$
$\Omega_{cc}^{+} \rightarrow \Xi_c^{+} K^0$	$2.31^{+0.09}_{-0.09}$	$1.38^{+0.96+1.44}_{-0.41-0.82}$	$1.32^{+0.94+1.42}_{-0.39-0.80}$	$0.25^{+0.16+0.05}_{-0.25-0.05}$	$0.67^{+0.02+0.04}_{-0.14-0.05}$	$0.70^{+0.10+0.03}_{-0.14-0.02}$
$\Omega_{cc}^{+} \rightarrow \Xi_c^{+} K^0$	$4.95^{+0.19}_{-0.19}$	$1.96^{+0.52+1.93}_{-0.41-1.14}$	$2.10^{+0.54+1.98}_{-0.43-1.19}$	$-0.32^{+0.07+0.04}_{-0.06-0.04}$	$-0.93^{+0.04+0.01}_{-0.030.00}$	$-0.19^{+0.09+0.09}_{-0.05-0.11}$

distance contribution-dominated processes, the numerical results are given in Tabs. VI-VIII. As do in Tab. III, we also consider two uncertainty sources for branching ratio and three asymmetry parameters. The first source of uncertainty stems from decay constants and strong couplings. The second one is from the parameter  $\eta = 0.9 \pm 0.2$ . Also for the branching ratio  $\mathcal{B}_{SD}$  not involving input parameters: strong couplings and  $\eta$ , there is only uncertainty from decay constants of light mesons. Then we can found that the uncertainty from decay constants is also much smaller than that from the strong coupling constants and  $\eta$ . And compared with the branching ratios, the decay asymmetry parameters are less affected by the two parameters. Therefore, the decay asymmetry parameter has a weaker dependence on the input parameter: strong coupling constants and  $\eta$ , compared to the branching ratios. In Tab. IV, we conduct a comparative analysis with other

theoretical works. In contrast to other studies, our work incorporates both real and imaginary contributions within the amplitudes, which will provide the strong phases naturally to understand the  $CP$  asymmetries and decay asymmetries. In Table IX, we present a comparison of our findings with both the experimental data and results from existing theoretical literature. The findings indicate that the diverse predictions do not entirely align with each other.

It can be found that the factorizable contributions of diagram amplitude  $T$  are dominant relative to the long-distance contributions of  $C'$  and  $E_2$ , as shown in Tab. V. On the other hand, from Tabs. VI-VIII, the long-distance contributions are dominated, since the short-distance amplitude  $C_{SD}$  is deeply suppressed by the effective Wilson coefficient  $a_2(m_c) = -0.017 < a_1(m_c) = 1.07$  at the charm mass scale. In this work,  $a_1(m_c) = 1.07$  has been used at the calculation of the weak decay vertex in the triangle diagram. Currently, there is no absolute branching fraction of  $\mathcal{B}_{cc} \rightarrow \mathcal{B}_c P$  been directly measured, but the branching fraction of  $\Xi_{cc}^{++} \rightarrow \Xi_c^+ \pi^+$  relative to  $\Xi_{cc}^{++} \rightarrow \Lambda_c^+ K^- \pi^+ \pi^+$  was measured to be [7]

$$\frac{\mathcal{B}(\Xi_{cc}^{++} \rightarrow \Xi_c^+ \pi^+) \times \mathcal{B}(\Xi_c^+ \rightarrow p K^- \pi^+)}{\mathcal{B}(\Xi_{cc}^{++} \rightarrow \Lambda_c^+ K^- \pi^+ \pi^+) \times \mathcal{B}(\Lambda_c^+ \rightarrow p K^- \pi^+)} = 0.035 \pm 0.009(\text{stat.}) \pm 0.003(\text{syst.}). \quad (59)$$

As pointed out in Ref. [139], using the measurements  $\mathcal{B}(\Lambda_c^+ \rightarrow p K^- \pi^+) = (6.24 \pm 0.28)\%$  and  $\mathcal{B}(\Xi_c^+ \rightarrow p K^- \pi^+) = (0.62 \pm 0.30)\%$  [1], and combining the theoretical predictions  $\mathcal{B}(\Xi_{cc}^{++} \rightarrow \Lambda_c^+ K^- \pi^+ \pi^+) \approx \frac{2}{3} \mathcal{B}(\Xi_{cc}^{++} \rightarrow \Sigma_c^{++} \bar{K}^{*0})$  [72] and  $\mathcal{B}(\Xi_{cc}^{++} \rightarrow \Sigma_c^{++} \bar{K}^{*0}) = 5.61\%$  [93], the branching fraction of  $\Xi_{cc}^{++} \rightarrow \Xi_c^+ \pi^+$  can be obtained

$$\mathcal{B}(\Xi_{cc}^{++} \rightarrow \Xi_c^+ \pi^+)_{\text{expt}} \approx (1.33 \pm 0.74)\%. \quad (60)$$

Nevertheless, the calculated branching fraction  $\mathcal{B}(\Xi_{cc}^{++} \rightarrow \Xi_c^+ \pi^+)_{\text{our}} = (3.98_{-0.27}^{+0.30+0.65})\%$  slightly larger than the expectation given by the above Eq. (60).

The decay asymmetry parameters, defined as ratios of the amplitudes ( $\mathcal{S}$ ,  $\mathcal{P}$ ), ( $A$ ,  $B$ ) or helicity amplitudes  $H_{\pm 1/2}$  in different form as given by Eqs. ((37)-(39)), exhibit less sensitivity to model and input parameters. The sensitivity to the  $\eta$  parameter is diminished for all three asymmetry parameters in comparison to branching ratios, regardless of whether the process is predominantly influenced by short-distance or long-distance contributions.

The dependence of the asymmetry parameters on the  $\eta$  parameter is shown in Fig.5. We can see that these parameters have a small dependence on the parameter  $\eta$ . The theoretical predictions for the decay asymmetry parameter  $\alpha$  for  $\Xi_{cc}^{++} \rightarrow \Xi_c^+ \pi^+$  given in this paper are consistent with those in Refs. [70, 72, 73, 75, 89, 138–140], which indicates that the calculations of relative magnitudes and phases of helicity amplitudes are reasonable.

## E. $CP$ violations

In this section, we provide our numerical calculation for direct charge parity ( $CP$ ) violation in the decays of doubly charmed baryons. Using the parameter  $\eta = 0.9 \pm 0.2$ , we give our predictions for  $CP$  violations in singly CKM suppressed decays in Tabs. X-XI.

In this study, we exclusively examine the  $CP$  violation in singly Cabibbo suppressed processes, which encompasses two CKM matrix elements:  $V_{cd}V_{ud}^*$  and  $V_{cs}V_{us}^*$ . Within the rescattering mechanism, these elements contribute to an identical process, resulting in a non-zero weak phase difference. Furthermore, long-distance final state interaction effect offer significant phase information for the decay process. Consequently, our theoretical framework is capable of directly determining the magnitude of  $CP$  violation and currently serves as the sole method to measure  $CP$  violation in

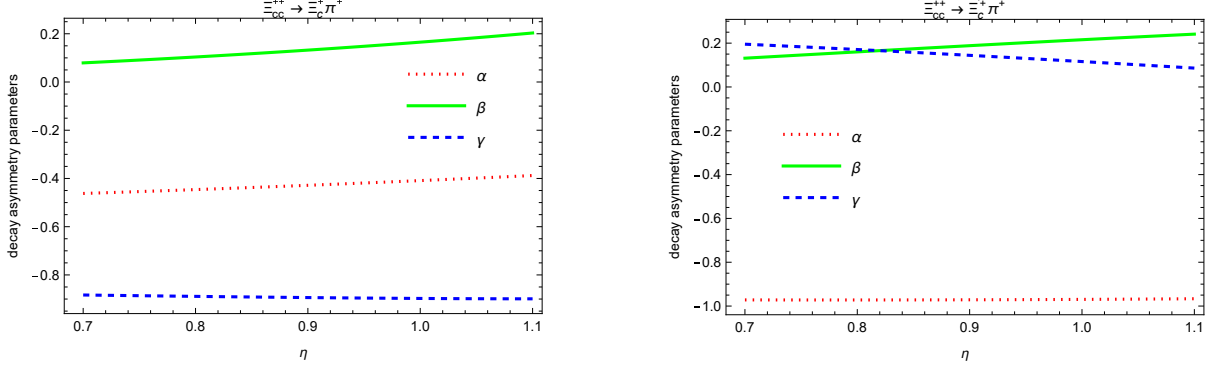


Figure 5: The dependence of decay asymmetry parameters on  $\eta$  for decays (a):  $\Xi_{cc}^{++} \rightarrow \Xi_c^{+} \pi^{+}$  and (b):  $\Xi_{cc}^{++} \rightarrow \Xi_c^{' +} \pi^{+}$  with  $\eta \sim [0.7, 1.1]$ .

Table IX: Comparison of the branching fractions, the decay asymmetry parameter  $\alpha$  and the ratio of branching fractions  $R_{\mathcal{B}'/\mathcal{B}}$  in various approaches. In this table, we list the experimental data from the LHCb collaboration [9] and the theoretical prediction from the pole approximation (PA) in tandem with the SU(3)F symmetry [138], the non-relativistic quark model (NRQM) [139], the pole model (PM) with current algebra (CA) [72], the Ab initio three-loop calculation (AITLC) [73], the heavy quark effective theory (HQET) with pole model (PM) [70], light-cone sum rules (LCSR) with HQET [75], the light front quark model (LFQM) with mixing mechanism [89], the rescattering mechanism (RM) with Cutkosky cutting rule (CCR) [76] and the bag model [140].

	$\mathcal{B}(\Xi_c^{+} \pi^{+})[\%]$	$\mathcal{B}(\Xi_c^{' +} \pi^{+})[\%]$	$\alpha(\Xi_c^{+} \pi^{+})$	$\alpha(\Xi_c^{' +} \pi^{+})$	$R_{\mathcal{B}'/\mathcal{B}}$
This work	$3.97^{+0.63}_{-0.64}$	$5.38^{+0.53}_{-0.42}$	$-0.43^{+0.03}_{-0.04}$	$-0.97^{+0.00}_{-0.00}$	$1.35^{+0.81}_{-0.61}$
PA+SU(3) [138]	$0.99 \pm 0.21$	$1.18 \pm 0.18$	$-0.19 \pm 0.07$	$-0.96 \pm 0.00$	$1.19 \pm 0.09$
NRQM [139]	1.83	2.86	-0.78	-0.89	1.56
PM+CA [72]	0.69	4.65	-0.41	-0.84	6.74
AITLC [73]	$0.71 \pm 0.11$	$3.39 \pm 0.51$	$-0.57 \pm 0.09$	$-0.93 \pm 0.14$	$4.33 \pm 0.65$
HQET+PM [70]	9.30	7.5	-0.99	-0.78	-0.81
LCSR+HQET [75]	$6.22 \pm 1.94$	$8.85 \pm 0.62$	+0.99	-0.64	$1.42 \pm 0.78$
LFQM+Mixing [89]	$2.14 \pm 0.18$	$3.02 \pm 0.1$	$-0.99 \pm 0.01$	$-0.09 \pm 0.07$	$1.41 \pm 0.20$
RM+CCR [76]	$8.48^{+2.27}_{-1.37}$	$4.72^{+0.02}_{-0.00}$	-	-	$0.56^{+0.10}_{-0.12}$
Bag Model [140]	2.24	3.25	-0.93	-0.63	1.45
LHCb [9]	-	-	-	-	$1.41 \pm 0.17 \pm 0.10$

charmed baryon decays. The decay amplitude, denoted by  $\mathcal{A} = \lambda_d \mathcal{A}_d + \lambda_s \mathcal{A}_s$ , where  $\lambda_q = V_{cq} V_{uq}^*$  and  $q = d, s$ , aids in the expression of  $CP$  violation,

$$A_{CP}^{\text{dir}} \approx -2 \frac{\text{Im}(\lambda_d^* \lambda_s)}{|\lambda_d|^2} \frac{\text{Im}(\mathcal{A}_d^* \mathcal{A}_s)}{|\mathcal{A}_d - \mathcal{A}_s|^2}. \quad (61)$$

From Eq. (41), we can see that the direct  $CP$  violation is proportional to  $\sin \Delta\phi$ , where  $\Delta\phi$  is the weak phase difference for tree-level operators in charmed baryon decays, which is about

Table X: The  $CP$  violation of the short-distance dynamics dominated modes. The first uncertainty comes from input parameters: decay constants and strong couplings, which have been listed in Tab. II. The second uncertainty is due to the variation of the phenomenological parameter  $\eta = 0.9 \pm 0.2$ .

channels	$\mathcal{A}_{CP}^{dir}[10^{-3}]$	$\alpha_{CP}[10^{-3}]$	$\beta_{CP}[10^{-3}]$	$\gamma_{CP}[10^{-3}]$
$\Xi_{cc}^{++} \rightarrow \Sigma_c^+ \pi^+$	$0.13^{+0.05+0.11}_{-0.02-0.07}$	$0.12^{+0.08+0.15}_{-0.04-0.07}$	$-0.35^{+0.04+0.06}_{-0.02-0.05}$	$-36.70^{+18.40+37.10}_{-18.20-36.20}$
$\Xi_{cc}^{++} \rightarrow \Lambda_c^+ \pi^+$	$-0.52^{+0.07+0.22}_{-0.02-0.18}$	$-0.26^{+0.03+0.09}_{-0.03-0.14}$	$-0.53^{+0.02+0.03}_{-0.03-0.02}$	$0.04^{+0.00+0.00}_{-0.00-0.01}$
$\Xi_{cc}^{++} \rightarrow \Xi_c'^+ K^+$	$-0.09^{+0.01+0.03}_{-0.01-0.03}$	$-0.02^{+0.00+0.01}_{-0.01-0.01}$	$-2.11^{+0.35+0.26}_{-0.72-0.37}$	$0.44^{+0.04+0.17}_{-0.06-0.15}$
$\Xi_{cc}^{++} \rightarrow \Xi_c^+ K^+$	$0.10^{+0.04+0.00}_{-0.15-0.13}$	$0.21^{+0.04+0.16}_{-0.04-0.10}$	$-1.62^{+0.20+0.18}_{-0.12-0.15}$	$-0.01^{+0.01+0.01}_{-0.00-0.00}$
$\Xi_{cc}^+ \rightarrow \Sigma_c^0 \pi^+$	$0.06^{+0.05+0.01}_{-0.02-0.03}$	$0.13^{+0.17+0.23}_{-0.05-0.08}$	$-0.44^{+0.04+0.16}_{-0.03-0.02}$	$-0.53^{+0.12+0.21}_{-0.15-0.23}$
$\Xi_{cc}^+ \rightarrow \Xi_c'^0 K^+$	$0.10^{+0.03+0.04}_{-0.02-0.04}$	$0.11^{+0.14+0.22}_{-0.04-0.08}$	$-0.01^{+0.01+0.05}_{-0.00-0.03}$	$-0.13^{+0.01+0.02}_{-0.00-0.01}$
$\Xi_{cc}^+ \rightarrow \Xi_c^0 K^+$	$-0.04^{+0.01+0.01}_{-0.01-0.01}$	$-0.06^{+0.01+0.02}_{-0.01-0.03}$	$18.40^{+6.08+14.50}_{-17.20-25.30}$	$0.03^{+0.01+0.02}_{-0.01-0.01}$
$\Omega_{cc}^+ \rightarrow \Xi_c^0 \pi^+$	$-0.18^{+0.08+0.05}_{-0.01-0.00}$	$-0.11^{+0.01+0.02}_{-0.01-0.00}$	$-2.86^{+0.55+0.67}_{-2.48-1.41}$	$0.02^{+0.00+0.00}_{-0.01-0.00}$
$\Omega_{cc}^+ \rightarrow \Xi_c'^0 \pi^+$	$-0.22^{+0.05+0.12}_{-0.08-0.26}$	$0.36^{+0.48+0.89}_{-0.12-0.23}$	$-0.58^{+0.04+0.05}_{-0.01-0.02}$	$2.43^{+0.81+1.14}_{-2.84-8.87}$
$\Omega_{cc}^+ \rightarrow \Omega_c^0 K^+$	$-0.08^{+0.02+0.02}_{-0.02-0.02}$	$-0.01^{+0.00+0.00}_{-0.00-0.00}$	$-1.69^{+0.18+0.22}_{-0.22-0.33}$	$0.71^{+0.13+0.37}_{-0.12-0.28}$

$6 \times 10^{-4}$  ( $\Delta\phi = \arctan[\text{Im}(V_{cd})/\text{Re}(V_{cd})]$ ). Therefore, the expected size of  $CP$  violation in doubly charmed baryon decays should be at this level, which is consistent with the theoretical expectations in Table X. For example, the decay channels  $\Xi_{cc}^{++} \rightarrow \Xi_c^+ K^+$  and  $\Xi_{cc}^{++} \rightarrow \Xi_c'^+ K^+$  are characterized by  $CP$  violation induced by tree-level operators mediated by CKM matrix elements  $V_{cd}V_{ud}$  and  $V_{cs}V_{us}$ . These elements contribute to the amplitudes in the triangle diagram, as depicted in Fig. 3. This influences the decay amplitude and induces a weak phase difference, denoted as  $\Delta\phi$ . The understanding and prediction of  $CP$  violation in charmed baryon decays heavily relies on this weak phase difference, in conjunction with the strong phases derived from the triangle integrals. To validate the reliability of the theoretical method for predicting the magnitude of  $CP$  violation, it is crucial to investigate the relationship between  $CP$  violation parameters and model parameters, such as  $\eta$ . For the decays  $\Xi_{cc}^{++} \rightarrow \Xi_c^+ K^+$  and  $\Xi_{cc}^{++} \rightarrow \Xi_c'^+ K^+$ , the relationship between their  $CP$  violation parameters and the  $\eta$  parameter is depicted in Fig. 6. This research offers a quantitative evaluation of the susceptibility of  $CP$  violation effects to alterations in the model parameter  $\eta$ . The study indicates that both the direct  $CP$  violation and the asymmetry parameter-induced  $CP$  violation exhibit minimal sensitivity to model parameters. The results show that the predictions for  $CP$  violation observables are independent of theoretical input parameters or model assumptions. This is important to check the robustness of the theoretical framework and to make sure that the predicted size of  $CP$  violation indeed corresponds to the physical effects driving these decays.

#### IV. SUMMARY

In this work, we introduced the whole theoretical framework of the rescattering mechanism by investigating the two-body nonleptonic weak decays  $\mathcal{B}_{cc} \rightarrow \mathcal{B}_c P$ , where  $\mathcal{B}_{cc} = (\Xi_{cc}^{++}, \Xi_{cc}^+, \Omega_{cc}^+)$  are the doubly charmed baryons,  $\mathcal{B}_c = (\mathcal{B}_3, \mathcal{B}_6)$  are the singly charmed baryons and  $P = (\pi, K, \eta_{1,8})$  are the light pseudoscalar mesons. It was interpreted in detail for the physical foundation of the rescattering mechanism at the hadron level. On the other hand, as a self-consistent test to the rescattering mechanism, the relations of topological diagrams and flavor  $SU(3)$  symmetry have

Table XI: CP violation of the nonleptonic weak decay of doubly charmed baryons  $\mathcal{B}_{cc} \rightarrow \mathcal{B}_c P$  which is the long-distance dominated singly Cabibbo-suppressed. The first uncertainty comes from input parameters: decay constants and strong couplings, which have been listed in Tab. II. The second uncertainty is due to the variation of the phenomenological parameter  $\eta = 0.9 \pm 0.2$ .

channels	$\mathcal{A}_{CP}^{dir}[10^{-4}]$	$\alpha_{CP}[10^{-4}]$	$\beta_{CP}[10^{-4}]$	$\gamma_{CP}[10^{-4}]$
$\Xi_{cc}^{++} \rightarrow \Sigma_c^{++} \pi^0$	$2.03^{+0.03+0.20}_{-0.06-0.13}$	$-0.48^{+0.06+0.30}_{-0.53-0.21}$	$-2.19^{+0.25+0.16}_{-1.41-0.32}$	$1.93^{+0.02+0.19}_{-0.13-0.30}$
$\Xi_{cc}^{++} \rightarrow \Sigma_c^{++} \eta_1$	$-32.30^{+0.89+2.21}_{-0.92-1.31}$	$-20.30^{+25.50+7.51}_{-5.44-25.90}$	$9.79^{+1.14+2.53}_{-1.61-4.62}$	$-57.20^{+28.10+9.86}_{-13.30-51.60}$
$\Xi_{cc}^{++} \rightarrow \Sigma_c^{++} \eta_8$	$2.31^{+0.62+0.04}_{-0.26-0.04}$	$0.20^{+0.20+0.02}_{-0.14-0.04}$	$6.60^{+0.00+0.40}_{-0.34-0.40}$	$-0.42^{+0.11+0.02}_{-0.34-0.02}$
$\Xi_{cc}^{+} \rightarrow \Sigma_c^{+} \pi^0$	$2.61^{+0.40+0.14}_{-0.31-0.21}$	$-3.03^{+0.71+0.16}_{-2.55-0.02}$	$29.20^{+13.00+34.40}_{-23.50-9.20}$	$0.77^{+0.92+0.88}_{-0.31-0.61}$
$\Xi_{cc}^{+} \rightarrow \Sigma_c^{+} \eta_1$	$-11.50^{+0.60+0.07}_{-0.57-0.05}$	$-0.35^{+13.80+0.08}_{-0.58-0.61}$	$69.90^{+11.40+9.96}_{-22.00-14.40}$	$-22.70^{+12.80+9.94}_{-8.97-64.30}$
$\Xi_{cc}^{+} \rightarrow \Sigma_c^{+} \eta_8$	$7.28^{+0.26+0.43}_{-0.53-0.40}$	$-0.29^{+1.78+0.04}_{-0.52-0.11}$	$4.57^{+0.27+0.11}_{-0.85-0.12}$	$-0.90^{+0.25+0.04}_{-1.20-0.05}$
$\Xi_{cc}^{+} \rightarrow \Lambda_c^{+} \pi^0$	$1.49^{+0.02+0.34}_{-0.08-0.23}$	$-5.66^{+0.28+0.69}_{-0.04-1.12}$	$5.28^{+0.49+0.33}_{-0.33-0.47}$	$-2.15^{+0.31+0.17}_{-0.42-0.33}$
$\Xi_{cc}^{+} \rightarrow \Lambda_c^{+} \eta_1$	$-6.57^{+0.20+0.33}_{-0.25-0.49}$	$68.40^{+31.30+39.90}_{-39.30-15.10}$	$2.36^{+0.97+3.57}_{-0.52-3.52}$	$-0.75^{+1.32+0.11}_{-1.10-0.42}$
$\Xi_{cc}^{+} \rightarrow \Lambda_c^{+} \eta_8$	$0.93^{+0.03+0.01}_{-0.06-0.03}$	$-2.79^{+0.44+0.24}_{-0.41-0.30}$	$2.87^{+0.55+0.27}_{-0.36-0.27}$	$-51.40^{+26.70+6.46}_{-22.70-4.47}$
$\Xi_{cc}^{+} \rightarrow \Sigma_c^{+} \pi^{-}$	$-0.62^{+0.26+0.02}_{-0.35-0.02}$	$-1.15^{+0.26+0.03}_{-0.16-0.01}$	$17.10^{+7.15+1.45}_{-4.20-0.77}$	$0.72^{+1.41+0.07}_{-0.24-0.05}$
$\Xi_{cc}^{+} \rightarrow \Xi_c^{+} K^0$	$-2.27^{+0.36+0.10}_{-0.62-0.09}$	$-0.34^{+0.24+0.04}_{-0.09-0.05}$	$6.83^{+4.62+0.87}_{-3.22-0.79}$	$-2.78^{+4.79+0.25}_{-2.99-0.28}$
$\Xi_{cc}^{+} \rightarrow \Xi_c^{+} K^0$	$-8.58^{+0.32+0.66}_{-0.58-0.67}$	$-13.20^{+1.84+1.96}_{-1.46-2.81}$	$-2.98^{+1.68+0.50}_{-0.72-0.48}$	$18.10^{+0.68+0.66}_{-3.24-0.76}$
$\Omega_{cc}^{+} \rightarrow \Sigma_c^{+} \bar{K}^0$	$0.87^{+0.37+0.01}_{-0.41-0.01}$	$3.48^{+1.38+0.40}_{-1.57-0.32}$	$-0.01^{+0.17+0.06}_{-0.02-0.06}$	$-1.96^{+0.08+0.07}_{-0.02-0.09}$
$\Omega_{cc}^{+} \rightarrow \Lambda_c^{+} \bar{K}^0$	$0.48^{+0.02+0.02}_{-0.06-0.02}$	$0.67^{+0.73+0.06}_{-0.40-0.04}$	$-0.49^{+0.89+0.06}_{-0.81-0.06}$	$0.32^{+0.71+0.11}_{-0.41-0.09}$
$\Omega_{cc}^{+} \rightarrow \Sigma_c^{+} K^{-}$	$-0.34^{+0.12+0.01}_{-0.10-0.01}$	$-3.78^{+6.13+0.35}_{-1.43-0.48}$	$1.14^{+2.65+0.14}_{-1.10-0.18}$	$0.36^{+0.60+0.04}_{-0.39-0.03}$
$\Omega_{cc}^{+} \rightarrow \Xi_c^{+} \pi^0$	$6.79^{+0.37+0.05}_{-0.30-0.26}$	$-1.58^{+0.19+0.21}_{-0.03-0.45}$	$2.35^{+0.10+0.33}_{-0.12-0.36}$	$-3.57^{+0.54+0.29}_{-1.08-0.46}$
$\Omega_{cc}^{+} \rightarrow \Xi_c^{+} \eta_1$	$-3.66^{+0.45+0.20}_{-0.60-0.22}$	$-0.16^{+0.01+0.04}_{-0.98-0.03}$	$3.47^{+1.81+0.50}_{-1.84-0.53}$	$-4.24^{+2.32+0.72}_{-2.23-1.02}$
$\Omega_{cc}^{+} \rightarrow \Xi_c^{+} \eta_8$	$-0.19^{+0.03+0.02}_{-0.08-0.02}$	$-0.37^{+0.04+0.02}_{-0.03-0.02}$	$5.32^{+0.21+0.71}_{-0.19-0.61}$	$0.13^{+0.04+0.00}_{-0.02-0.00}$
$\Omega_{cc}^{+} \rightarrow \Xi_c^{+} \pi^0$	$5.32^{+1.00+0.01}_{-0.58-0.17}$	$-2.03^{+0.14+0.17}_{-0.08-0.26}$	$2.34^{+0.41+0.62}_{-0.39-0.42}$	$-0.64^{+0.12+0.04}_{-0.21-0.02}$
$\Omega_{cc}^{+} \rightarrow \Xi_c^{+} \eta_1$	$-1.49^{+0.00+0.08}_{-0.00-0.09}$	$-5.81^{+2.76+0.28}_{-2.39-0.37}$	$-1.07^{+0.24+0.27}_{-0.86-0.30}$	$0.03^{+0.17+0.01}_{-0.00-0.01}$
$\Omega_{cc}^{+} \rightarrow \Xi_c^{+} \eta_8$	$-0.33^{+0.10+0.00}_{-0.19-0.00}$	$-0.25^{+0.03+0.01}_{-0.02-0.01}$	$-2.95^{+2.09+0.35}_{-0.89-0.40}$	$0.68^{+0.11+0.02}_{-0.11-0.02}$

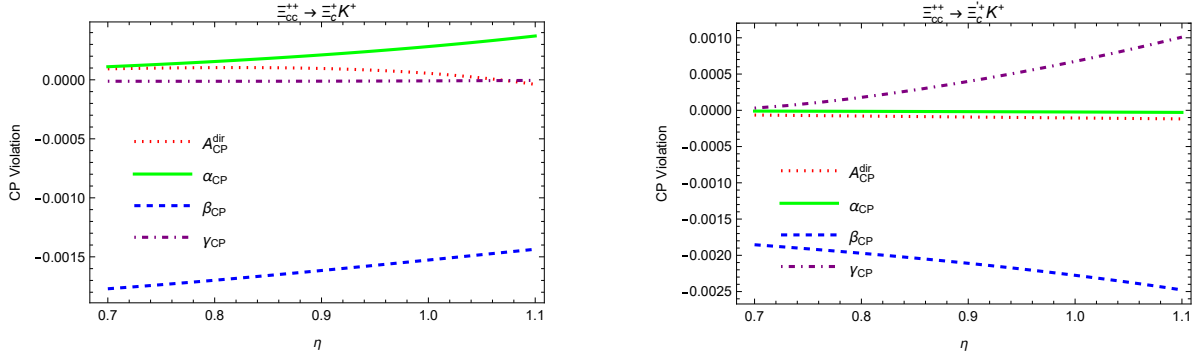


Figure 6: The dependence of the CP violation on  $\eta$  for decays (a):  $\Xi_{cc}^{++} \rightarrow \Xi_c^{+} K^{+}$  and (b):  $\Xi_{cc}^{++} \rightarrow \Xi_c^{+} K^{+}$  with  $\eta \sim [0.7, 1.1]$ .

been discussed. The main points are the following:

- (1) We present a topological analysis of the two-body nonleptonic weak decays  $\mathcal{B}_{cc} \rightarrow \mathcal{B}_c P$  and give the amplitudes of each decay mode within the rescattering mechanism at the hadron level.
- (2) Using the experiment data [9]

$$\mathcal{RB} = \frac{\mathcal{B}(\Xi_{cc}^{++} \rightarrow \Xi_c^{+} \pi^{+})}{\mathcal{B}(\Xi_{cc}^{++} \rightarrow \Xi_c^{+} \pi^{+})} = 1.41 \pm 0.17 \pm 0.10, \quad (62)$$

this parameter can be determined as  $\eta = 0.9 \pm 0.2$ .

- (3) After the calculation of the amplitude of each decay mode, we conduct a comparative analysis with other theoretical works. In contrast to other studies, our work include both real and imaginary contributions of the amplitudes. As illustrated in Tab. III, the uncertainty from decay constants is much smaller than that from the strong coupling constants and  $\eta$ . This is because almost of these decay constants have been precisely determined using experimental data [1]. Nevertheless, there is a significant lack of experimental data available for determining the parameters: strong couplings and  $\eta$ .
- (4) Also, we obtain the same counting rules as the analysis in SCET for the topological amplitudes in charm decays, that is  $\frac{|C|}{|T|} \sim \frac{|C'|}{|C|} \sim \frac{|E_1|}{|C|} \sim \frac{|E_2|}{|C|} \sim O(\frac{\Lambda_{\text{QCD}}^b}{m_c}) \sim O(1)$ , which will be significant guidance for the following studies to charmed baryon decays. After the calculation of the decay width of each decay mode, we find that large  $SU(3)$  symmetry breaking effects exist in our work. It requires more studies on the  $SU(3)$  breaking effects of the doubly charmed baryon decays in the future.
- (5) With  $\eta = 0.9 \pm 0.2$ , we theoretically predict the branching ratios, decay asymmetry parameters and CP violation of all considered  $\mathcal{B}_{cc} \rightarrow \mathcal{B}_c P$  and some discussions on the dependence of the parameter  $\eta$ . As depicted in Fig.4(a), the branching fraction  $\mathcal{B}(\Xi_{cc}^{++} \rightarrow \Xi_c^+ \pi^+)_{\text{our}} = (3.98_{-0.27-0.63}^{+0.30+0.65})\%$  is slightly larger than the expectation in Ref. [139]. The numerical results of the branching ratios exhibited the same conclusion with the charm meson decays: the non-factorizable long-distance contributions play an important role in doubly charmed baryon decays.
- (6) From Tabs. V-VIII, we can found that the decay asymmetry parameters are less affected by the two parameters: strong coupling constants and  $\eta$ , compared with the branching ratios. Therefore, the decay asymmetry parameter has a weaker dependence on the input parameter, compared to the branching ratios.
- (7) The study indicates that both the direct CP violation and the asymmetry parameter-induced CP violation exhibit minimal sensitivity to model parameters.

## Acknowledgments

The authors are very grateful to Jia-Jie Han and Hua-Yu Jiang for useful discussions. This work is supported in part by the National Natural Science Foundation of China under Grant No. 12005294 and No. 12335003, the youth Foundation JN210003, of China University of mining and technology, the opening Issues Foundation No.12247101, of Lanzhou Center for Theoretical Physics, and by the Fundamental Research Funds for the Central Universities under No. lzujbky-2024-oy02.

**Data Availability Statement:** No Data associated in the manuscript.

## Appendix A: Amplitudes of each mode

The expressions of amplitudes for all the forty-seven  $\mathcal{B}_{cc} \rightarrow \mathcal{B}_c P$  decays considered in this paper are collected in this Appendix. Twenty amplitudes for the short-distance dominated modes are



given as follows.

$$\mathcal{A}(\Omega_{cc}^+ \rightarrow \Omega_c^0 \pi^+) = \mathcal{T}_{SD}(\Omega_{cc}^+ \rightarrow \Omega_c^0 \pi^+), \quad (\text{A15})$$

$$\begin{aligned} \mathcal{A}(\Omega_{cc}^+ \rightarrow \Xi_c^0 \pi^+) &= \mathcal{T}_{SD}(\Omega_{cc}^+ \rightarrow \Xi_c^0 \pi^+) + \mathcal{M}(\pi^+, \Xi_c^{(\prime)0}; \rho^0) + \mathcal{M}(\rho^+, \Xi_c^{(\prime)0}; \pi^0) + \mathcal{M}(K^+, \Omega_c^0; K^{*0}) \\ &\quad + \mathcal{M}(K^{*+}, \Omega_c^0; K^0) + \mathcal{M}(\rho^+, \Xi_c^{(\prime)0}; \rho^0) + \mathcal{M}(K^{*+}, \Omega_c^0; K^{*0}), \end{aligned} \quad (\text{A16})$$

$$\begin{aligned} \mathcal{A}(\Omega_{cc}^+ \rightarrow \Xi_c^{\prime 0} \pi^+) &= \mathcal{T}_{SD}(\Omega_{cc}^+ \rightarrow \Xi_c^{\prime 0} \pi^+) + \mathcal{M}(\pi^+, \Xi_c^{(\prime)0}; \rho^0) + \mathcal{M}(\rho^+, \Xi_c^{(\prime)0}; \pi^0) + \mathcal{M}(K^+, \Omega_c^0; K^{*0}) \\ &\quad + \mathcal{M}(K^{*+}, \Omega_c^0; K^0) + \mathcal{M}(\rho^+, \Xi_c^{(\prime)0}; \rho^0) + \mathcal{M}(K^{*+}, \Omega_c^0; K^{*0}), \end{aligned} \quad (\text{A17})$$

$$\begin{aligned} \mathcal{A}(\Omega_{cc}^+ \rightarrow \Omega_c^0 K^+) &= \mathcal{T}_{SD}(\Omega_{cc}^+ \rightarrow \Omega_c^0 K^+) + \mathcal{M}(\pi^+, \Xi_c^{(\prime)0}; \bar{K}^{*0}) + \mathcal{M}(\rho^+, \Xi_c^{(\prime)0}; \bar{K}^0) \\ &\quad + \mathcal{M}(K^+, \Omega_c^0; \phi) + \mathcal{M}(K^{*+}, \Omega_c^0; \eta_8) + \mathcal{M}(\rho^+, \Xi_c^{(\prime)0}; \bar{K}^{*0}) + \mathcal{M}(K^{*+}, \Omega_c^0; \phi), \end{aligned} \quad (\text{A18})$$

$$\begin{aligned} \mathcal{A}(\Omega_{cc}^+ \rightarrow \Xi_c^0 K^+) &= \mathcal{T}_{SD}(\Omega_{cc}^+ \rightarrow \Xi_c^0 K^+) + \mathcal{M}(K^+, \Xi_c^{(\prime)0}; \phi) + \mathcal{M}(K^{*+}, \Xi_c^{(\prime)0}; \eta_8) + \mathcal{M}(K^{*+}, \Xi_c^{(\prime)0}; \phi), \\ \mathcal{A}(\Omega_{cc}^+ \rightarrow \Xi_c^{(\prime)0} K^+) &= \mathcal{T}_{SD}(\Omega_{cc}^+ \rightarrow \Xi_c^{(\prime)0} K^+) + \mathcal{M}(K^+, \Xi_c^{(\prime)0}; \phi) + \mathcal{M}(K^{*+}, \Xi_c^{(\prime)0}; \eta_8) + \mathcal{M}(K^{*+}, \Xi_c^{(\prime)0}; \phi). \end{aligned} \quad (\text{A19})$$

The amplitudes for long-distance dominated and Cabibbo flavored modes can be given as follows.

$$\begin{aligned} \mathcal{A}(\Xi_{cc}^{++} \rightarrow \Sigma_c^{++} \bar{K}^0) &= \mathcal{C}_{SD}(\Xi_{cc}^{++} \rightarrow \Sigma_c^{++} \bar{K}^0) + \mathcal{M}(\pi^+, \Xi_c^{(\prime)+}; K^{*+}) + \mathcal{M}(\rho^+, \Xi_c^{(\prime)+}; K^+) + \mathcal{M}(\rho^+, \Xi_c^{(\prime)+}; K^{*+}) \\ &\quad + \mathcal{M}(\Xi_c^{(\prime)+}, \pi^+; \Lambda_c^+ / \Sigma_c^+) + \mathcal{M}(\Xi_c^{(\prime)+}, \rho^+; \Lambda_c^+ / \Sigma_c^+) + \mathcal{M}(\Xi_c^{(\prime)+}, \pi^+; \Sigma_c^{*+}) + \mathcal{M}(\Xi_c^{(\prime)+}, \rho^+; \Sigma_c^{*+}), \end{aligned} \quad (\text{A20})$$

$$\mathcal{A}(\Xi_{cc}^+ \rightarrow \Omega_c^0 K^+) = \mathcal{M}(\pi^+, \Xi_c^{(\prime)0}; \bar{K}^{*0}) + \mathcal{M}(\rho^+, \Xi_c^{(\prime)0}; \bar{K}^0) + \mathcal{M}(\rho^+, \Xi_c^{(\prime)0}; \bar{K}^{*0}), \quad (\text{A21})$$

$$\begin{aligned} \mathcal{A}(\Xi_{cc}^+ \rightarrow \Sigma_c^+ \bar{K}^0) &= \mathcal{C}_{SD}(\Xi_{cc}^+ \rightarrow \Sigma_c^+ \bar{K}^0) + \mathcal{M}(\pi^+, \Xi_c^{(\prime)0}; K^{*+}) + \mathcal{M}(\rho^+, \Xi_c^{(\prime)0}; K^+) + \mathcal{M}(\rho^+, \Xi_c^{(\prime)0}; K^{*+}) \\ &\quad + \mathcal{M}(\Xi_c^{(\prime)0}, \pi^+; \Sigma_c^0) + \mathcal{M}(\Xi_c^{(\prime)0}, \rho^+; \Sigma_c^0) + \mathcal{M}(\Xi_c^{(\prime)0}, \pi^+; \Sigma_c^{*0}) + \mathcal{M}(\Xi_c^{(\prime)0}, \rho^+; \Sigma_c^{*0}), \end{aligned} \quad (\text{A22})$$

$$\begin{aligned} \mathcal{A}(\Xi_{cc}^+ \rightarrow \Lambda_c^+ \bar{K}^0) &= \mathcal{C}_{SD}(\Xi_{cc}^+ \rightarrow \Lambda_c^+ \bar{K}^0) + \mathcal{M}(\pi^+, \Xi_c^{(\prime)0}; K^{*+}) + \mathcal{M}(\rho^+, \Xi_c^{(\prime)0}; K^+) + \mathcal{M}(\rho^+, \Xi_c^{(\prime)0}; K^{*+}) \\ &\quad + \mathcal{M}(\Xi_c^{(\prime)0}, \pi^+; \Sigma_c^0) + \mathcal{M}(\Xi_c^{(\prime)0}, \rho^+; \Sigma_c^0) + \mathcal{M}(\Xi_c^{(\prime)0}, \pi^+; \Sigma_c^{*0}) + \mathcal{M}(\Xi_c^{(\prime)0}, \rho^+; \Sigma_c^{*0}), \end{aligned} \quad (\text{A23})$$

$$\mathcal{A}(\Xi_{cc}^+ \rightarrow \Sigma_c^{++} K^-) = \mathcal{M}(\Xi_c^{(\prime)0}, \pi^+; \Lambda_c^+ / \Sigma_c^+) + \mathcal{M}(\Xi_c^{(\prime)0}, \rho^+; \Lambda_c^+ / \Sigma_c^+) + \mathcal{M}(\Xi_c^{(\prime)0}, \pi^+; \Sigma_c^{*+}) + \mathcal{M}(\Xi_c^{(\prime)0}, \rho^+; \Sigma_c^{*+}), \quad (\text{A24})$$

$$\begin{aligned} \mathcal{A}(\Xi_{cc}^+ \rightarrow \Xi_c^+ \pi^0) &= \mathcal{C}_{SD}(\Xi_{cc}^+ \rightarrow \Xi_c^+ \pi^0) + \mathcal{M}(\pi^+, \Xi_c^{(\prime)0}; \rho^+) + \mathcal{M}(\rho^+, \Xi_c^{(\prime)0}; \pi^+) + \mathcal{M}(\rho^+, \Xi_c^{(\prime)0}; \rho^+) \\ &\quad + \mathcal{M}(\Xi_c^{(\prime)0}, \pi^+; \Xi_c^{(\prime)0}) + \mathcal{M}(\Xi_c^{(\prime)0}, \rho^+; \Xi_c^{(\prime)0}) + \mathcal{M}(\Xi_c^{(\prime)0}, \pi^+; \Xi_c^{\prime *0}) + \mathcal{M}(\Xi_c^{(\prime)0}, \rho^+; \Xi_c^{\prime *0}), \end{aligned} \quad (\text{A25})$$

$$\begin{aligned} \mathcal{A}(\Xi_{cc}^+ \rightarrow \Xi_c^+ \eta_1) &= \mathcal{M}(\Xi_c^0, \pi^+; \Xi_c^0) + \mathcal{M}(\Xi_c^0, \pi^+; \Xi_c^{\prime 0}) + \mathcal{M}(\Xi_c^0, \rho^+; \Xi_c^0) + \mathcal{M}(\Xi_c^0, \rho^+; \Xi_c^{\prime 0}) \\ &\quad + \mathcal{M}(\Xi_c^0, \pi^+; \Xi_c^{\prime *0}) + \mathcal{M}(\Xi_c^0, \rho^+; \Xi_c^{\prime *0}), \end{aligned} \quad (\text{A26})$$

$$\mathcal{A}(\Xi_{cc}^+ \rightarrow \Xi_c^+ \eta_8) = \mathcal{M}(\Xi_c^{(\prime)0}, \pi^+; \Xi_c^{(\prime)0}) + \mathcal{M}(\Xi_c^{(\prime)0}, \rho^+; \Xi_c^{(\prime)0}) + \mathcal{M}(\Xi_c^{(\prime)0}, \pi^+; \Xi_c^{\prime *0}) + \mathcal{M}(\Xi_c^{(\prime)0}, \rho^+; \Xi_c^{\prime *0}), \quad (\text{A27})$$

$$\begin{aligned} \mathcal{A}(\Xi_{cc}^+ \rightarrow \Xi_c^{\prime +} \pi^0) &= \mathcal{C}_{SD}(\Xi_{cc}^+ \rightarrow \Xi_c^{\prime +} \pi^0) + \mathcal{M}(\pi^+, \Xi_c^{(\prime)0}; \rho^+) + \mathcal{M}(\rho^+, \Xi_c^{(\prime)0}; \pi^+) + \mathcal{M}(\rho^+, \Xi_c^{(\prime)0}; \rho^+) \\ &\quad + \mathcal{M}(\Xi_c^{(\prime)0}, \pi^+; \Xi_c^{(\prime)0}) + \mathcal{M}(\Xi_c^{(\prime)0}, \rho^+; \Xi_c^{(\prime)0}) + \mathcal{M}(\Xi_c^{(\prime)0}, \pi^+; \Xi_c^{\prime *0}) + \mathcal{M}(\Xi_c^{(\prime)0}, \rho^+; \Xi_c^{\prime *0}), \end{aligned} \quad (\text{A28})$$

$$\begin{aligned} \mathcal{A}(\Xi_{cc}^+ \rightarrow \Xi_c^{\prime +} \eta_1) &= \mathcal{M}(\Xi_c^0, \pi^+; \Xi_c^0) + \mathcal{M}(\Xi_c^0, \pi^+; \Xi_c^{\prime 0}) + \mathcal{M}(\Xi_c^0, \rho^+; \Xi_c^0) + \mathcal{M}(\Xi_c^0, \rho^+; \Xi_c^{\prime 0}) \\ &\quad + \mathcal{M}(\Xi_c^0, \pi^+; \Xi_c^{\prime *0}) + \mathcal{M}(\Xi_c^0, \rho^+; \Xi_c^{\prime *0}), \end{aligned} \quad (\text{A29})$$

$$\mathcal{A}(\Xi_{cc}^+ \rightarrow \Xi_c^{\prime +} \eta_8) = \mathcal{M}(\Xi_c^{(\prime)0}, \pi^+; \Xi_c^{(\prime)0}) + \mathcal{M}(\Xi_c^{(\prime)0}, \rho^+; \Xi_c^{(\prime)0}) + \mathcal{M}(\Xi_c^{(\prime)0}, \pi^+; \Xi_c^{\prime *0}) + \mathcal{M}(\Xi_c^{(\prime)0}, \rho^+; \Xi_c^{\prime *0}), \quad (\text{A30})$$

$$\begin{aligned} \mathcal{A}(\Omega_{cc}^+ \rightarrow \Xi_c^+ \bar{K}^0) &= \mathcal{C}_{SD}(\Omega_{cc}^+ \rightarrow \Xi_c^+ \bar{K}^0) + \mathcal{M}(\pi^+, \Omega_c^0; K^{*+}) + \mathcal{M}(\rho^+, \Omega_c^0; K^+) + \mathcal{M}(\rho^+, \Omega_c^0; K^{*+}) \\ &\quad + \mathcal{M}(\Omega_c^0, \pi^+; \Xi_c^{(\prime)0}) + \mathcal{M}(\Omega_c^0, \rho^+; \Xi_c^{(\prime)0}) + \mathcal{M}(\Omega_c^0, \pi^+; \Xi_c^{\prime *0}) + \mathcal{M}(\Omega_c^0, \rho^+; \Xi_c^{\prime *0}), \end{aligned} \quad (\text{A31})$$

$$\begin{aligned} \mathcal{A}(\Omega_{cc}^+ \rightarrow \Xi_c^{\prime +} \bar{K}^0) &= \mathcal{C}_{SD}(\Omega_{cc}^+ \rightarrow \Xi_c^{\prime +} \bar{K}^0) + \mathcal{M}(\pi^+, \Omega_c^0; K^{*+}) + \mathcal{M}(\rho^+, \Omega_c^0; K^+) + \mathcal{M}(\rho^+, \Omega_c^0; K^{*+}) \\ &\quad + \mathcal{M}(\Omega_c^0, \pi^+; \Xi_c^{(\prime)0}) + \mathcal{M}(\Omega_c^0, \rho^+; \Xi_c^{(\prime)0}) + \mathcal{M}(\Omega_c^0, \pi^+; \Xi_c^{\prime *0}) + \mathcal{M}(\Omega_c^0, \rho^+; \Xi_c^{\prime *0}). \end{aligned} \quad (\text{A32})$$

The amplitudes for long-distance dominated singly Cabibbo suppressed modes can be given as follows.

$$\begin{aligned} \mathcal{A}(\Xi_{cc}^{++} \rightarrow \Sigma_c^{++} \pi^0) &= \mathcal{C}_{SD}(\Xi_{cc}^{++} \rightarrow \Sigma_c^{++} \pi^0) + \mathcal{M}(\pi^+, \Lambda_c^+ / \Sigma_c^+; \rho^+) + \mathcal{M}(\rho^+, \Lambda_c^+ / \Sigma_c^+; \pi^+) + \mathcal{M}(\rho^+, \Lambda_c^+ / \Sigma_c^+; \rho^+) \\ &\quad + \mathcal{M}(K^+, \Xi_c^{(\prime)+}; K^{*+}) + \mathcal{M}(K^{*+}, \Xi_c^{(\prime)+}; K^+) + \mathcal{M}(\Xi_c^{(\prime)+}, K^+; \Xi_c^{(\prime)+}) + \mathcal{M}(\Xi_c^{(\prime)+}, K^{*+}; \Xi_c^{(\prime)+}) \\ &\quad + \mathcal{M}(\Lambda_c^+, \pi^+; \Sigma_c^+) + \mathcal{M}(\Sigma_c^+, \pi^+; \Lambda_c^+) + \mathcal{M}(\Lambda_c^+, \rho^+; \Sigma_c^+) + \mathcal{M}(\Sigma_c^+, \rho^+; \Lambda_c^+) \\ &\quad + \mathcal{M}(\Xi_c^{(\prime)+}, K^+; \Xi_c^{\prime *+}) + \mathcal{M}(\Xi_c^{(\prime)+}, K^{*+}; \Xi_c^{\prime *+}) + \mathcal{M}(\Lambda_c^+, \pi^+; \Sigma_c^{*+}) + \mathcal{M}(\Lambda_c^+, \rho^+; \Sigma_c^{*+}), \end{aligned} \quad (\text{A33})$$

$$\begin{aligned} \mathcal{A}(\Xi_{cc}^{++} \rightarrow \Sigma_c^{++} \eta_1) &= \mathcal{C}_{SD}(\Xi_{cc}^{++} \rightarrow \Sigma_c^{++} \eta_1) \\ &\quad + \mathcal{M}(\Sigma_c^+, \pi^+; \Sigma_c^+) + \mathcal{M}(\Lambda_c^+, \pi^+; \Lambda_c^+) + \mathcal{M}(\Sigma_c^+, \rho^+; \Sigma_c^+) + \mathcal{M}(\Lambda_c^+, \rho^+; \Lambda_c^+) \\ &\quad + \mathcal{M}(\Xi_c^+, K^+; \Xi_c^+) + \mathcal{M}(\Xi_c^+, K^+; \Xi_c^{\prime +}) + \mathcal{M}(\Xi_c^+, K^{*+}; \Xi_c^+) + \mathcal{M}(\Xi_c^+, K^{*+}; \Xi_c^{\prime +}) \\ &\quad + \mathcal{M}(\Sigma_c^+, \pi^+; \Sigma_c^{*+}) + \mathcal{M}(\Sigma_c^+, \rho^+; \Sigma_c^{*+}) + \mathcal{M}(\Xi_c^+, K^+; \Xi_c^{\prime *+}) + \mathcal{M}(\Xi_c^+, K^{*+}; \Xi_c^{\prime *+}), \end{aligned} \quad (\text{A34})$$



$$\begin{aligned} \mathcal{A}(\Omega_{cc}^+ \rightarrow \Xi_c^+ \eta_1) = & \mathcal{C}_{SD}(\Omega_{cc}^+ \rightarrow \Xi_c^+ \eta_1) + \mathcal{M}(\Omega_c^0, K^+; \Omega_c^0) + \mathcal{M}(\Omega_c^0, K^{*+}; \Omega_c^0) + \mathcal{M}(\Xi_c^0, \pi^+; \Xi_c^0) \\ & + \mathcal{M}(\Xi_c^{\prime 0}, \pi^+; \Xi_c^{\prime 0}) + \mathcal{M}(\Xi_c^0, \rho^+; \Xi_c^0) + \mathcal{M}(\Xi_c^{\prime 0}, \rho^+; \Xi_c^{\prime 0}) \\ & + \mathcal{M}(\Omega_c^0, K^+; \Omega_c^{*0}) + \mathcal{M}(\Omega_c^0, K^{*+}; \Omega_c^{*0}) + \mathcal{M}(\Xi_c^{\prime 0}, \pi^+; \Xi_c^{\prime *0}) + \mathcal{M}(\Xi_c^{\prime 0}, \rho^+; \Xi_c^{\prime *0}), \end{aligned} \quad (\text{A49})$$

$$\begin{aligned}
\mathcal{A}(\Omega_{cc}^+ \rightarrow \Xi_c^+ \eta_8) = & \mathcal{C}_{SD}(\Omega_{cc}^+ \rightarrow \Xi_c^+ \eta_8) + \mathcal{M}(K^+, \Omega_c^0, K^{*+}) + \mathcal{M}(K^{*+}, \Omega_c^0, K^+) + \mathcal{M}(K^{*+}, \Omega_c^0, K^{*+}) \\
& + \mathcal{M}(\Omega_c^0, K^+, \Omega_c^0) + \mathcal{M}(\Omega_c^0, K^{*+}, \Omega_c^0) + \mathcal{M}(\Xi_c^{(\prime)0}, \pi^+, \Xi_c^{(\prime)0}) + \mathcal{M}(\Xi_c^{(\prime)0}, \rho^+, \Xi_c^{(\prime)0}) \\
& + \mathcal{M}(\Omega_c^0, K^+, \Omega_c^{*0}) + \mathcal{M}(\Omega_c^0, K^{*+}, \Omega_c^{*0}) + \mathcal{M}(\Xi_c^{(\prime)0}, \pi^+, \Xi_c^{*0}) + \mathcal{M}(\Xi_c^{(\prime)0}, \rho^+, \Xi_c^{*0}), \quad (\text{A50})
\end{aligned}$$

$$\begin{aligned} \mathcal{A}(\Omega_{cc}^+ \rightarrow \Xi_c'^+ \pi^0) = & \mathcal{C}_{SD}(\Omega_{cc}^+ \rightarrow \Xi_c'^+ \pi^0) + \mathcal{M}(\pi^+, \Xi_c^{(\prime)0}; \rho^+) + \mathcal{M}(\rho^+, \Xi_c^{(\prime)0}; \pi^+) \\ & + \mathcal{M}(K^+, \Omega_c^0; K^{*+}) + \mathcal{M}(K^{*+}, \Omega_c^0; K^+) + \mathcal{M}(\rho^+, \Xi_c^{(\prime)0}; \rho^+) + \mathcal{M}(K^{*+}, \Omega_c^0; K^{*+}) \\ & + \mathcal{M}(\Xi_c^{(\prime)0}, \pi^+; \Xi_c^{(\prime)0}) + \mathcal{M}(\Xi_c^{(\prime)0}, \rho^+; \Xi_c^{(\prime)0}) + \mathcal{M}(\Xi_c^{(\prime)0}, \pi^+; \Xi_c'^{*0}) + \mathcal{M}(\Xi_c^{(\prime)0}, \rho^+; \Xi_c'^{*0}), \end{aligned} \quad (\text{A51})$$

$$\begin{aligned}\mathcal{A}(\Omega_{cc}^+ \rightarrow \Xi_c'^+ \eta_1) = & \mathcal{C}_{SD}(\Omega_{cc}^+ \rightarrow \Xi_c'^+ \eta_1) + \mathcal{M}(\Omega_c^0, K^+; \Omega_c^0) + \mathcal{M}(\Omega_c^0, K^{*+}; \Omega_c^0) + \mathcal{M}(\Xi_c^0, \pi^+; \Xi_c^0) \\ & + \mathcal{M}(\Xi_c^0, \pi^+; \Xi_c'^0) + \mathcal{M}(\Xi_c^0, \rho^+; \Xi_c^0) + \mathcal{M}(\Xi_c^0, \rho^+; \Xi_c'^0) \\ & + \mathcal{M}(\Omega_c^0, K^+; \Omega_c^{*0}) + \mathcal{M}(\Omega_c^0, K^{*+}; \Omega_c^{*0}) + \mathcal{M}(\Xi_c'^0, \pi^+; \Xi_c'^{*0}) + \mathcal{M}(\Xi_c'^0, \rho^+; \Xi_c'^{*0}),\end{aligned}\quad (\text{A52})$$

$$\begin{aligned}
\mathcal{A}(\Omega_{cc}^+ \rightarrow \Xi_c'^+ \eta_8) = & \mathcal{C}_{SD}(\Omega_{cc}^+ \rightarrow \Xi_c'^+ \eta_8) + \mathcal{M}(K^+, \Omega_c^0; K^{*+}) + \mathcal{M}(K^{*+}, \Omega_c^0; K^+) + \mathcal{M}(K^{*+}, \Omega_c^0; K^{*+}) \\
& + \mathcal{M}(\Omega_c^0, K^+; \Omega_c^0) + \mathcal{M}(\Omega_c^0, K^{*+}; \Omega_c^0) + \mathcal{M}(\Xi_c'^{(\prime)0}, \pi^+; \Xi_c'^{(\prime)0}) + \mathcal{M}(\Xi_c'^{(\prime)0}, \rho^+; \Xi_c'^{(\prime)0}) \\
& + \mathcal{M}(\Omega_c^0, K^+; \Omega_c^{*0}) + \mathcal{M}(\Omega_c^0, K^{*+}; \Omega_c^{*0}) + \mathcal{M}(\Xi_c'^{(\prime)0}, \pi^+; \Xi_c'^{*0}) + \mathcal{M}(\Xi_c'^{(\prime)0}, \rho^+; \Xi_c'^{*0}). \quad (\text{A53})
\end{aligned}$$

The amplitudes for long-distance dominated doubly Cabibbo suppressed can be given as follows.

$$\begin{aligned} \mathcal{A}(\Xi_{cc}^{++} \rightarrow \Sigma_c^{++} K^0) &= \mathcal{C}_{SD}(\Xi_{cc}^{++} \rightarrow \Sigma_c^{++} K^0) + \mathcal{M}(K^{*+}, \Lambda_c^+ / \Sigma_c^+; \pi^+) + \mathcal{M}(K^+, \Lambda_c^+ / \Sigma_c^+; \rho^+) \\ &\quad + \mathcal{M}(K^{*+}, \Lambda_c^+ / \Sigma_c^+; \rho^+) + \mathcal{M}(\Lambda_c^+ / \Sigma_c^+, K^+; \Xi_c^{(\prime)+}) + \mathcal{M}(\Lambda_c^+ / \Sigma_c^+, K^{*+}; \Xi_c^{(\prime)+}) \\ &\quad + \mathcal{M}(\Lambda_c^+ / \Sigma_c^+, K^+; \Xi_c^{\prime*+}) + \mathcal{M}(\Lambda_c^+ / \Sigma_c^+, K^{*+}; \Xi_c^{\prime*+}), \end{aligned} \quad (\text{A54})$$

$$\begin{aligned} \mathcal{A}(\Xi_{cc}^+ \rightarrow \Sigma_c^+ K^0) = & \mathcal{C}_{SD}(\Xi_{cc}^+ \rightarrow \Sigma_c^+ K^0) + \mathcal{M}(K^+, \Sigma_c^0; \rho^+) + \mathcal{M}(K^{*+}, \Sigma_c^0; \pi^+) + \mathcal{M}(K^{*+}, \Sigma_c^0; \rho^+) \\ & + \mathcal{M}(\Sigma_c^0, K^+; \Xi_c^{(\prime)0}) + \mathcal{M}(\Sigma_c^0, K^{*+}; \Xi_c^{(\prime)*0}) + \mathcal{M}(\Sigma_c^0, K^+; \Xi_c^{*0}) + \mathcal{M}(\Sigma_c^0, K^{*+}; \Xi_c^{*0}), \end{aligned} \quad (\text{A55})$$

$$\begin{aligned} \mathcal{A}(\Xi_{cc}^+ \rightarrow \Lambda_c^+ K^0) = & \mathcal{C}_{SD}(\Xi_{cc}^+ \rightarrow \Lambda_c^+ K^0) + \mathcal{M}(K^+, \Sigma_c^0; \rho^+) + \mathcal{M}(K^{*+}, \Sigma_c^0; \pi^+) + \mathcal{M}(K^{*+}, \Sigma_c^0; \rho^+) \\ & + \mathcal{M}(\Sigma_c^0, K^+; \Xi_c^{(\prime)0}) + \mathcal{M}(\Sigma_c^0, K^{*+}; \Xi_c^{(\prime)*0}) + \mathcal{M}(\Sigma_c^0, K^+; \Xi_c'^0) + \mathcal{M}(\Sigma_c^0, K^{*+}; \Xi_c'^{*0}), \end{aligned} \quad (\text{A56})$$

$$\begin{aligned} \mathcal{A}(\Omega_{cc}^+ \rightarrow \Sigma_c^+ \pi^0) = & \mathcal{M}(K^+, \Xi_c^{(\prime)0}; K^{*+}) + \mathcal{M}(K^{*+}, \Xi_c^{(\prime)0}; K^+) + \mathcal{M}(K^{*+}, \Xi_c^{(\prime)0}; K^{*+}) \\ & + \mathcal{M}(\Xi_c^{(\prime)0}, K^+; \Xi_c^{(\prime)0}) + \mathcal{M}(\Xi_c^{(\prime)0}, K^{*+}; \Xi_c^{(\prime)0}) + \mathcal{M}(\Xi_c^{(\prime)0}, K^+; \Xi_c^{(*0})} + \mathcal{M}(\Xi_c^{(\prime)0}, K^{*+}; \Xi_c^{(*0)}), \end{aligned} \quad (\text{A57})$$

$$\begin{aligned} \mathcal{A}(\Omega_{cc}^+ \rightarrow \Sigma_c^+ \eta_1) = & \mathcal{C}_{SD}(\Omega_{cc}^+ \rightarrow \Sigma_c^+ \eta_1) \\ & + \mathcal{M}(\Xi_c^0, K^+; \Xi_c^0) + \mathcal{M}(\Xi_c'^0, K^+; \Xi_c'^0) + \mathcal{M}(\Xi_c^0, K^{*+}; \Xi_c^0) + \mathcal{M}(\Xi_c'^0, K^{*+}; \Xi_c'^0) \\ & + \mathcal{M}(\Xi_c'^0, K^+; \Xi_c'^{*0}) + \mathcal{M}(\Xi_c'^0, K^{*+}; \Xi_c'^{*0}), \end{aligned} \quad (\text{A58})$$

$$\begin{aligned} \mathcal{A}(\Omega_{cc}^+ \rightarrow \Sigma_c^+ \eta_8) = & \mathcal{C}_{SD}(\Omega_{cc}^+ \rightarrow \Sigma_c^+ \eta_8) + \mathcal{M}(K^+, \Xi_c^{(\prime)0}; K^{*+}) + \mathcal{M}(K^{*+}, \Xi_c^{(\prime)0}; K^+) + \mathcal{M}(K^{*+}, \Xi_c^{(\prime)0}; K^{*+}) \\ & + \mathcal{M}(\Xi_c^{(\prime)0}, K^+; \Xi_c^{(\prime)0}) + \mathcal{M}(\Xi_c^{(\prime)0}, K^{*+}; \Xi_c^{(\prime)0}) + \mathcal{M}(\Xi_c^{(\prime)0}, K^+; \Xi_c^{*\prime 0}) + \mathcal{M}(\Xi_c^{(\prime)0}, K^{*+}; \Xi_c^{*\prime 0}), \end{aligned} \quad (\text{A59})$$

$$\begin{aligned} \mathcal{A}(\Omega_{cc}^+ \rightarrow \Lambda_c^+ \pi^0) = & +\mathcal{M}(K^+, \Xi_c^{(\prime)0}; K^{*+}) + \mathcal{M}(K^{*+}, \Xi_c^{(\prime)0}; K^+) + \mathcal{M}(K^{*+}, \Xi_c^{(\prime)0}; K^{*+}) \\ & + \mathcal{M}(\Xi_c^{(\prime)0}, K^+; \Xi_c^{(\prime)0}) + \mathcal{M}(\Xi_c^{(\prime)0}, K^{*+}; \Xi_c^{(\prime)0}) + \mathcal{M}(\Xi_c^{(\prime)0}, K^+; \Xi_c'^{*0}) + \mathcal{M}(\Xi_c^{(\prime)0}, K^{*+}; \Xi_c'^{*0}), \end{aligned} \quad (\text{A60})$$

$$\begin{aligned} \mathcal{A}(\Omega_{cc}^+ \rightarrow \Lambda_c^+ \eta_1) = & \mathcal{C}_{SD}(\Omega_{cc}^+ \rightarrow \Lambda_c^+ \eta_1) \\ & + \mathcal{M}(\Xi_c^0, K^+; \Xi_c^0) + \mathcal{M}(\Xi_c'^0, K^+; \Xi_c'^0) + \mathcal{M}(\Xi_c^0, K^{*+}; \Xi_c^0) + \mathcal{M}(\Xi_c'^0, K^{*+}; \Xi_c'^0) \\ & + \mathcal{M}(\Xi_c'^0, K^+; \Xi_c'^{*0}) + \mathcal{M}(\Xi_c'^0, K^{*+}; \Xi_c'^{*0}), \end{aligned} \quad (\text{A61})$$

$$\begin{aligned} \mathcal{A}(\Omega_{cc}^+ \rightarrow \Lambda_c^+ \eta_8) = & \mathcal{C}_{SD}(\Omega_{cc}^+ \rightarrow \Lambda_c^+ \eta_8) + \mathcal{M}(K^+, \Xi_c^{(\prime)0}; K^{*+}) + \mathcal{M}(K^{*+}, \Xi_c^{(\prime)0}; K^+) + \mathcal{M}(K^{*+}, \Xi_c^{(\prime)0}; K^{*+}) \\ & + \mathcal{M}(\Xi_c^{(\prime)0}, K^+; \Xi_c^{(\prime)0}) + \mathcal{M}(\Xi_c^{(\prime)0}, K^{*+}; \Xi_c^{(\prime)0}) + \mathcal{M}(\Xi_c^{(\prime)0}, K^+; \Xi_c^{*\prime 0}) + \mathcal{M}(\Xi_c^{(\prime)0}, K^{*+}; \Xi_c^{*\prime 0}), \end{aligned} \quad (\text{A62})$$

$$\mathcal{A}(\Omega_{cc}^+ \rightarrow \Sigma_c^0 \pi^+) = \mathcal{M}(K^+, \Xi_c^{(\prime)0}; K^{*0}) + \mathcal{M}(K^{*+}, \Xi_c^{(\prime)0}; K^0) + \mathcal{M}(K^{*+}, \Xi_c^{(\prime)0}; K^{*0}), \quad (\text{A63})$$

$$\mathcal{A}(\Omega_{cc}^+ \rightarrow \Sigma_c^{++} \pi^-) = \mathcal{M}(\Xi_c^{(\prime)0}, K^+; \Xi_c^{(\prime)+}) + \mathcal{M}(\Xi_c^{(\prime)0}, K^{*+}; \Xi_c^{(\prime)+}) + \mathcal{M}(\Xi_c^{(\prime)0}, K^+; \Xi_c^{\prime*+}) + \mathcal{M}(\Xi_c^{(\prime)0}, K^{*+}; \Xi_c^{\prime*+}), \quad (\text{A64})$$

$$\begin{aligned} \mathcal{A}(\Omega_{cc}^+ \rightarrow \Xi_c^+ K^0) = & \mathcal{C}_{SD}(\Omega_{cc}^+ \rightarrow \Xi_c^+ K^0) + \mathcal{M}(K^+, \Xi_c^{(\prime)0}; \rho^+) + \mathcal{M}(K^{*+}, \Xi_c^{(\prime)0}; \pi^+) + \mathcal{M}(K^{*+}, \Xi_c^{(\prime)0}; \rho^+) \\ & + \mathcal{M}(\Xi_c^{(\prime)0}, K^+; \Omega_c^0) + \mathcal{M}(\Xi_c^{(\prime)0}, K^{*+}; \Omega_c^0) + \mathcal{M}(\Xi_c^{(\prime)0}, K^+; \Omega_c^{*0}) + \mathcal{M}(\Xi_c^{(\prime)0}, K^{*+}; \Omega_c^{*0}), \end{aligned} \quad (\text{A65})$$

$$\begin{aligned} \mathcal{A}(\Omega_{cc}^+ \rightarrow \Xi_c'^+ K^0) = & \mathcal{C}_{SD}(\Omega_{cc}^+ \rightarrow \Xi_c^{(\prime)+} K^0) + \mathcal{M}(K^+, \Xi_c^{(\prime)0}; \rho^+) + \mathcal{M}(K^{*+}, \Xi_c^{(\prime)0}; \pi^+) + \mathcal{M}(K^{*+}, \Xi_c^{(\prime)0}; \rho^+) \\ & + \mathcal{M}(\Xi_c^{(\prime)0}, K^+; \Omega_{cc}^0) + \mathcal{M}(\Xi_c^{(\prime)0}, K^{*+}; \Omega_{cc}^0) + \mathcal{M}(\Xi_c^{(\prime)0}, K^+; \Omega_{cc}^{*0}) + \mathcal{M}(\Xi_c^{(\prime)0}, K^{*+}; \Omega_{cc}^{*0}). \end{aligned} \quad (\text{A66})$$

## Appendix B: Strong couplings

In general, meson-baryon and meson-meson strong couplings can be obtained from the SU(3)-invariant strong Hamiltonian. In the present work, we use the SU(3) flavor symmetry to analysis the vector-vector-pseudoscalar (VVP), vector-pseudoscalar-pseudoscalar (VPP), baryon-baryon-pseudoscalar ( $BBP/BB^*P$ ) and baryon-baryon-vector ( $BBV/BB^*V$ ) couplings. Under SU(3) flavor symmetry, the pseudoscalar and vector meson can be written as follows,

$$P(J^P = 0^-) = \begin{pmatrix} \frac{\pi^0}{\sqrt{2}} + \frac{\eta_8}{\sqrt{6}} & \pi^+ & K^+ \\ \pi^- & -\frac{\pi^0}{\sqrt{2}} + \frac{\eta_8}{\sqrt{6}} & K^0 \\ K^- & \bar{K}^0 & -\sqrt{\frac{2}{3}}\eta_8 \end{pmatrix} + \frac{1}{\sqrt{3}} \begin{pmatrix} \eta_1 & 0 & 0 \\ 0 & \eta_1 & 0 \\ 0 & 0 & \eta_1 \end{pmatrix}, \quad (\text{B1})$$

$$V(J^P = 1^-) = \begin{pmatrix} \frac{\rho^0}{\sqrt{2}} + \frac{\omega}{\sqrt{2}} & \rho^+ & K^{*+} \\ \rho^- & -\frac{\rho^0}{\sqrt{2}} + \frac{\omega}{\sqrt{2}} & K^{*0} \\ K^{*-} & \bar{K}^{*0} & \phi \end{pmatrix}. \quad (\text{B2})$$

And the spin-parity  $1/2^+$  singly charmed baryons include anti-triplet  $\mathcal{B}_{\bar{3}}$  and sextet  $\mathcal{B}_6$ , which can given as follows,

$$B_6(J^P = \frac{1}{2}^+) = \begin{pmatrix} \Sigma_c^{++} & \frac{\Sigma_c^+}{\sqrt{2}} & \frac{\Xi_c'^+}{\sqrt{2}} \\ \frac{\Sigma_c^+}{\sqrt{2}} & \Sigma_c^0 & \frac{\Xi_c'^0}{\sqrt{2}} \\ \frac{\Xi_c'^+}{\sqrt{2}} & \frac{\Xi_c'^0}{\sqrt{2}} & \Omega_c^0 \end{pmatrix}, \quad B_{\bar{3}}(J^P = \frac{1}{2}^+) = \begin{pmatrix} 0 & \Lambda_c^+ & \Xi_c^+ \\ -\Lambda_c^+ & 0 & \Xi_c^0 \\ -\Xi_c^+ & -\Xi_c^0 & 0 \end{pmatrix}. \quad (\text{B3})$$

In addition, the spin-parity  $3/2^+$  singly charmed baryons sextet  $\mathcal{B}_6$  can given as follows,

$$B_6^*(J^P = \frac{3}{2}^+) = \begin{pmatrix} \Sigma_c^{*++} & \frac{\Sigma_c^{*+}}{\sqrt{2}} & \frac{\Xi_c^{*+}}{\sqrt{2}} \\ \frac{\Sigma_c^{*+}}{\sqrt{2}} & \Sigma_c^{*0} & \frac{\Xi_c^{*0}}{\sqrt{2}} \\ \frac{\Xi_c^{*+}}{\sqrt{2}} & \frac{\Xi_c^{*0}}{\sqrt{2}} & \Omega_c^{*0} \end{pmatrix}. \quad (\text{B4})$$

Then with the help of Eqs. (B2)-(B4), we can obtain the relationships of these strong couplings, as shown in Tabs. XII-XV.

- 
- [1] S. Navas *et al.* [Particle Data Group], Phys. Rev. D **110**, no.3, 030001 (2024) doi:10.1103/PhysRevD.110.030001
  - [2] S. P. Ratti, Nucl. Phys. B Proc. Suppl. **115**, 33-36 (2003) doi:10.1016/S0920-5632(02)01948-5
  - [3] B. Aubert *et al.* [BaBar], Phys. Rev. D **74**, 011103 (2006) doi:10.1103/PhysRevD.74.011103 [arXiv:hep-ex/0605075 [hep-ex]].
  - [4] R. Chistov *et al.* [Belle], Phys. Rev. Lett. **97**, 162001 (2006) doi:10.1103/PhysRevLett.97.162001 [arXiv:hep-ex/0606051 [hep-ex]].
  - [5] R. Aaij *et al.* [LHCb], JHEP **12**, 090 (2013) doi:10.1007/JHEP12(2013)090 [arXiv:1310.2538 [hep-ex]].
  - [6] R. Aaij *et al.* [LHCb], Phys. Rev. Lett. **119**, no.11, 112001 (2017) doi:10.1103/PhysRevLett.119.112001 [arXiv:1707.01621 [hep-ex]].
  - [7] R. Aaij *et al.* [LHCb], Phys. Rev. Lett. **121**, no.16, 162002 (2018) doi:10.1103/PhysRevLett.121.162002 [arXiv:1807.01919 [hep-ex]].
  - [8] R. Aaij *et al.* [LHCb], Phys. Rev. Lett. **121**, no.5, 052002 (2018) doi:10.1103/PhysRevLett.121.052002 [arXiv:1806.02744 [hep-ex]].

Table XII: The strong coupling constants between the vector mesons and two pseudoscalar mesons  $g_{VPP}$  can be obtained by using the coupling  $g_{\rho\pi\pi} = 6.05 = -\frac{g_{VPP}}{\sqrt{2}}$  [115] and SU(3) relations.

Vertex	g	Vertex	g	Vertex	g	Vertex	g
$\rho^0\pi^+\pi^-$	$-\frac{g_{VPP}}{\sqrt{2}}$	$\rho^0\pi^0\eta_8$	$\frac{g_{VPP}}{\sqrt{6}}$	$\rho^0\pi^0\eta_1$	$\frac{g_{VPP}}{\sqrt{3}}$	$\rho^0\pi^-\pi^+$	$\frac{g_{VPP}}{\sqrt{2}}$
$\rho^0\bar{K}^0K^0$	$-\frac{g_{VPP}}{\sqrt{2}}$	$\rho^0K^-K^+$	$\frac{g_{VPP}}{\sqrt{2}}$	$\rho^0\eta_8\pi^0$	$\frac{g_{VPP}}{\sqrt{6}}$	$\rho^0\eta_1\pi^0$	$\frac{g_{VPP}}{\sqrt{3}}$
$\omega\pi^+\pi^-$	$\frac{g_{VPP}}{\sqrt{2}}$	$\omega\pi^0\pi^0$	$\frac{g_{VPP}}{\sqrt{2}}$	$\omega\pi^-\pi^+$	$\frac{g_{VPP}}{\sqrt{2}}$	$\omega\bar{K}^0K^0$	$\frac{g_{VPP}}{\sqrt{2}}$
$\omega K^-K^+$	$\frac{g_{VPP}}{\sqrt{2}}$	$\omega\eta_8\eta_8$	$\frac{g_{VPP}}{3\sqrt{2}}$	$\omega\eta_8\eta_1$	$\frac{g_{VPP}}{3}$	$\omega\eta_1\eta_8$	$\frac{g_{VPP}}{3}$
$\omega\eta_1\eta_1$	$\frac{\sqrt{2}g_{VPP}}{3}$	$\rho^+\pi^+\pi^0$	$\frac{g_{VPP}}{\sqrt{2}}$	$\rho^+\pi^+\eta_8$	$\frac{g_{VPP}}{\sqrt{6}}$	$\rho^+\pi^+\eta_1$	$\frac{g_{VPP}}{\sqrt{3}}$
$\rho^+\pi^0\pi^+$	$-\frac{g_{VPP}}{\sqrt{2}}$	$\rho^+\bar{K}^0K^+$	$g_{VPP}$	$\rho^+\eta_8\pi^+$	$\frac{g_{VPP}}{\sqrt{6}}$	$\rho^+\eta_1\pi^+$	$\frac{g_{VPP}}{\sqrt{3}}$
$K^{*+}K^+\pi^0$	$\frac{g_{VPP}}{\sqrt{2}}$	$K^{*+}K^+\eta_8$	$\frac{g_{VPP}}{\sqrt{6}}$	$K^{*+}K^+\eta_1$	$\frac{g_{VPP}}{\sqrt{3}}$	$K^{*+}K^0\pi^+$	$g_{VPP}$
$K^{*+}\eta_8K^+$	$-\sqrt{\frac{2}{3}}g_{VPP}$	$K^{*+}\eta_1K^+$	$\frac{g_{VPP}}{\sqrt{3}}$	$\rho^-\pi^0\pi^-$	$\frac{g_{VPP}}{\sqrt{2}}$	$\rho^-\pi^-\pi^0$	$-\frac{g_{VPP}}{\sqrt{2}}$
$\rho^-\pi^-\eta_8$	$\frac{g_{VPP}}{\sqrt{6}}$	$\rho^-\pi^-\eta_1$	$\frac{g_{VPP}}{\sqrt{3}}$	$\rho^-K^-K^0$	$g_{VPP}$	$\rho^-\eta_8\pi^-$	$\frac{g_{VPP}}{\sqrt{6}}$
$\rho^-\eta_1\pi^-$	$\frac{g_{VPP}}{\sqrt{3}}$	$K^{*0}K^+\pi^-$	$g_{VPP}$	$K^{*0}K^0\pi^0$	$-\frac{g_{VPP}}{\sqrt{2}}$	$K^{*0}K^0\eta_8$	$\frac{g_{VPP}}{\sqrt{6}}$
$K^{*0}K^0\eta_1$	$\frac{g_{VPP}}{\sqrt{3}}$	$K^{*0}\eta_8K^0$	$-\sqrt{\frac{2}{3}}g_{VPP}$	$K^{*0}\eta_1K^0$	$\frac{g_{VPP}}{\sqrt{3}}$	$K^{*-}\pi^0K^-$	$\frac{g_{VPP}}{\sqrt{2}}$
$K^{*-}\pi^-\bar{K}^0$	$g_{VPP}$	$K^{*-}K^-\eta_8$	$-\sqrt{\frac{2}{3}}g_{VPP}$	$K^{*-}K^-\eta_1$	$\frac{g_{VPP}}{\sqrt{3}}$	$K^{*-}\eta_8K^-$	$\frac{g_{VPP}}{\sqrt{6}}$
$K^{*-}\eta_1K^-$	$\frac{g_{VPP}}{\sqrt{3}}$	$\bar{K}^{*0}\pi^+K^-$	$g_{VPP}$	$\bar{K}^{*0}\pi^0K^0$	$-\frac{g_{VPP}}{\sqrt{2}}$	$\bar{K}^{*0}\bar{K}^0\eta_8$	$-\sqrt{\frac{2}{3}}g_{VPP}$
$\bar{K}^{*0}\bar{K}^0\eta_1$	$\frac{g_{VPP}}{\sqrt{3}}$	$\bar{K}^{*0}\eta_8\bar{K}^0$	$\frac{g_{VPP}}{\sqrt{6}}$	$\bar{K}^{*0}\eta_1\bar{K}^0$	$\frac{g_{VPP}}{\sqrt{3}}$	$\phi K^+K^-$	$g_{VPP}$
$\phi K^0\bar{K}^0$	$g_{VPP}$	$\phi\eta_8\eta_8$	$\frac{2g_{VPP}}{3}$	$\phi\eta_8\eta_1$	$-\frac{1}{3}\sqrt{2}g_{VPP}$	$\phi\eta_1\eta_8$	$-\frac{1}{3}\sqrt{2}g_{VPP}$
$\phi\eta_1\eta_1$	$\frac{g_{VPP}}{3}$						

Table XIII: The strong couplings between the pseudoscalar meson (P) and two vector mesons (V) can be obtained by using the coupling constant  $g_{\omega\rho\pi} = g_{VVP}/\sqrt{2} = -10$  [131] and SU(3) relationships.

Vertex	g	Vertex	g	Vertex	g	Vertex	g
$\pi^+\rho^0\rho^+$	$-\frac{g_{VVP}}{\sqrt{2}}$	$\pi^+\omega\rho^+$	$\frac{g_{VVP}}{\sqrt{2}}$	$\pi^+\rho^+\rho^0$	$\frac{g_{VVP}}{\sqrt{2}}$	$\pi^+\rho^+\omega$	$\frac{g_{VVP}}{\sqrt{2}}$
$\pi^+\bar{K}^{*0}K^{*+}$	$g_{VVP}$	$\pi^0\rho^0\omega$	$\frac{g_{VVP}}{\sqrt{2}}$	$\pi^0\omega\rho^0$	$\frac{g_{VVP}}{\sqrt{2}}$	$\pi^0\rho^+\rho^-$	$-\frac{g_{VVP}}{\sqrt{2}}$
$\pi^0\rho^-\rho^+$	$\frac{g_{VVP}}{\sqrt{2}}$	$\pi^0K^{*-}K^{*+}$	$\frac{g_{VVP}}{\sqrt{2}}$	$\pi^0\bar{K}^{*0}K^{*0}$	$-\frac{g_{VVP}}{\sqrt{2}}$	$\pi^-\rho^0\rho^-$	$\frac{g_{VVP}}{\sqrt{2}}$
$\pi^-\omega\rho^-$	$\frac{g_{VVP}}{\sqrt{2}}$	$\pi^-\rho^-\rho^0$	$-\frac{g_{VVP}}{\sqrt{2}}$	$\pi^-\rho^-\omega$	$\frac{g_{VVP}}{\sqrt{2}}$	$\pi^-\bar{K}^{*0}K^{*0}$	$g_{VVP}$
$K^+K^{*+}\rho^0$	$\frac{g_{VVP}}{\sqrt{2}}$	$K^+K^{*+}\omega$	$\frac{g_{VVP}}{\sqrt{2}}$	$K^+K^{*0}\rho^+$	$g_{VVP}$	$K^+\phi K^{*+}$	$g_{VVP}$
$K^0K^{*+}\rho^-$	$g_{VVP}$	$K^0K^{*0}\rho^0$	$-\frac{g_{VVP}}{\sqrt{2}}$	$K^0K^{*0}\omega$	$\frac{g_{VVP}}{\sqrt{2}}$	$K^0\phi K^{*0}$	$g_{VVP}$
$\bar{K}^0\rho^0\bar{K}^{*0}$	$-\frac{g_{VVP}}{\sqrt{2}}$	$\bar{K}^0\omega\bar{K}^{*0}$	$\frac{g_{VVP}}{\sqrt{2}}$	$\bar{K}^0\rho^+K^{*-}$	$g_{VVP}$	$\bar{K}^0\bar{K}^{*0}\phi$	$g_{VVP}$
$K^-\rho^0K^{*-}$	$\frac{g_{VVP}}{\sqrt{2}}$	$K^-\omega K^{*-}$	$\frac{g_{VVP}}{\sqrt{2}}$	$K^-\rho^-\bar{K}^{*0}$	$g_{VVP}$	$K^-K^{*-}\phi$	$g_{VVP}$
$\eta_8\rho^0\rho^0$	$\frac{g_{VVP}}{\sqrt{6}}$	$\eta_8\omega\omega$	$\frac{g_{VVP}}{\sqrt{6}}$	$\eta_8\rho^+\rho^-$	$\frac{g_{VVP}}{\sqrt{6}}$	$\eta_8K^{*+}K^{*-}$	$-\sqrt{\frac{2}{3}}g_{VVP}$
$\eta_8\rho^-\rho^+$	$\frac{g_{VVP}}{\sqrt{6}}$	$\eta_8K^{*0}\bar{K}^{*0}$	$-\sqrt{\frac{2}{3}}g_{VVP}$	$\eta_8K^{*-}K^{*+}$	$\frac{g_{VVP}}{\sqrt{6}}$	$\eta_8\bar{K}^{*0}K^{*0}$	$\frac{g_{VVP}}{\sqrt{6}}$
$\eta_8\phi\phi$	$-\sqrt{\frac{2}{3}}g_{VVP}$	$\eta_1\rho^0\rho^0$	$\frac{g_{VVP}}{\sqrt{3}}$	$\eta_1\omega\omega$	$\frac{g_{VVP}}{\sqrt{3}}$	$\eta_1\rho^+\rho^-$	$\frac{g_{VVP}}{\sqrt{3}}$
$\eta_1K^{*+}K^{*-}$	$\frac{g_{VVP}}{\sqrt{3}}$	$\eta_1\rho^-\rho^+$	$\frac{g_{VVP}}{\sqrt{3}}$	$\eta_1K^{*0}\bar{K}^{*0}$	$\frac{g_{VVP}}{\sqrt{3}}$	$\eta_1K^{*-}K^{*+}$	$\frac{g_{VVP}}{\sqrt{3}}$
$\eta_1\bar{K}^{*0}K^{*0}$	$\frac{g_{VVP}}{\sqrt{3}}$	$\eta_1\phi\phi$	$\frac{g_{VVP}}{\sqrt{3}}$				

Table XIV: The spin 1/2 singly charmed baryons ground states include anti-triplet  $\mathcal{B}_{\bar{3}}$  and sextet  $\mathcal{B}_6$ . The strong couplings of  $\mathcal{B}_{\bar{3}}\mathcal{B}_{\bar{3}}P$ ,  $\mathcal{B}_6\mathcal{B}_{\bar{3}}P$  and  $\mathcal{B}_6\mathcal{B}_6P$  can be obtained by using the coupling constant  $g_{\Xi_c^+\Xi_c^+\pi^0} = 0.7 = \frac{g_{PBB1}}{\sqrt{2}}$ ,  $g_{\Xi_c^+\Xi_c^+\pi^0} = 3.1 = \frac{g_{PBB2}}{2}$  and  $\Sigma_c^+\Sigma_c^0\pi^+ = 8.0 = \frac{g_{PBB3}}{\sqrt{2}}$  [118], respectively. Since the matrix forms of the spin-3/2 singly charmed baryon ground state  $\mathcal{B}_6^*$  and the 1/2 sextet  $\mathcal{B}_6$  under symmetry are similar, the derived relations are identical. Then the couplings  $\mathcal{B}_6^*\mathcal{B}_{\bar{3}}P$  and  $\mathcal{B}_6^*\mathcal{B}_6P$  can be get from  $g_{\Sigma_c^{*0}\Lambda_c^+\pi^-} = 3.9 = g_{PB^*B2}$  and  $g_{\Sigma_c^{*+}\Sigma_c^0\pi^+} = 4.3 = \frac{g_{PB^*B3}}{\sqrt{2}}$  [132], respectively.

Vertex	g	Vertex	g	Vertex	g	Vertex	g
$\Lambda_c^+\Lambda_c^+\eta_8$	$\sqrt{\frac{2}{3}}g_{PBB1}$	$\Lambda_c^+\Lambda_c^+\eta_1$	$\frac{2g_{PBB1}}{\sqrt{3}}$	$\Lambda_c^+\Xi_c^+K^0$	$g_{PBB1}$	$\Lambda_c^+\Xi_c^0K^+$	$-g_{PBB1}$
$\Xi_c^+\Lambda_c^+\bar{K}^0$	$g_{PBB1}$	$\Xi_c^+\Xi_c^+\pi^0$	$\frac{g_{PBB1}}{\sqrt{2}}$	$\Xi_c^+\Xi_c^+\eta_8$	$-\frac{g_{PBB1}}{\sqrt{6}}$	$\Xi_c^+\Xi_c^+\eta_1$	$\frac{2g_{PBB1}}{\sqrt{3}}$
$\Xi_c^+\Xi_c^+\pi^+$	$g_{PBB1}$	$\Xi_c^0\Lambda_c^+K^-$	$-g_{PBB1}$	$\Xi_c^0\Xi_c^+\pi^-$	$g_{PBB1}$	$\Xi_c^0\Xi_c^0\pi^0$	$-\frac{g_{PBB1}}{\sqrt{2}}$
$\Xi_c^0\Xi_c^0\eta_8$	$-\frac{g_{PBB1}}{\sqrt{6}}$	$\Xi_c^0\Xi_c^0\eta_1$	$\frac{2g_{PBB1}}{\sqrt{3}}$				
$\Sigma_c^{++}\Lambda_c^+\pi^+$	$-g_{PBB2}$	$\Sigma_c^{++}\Xi_c^+K^+$	$-g_{PBB2}$	$\Sigma_c^+\Lambda_c^+\pi^0$	$g_{PBB2}$	$\Sigma_c^+\Xi_c^+K^0$	$-\frac{g_{PBB2}}{\sqrt{2}}$
$\Sigma_c^+\Xi_c^0K^+$	$-\frac{g_{PBB2}}{\sqrt{2}}$	$\Sigma_c^0\Lambda_c^+\pi^-$	$g_{PBB2}$	$\Sigma_c^0\Xi_c^0K^0$	$-g_{PBB2}$	$\Xi_c^+\Lambda_c^+\bar{K}^0$	$-\frac{g_{PBB2}}{\sqrt{2}}$
$\Xi_c^+\Xi_c^+\pi^0$	$\frac{g_{PBB2}}{2}$	$\Xi_c^+\Xi_c^+\eta_8$	$\frac{\sqrt{3}g_{PBB2}}{2}$	$\Xi_c^+\Xi_c^0\pi^+$	$\frac{g_{PBB2}}{\sqrt{2}}$	$\Xi_c^0\Lambda_c^+K^-$	$-\frac{g_{PBB2}}{\sqrt{2}}$
$\Xi_c^0\Xi_c^+\pi^-$	$\frac{g_{PBB2}}{\sqrt{2}}$	$\Xi_c^0\Xi_c^0\pi^0$	$-\frac{g_{PBB2}}{2}$	$\Xi_c^0\Xi_c^0\eta_8$	$\frac{\sqrt{3}g_{PBB2}}{2}$	$\Omega_c^0\Xi_c^+K^-$	$g_{PBB2}$
$\Omega_c^0\Xi_c^0\bar{K}^0$	$g_{PBB2}$						
$\Sigma_c^{++}\Sigma_c^{++}\pi^0$	$\frac{g_{PBB3}}{\sqrt{2}}$	$\Sigma_c^{++}\Sigma_c^{++}\eta_8$	$\frac{g_{PBB3}}{\sqrt{6}}$	$\Sigma_c^{++}\Sigma_c^{++}\eta_1$	$\frac{g_{PBB3}}{\sqrt{3}}$	$\Sigma_c^{++}\Sigma_c^+\pi^+$	$\frac{g_{PBB3}}{\sqrt{2}}$
$\Sigma_c^{++}\Xi_c^+K^+$	$\frac{g_{PBB3}}{\sqrt{2}}$	$\Sigma_c^+\Sigma_c^{++}\pi^-$	$\frac{g_{PBB3}}{\sqrt{2}}$	$\Sigma_c^+\Sigma_c^+\eta_8$	$\frac{g_{PBB3}}{\sqrt{6}}$	$\Sigma_c^+\Sigma_c^+\eta_1$	$\frac{g_{PBB3}}{\sqrt{3}}$
$\Sigma_c^+\Sigma_c^0\pi^+$	$\frac{g_{PBB3}}{\sqrt{2}}$	$\Sigma_c^+\Xi_c^+K^0$	$\frac{g_{PBB3}}{2}$	$\Sigma_c^+\Xi_c^0K^+$	$\frac{g_{PBB3}}{2}$	$\Sigma_c^0\Sigma_c^+\pi^-$	$\frac{g_{PBB3}}{\sqrt{2}}$
$\Sigma_c^0\Sigma_c^0\pi^0$	$-\frac{g_{PBB3}}{\sqrt{2}}$	$\Sigma_c^0\Sigma_c^0\eta_8$	$\frac{g_{PBB3}}{\sqrt{6}}$	$\Sigma_c^0\Sigma_c^0\eta_1$	$\frac{g_{PBB3}}{\sqrt{3}}$	$\Sigma_c^0\Xi_c^0K^0$	$\frac{g_{PBB3}}{\sqrt{2}}$
$\Xi_c^+\Sigma_c^{++}K^-$	$\frac{g_{PBB3}}{\sqrt{2}}$	$\Xi_c^+\Sigma_c^+K^0$	$\frac{g_{PBB3}}{2}$	$\Xi_c^+\Xi_c^+\pi^0$	$\frac{g_{PBB3}}{2\sqrt{2}}$	$\Xi_c^+\Xi_c^+\eta_8$	$-\frac{g_{PBB3}}{2\sqrt{6}}$
$\Xi_c^+\Xi_c^+\eta_1$	$\frac{g_{PBB3}}{\sqrt{3}}$	$\Xi_c^+\Xi_c^0\pi^+$	$\frac{g_{PBB3}}{2}$	$\Xi_c^+\Omega_c^0K^+$	$\frac{g_{PBB3}}{\sqrt{2}}$	$\Xi_c^0\Sigma_c^+K^-$	$\frac{g_{PBB3}}{2}$
$\Xi_c^0\Sigma_c^0\bar{K}^0$	$\frac{g_{PBB3}}{\sqrt{2}}$	$\Xi_c^0\Xi_c^+\pi^-$	$\frac{g_{PBB3}}{2}$	$\Xi_c^0\Xi_c^0\pi^0$	$-\frac{g_{PBB3}}{2\sqrt{2}}$	$\Xi_c^0\Xi_c^0\eta_8$	$-\frac{g_{PBB3}}{2\sqrt{6}}$
$\Xi_c^0\Xi_c^0\eta_1$	$\frac{g_{PBB3}}{\sqrt{3}}$	$\Xi_c^0\Omega_c^0K^0$	$\frac{g_{PBB3}}{\sqrt{2}}$	$\Omega_c^0\Xi_c^+K^-$	$\frac{g_{PBB3}}{\sqrt{2}}$	$\Omega_c^0\Xi_c^0\bar{K}^0$	$\frac{g_{PBB3}}{\sqrt{2}}$
$\Omega_c^0\Omega_c^0\eta_8$	$-\sqrt{\frac{2}{3}}g_{PBB3}$	$\Omega_c^0\Omega_c^0\eta_1$	$\frac{g_{PBB3}}{\sqrt{3}}$				

- [9] R. Aaij *et al.* [LHCb], Chin. Phys. C **44**, no.2, 022001 (2020) doi:10.1088/1674-1137/44/2/022001 [arXiv:1910.11316 [hep-ex]].
- [10] R. Aaij *et al.* [LHCb], JHEP **05**, 038 (2022) doi:10.1007/JHEP05(2022)038 [arXiv:2202.05648 [hep-ex]].
- [11] R. Aaij *et al.* [LHCb], JHEP **12**, 107 (2021) doi:10.1007/JHEP12(2021)107 [arXiv:2109.07292 [hep-ex]].
- [12] R. Aaij *et al.* [LHCb], Sci. China Phys. Mech. Astron. **63**, no.2, 221062 (2020) doi:10.1007/s11433-019-1471-8 [arXiv:1909.12273 [hep-ex]].
- [13] R. Aaij *et al.* [LHCb], Sci. China Phys. Mech. Astron. **64**, no.10, 101062 (2021) doi:10.1007/s11433-021-1742-7 [arXiv:2105.06841 [hep-ex]].
- [14] R. Aaij *et al.* [LHCb], Chin. Phys. C **47**, no.9, 093001 (2023) doi:10.1088/1674-1137/ace9c8 [arXiv:2204.09541 [hep-ex]].
- [15] R. Aaij *et al.* [LHCb], JHEP **11**, 095 (2020) doi:10.1007/JHEP11(2020)095 [arXiv:2009.02481 [hep-ex]].
- [16] R. Aaij *et al.* [LHCb], Chin. Phys. C **45**, no.9, 093002 (2021) doi:10.1088/1674-1137/ac0c70 [arXiv:2104.04759 [hep-ex]].
- [17] R. Aaij *et al.* [LHCb], Nature Phys. **18**, no.7, 751-754 (2022) doi:10.1038/s41567-022-01614-y [arXiv:2109.01038 [hep-ex]].
- [18] R. Aaij *et al.* [LHCb], Nature Commun. **13**, no.1, 3351 (2022) doi:10.1038/s41467-022-30206-w

Table XV: similar with Tab. XIV, the strong couplings of  $\mathcal{B}_3\mathcal{B}_3V$ ,  $\mathcal{B}_6\mathcal{B}_3V$  and  $\mathcal{B}_6\mathcal{B}_6V$  can be obtained by using the coupling constant  $g_{\Xi_c^0\Lambda_c^+K^{*-}} = \{4.6, 6\} = g_{VBB1}$ ,  $g_{\Sigma_c^0\Lambda_c^+\rho^-} = \{2.6, 16\} = g_{VBB2}$  and  $g_{\Sigma_c^+\Sigma_c^0\rho^+} = \{4.0, 27\} = \frac{g_{VBB3}}{\sqrt{2}}$  [123], respectively. Then the couplings  $\mathcal{B}_6^*\mathcal{B}_3V$  and  $\mathcal{B}_6^*\mathcal{B}_6V$  can be get from  $g_{\Sigma_c^{*+}\Lambda_c^+\rho^0} = 10 = g_{VB^*B2}$  and  $g_{\Sigma_c^{*0}\Sigma_c^+\rho^-} = 5.77 = \frac{g_{VB^*B3}}{\sqrt{2}}$  [113], respectively.

Vertex	g	Vertex	g	Vertex	g	Vertex	g
$\Lambda_c^+\Lambda_c^+\omega$	$-\sqrt{2}g_{VBB1}$	$\Lambda_c^+\Xi_c^+K^{*0}$	$-g_{VBB1}$	$\Lambda_c^+\Xi_c^0K^{*+}$	$g_{VBB1}$	$\Xi_c^+\Lambda_c^+\bar{K}^{*0}$	$-g_{VBB1}$
$\Xi_c^+\Xi_c^+\rho^0$	$-\frac{g_{VBB1}}{\sqrt{2}}$	$\Xi_c^+\Xi_c^+\omega$	$-\frac{g_{VBB1}}{\sqrt{2}}$	$\Xi_c^+\Xi_c^+\phi$	$-g_{VBB1}$	$\Xi_c^+\Xi_c^0\rho^+$	$-g_{VBB1}$
$\Xi_c^0\Lambda_c^+K^{*-}$	$g_{VBB1}$	$\Xi_c^0\Xi_c^+\rho^-$	$-g_{VBB1}$	$\Xi_c^0\Xi_c^0\rho^0$	$\frac{g_{VBB1}}{\sqrt{2}}$	$\Xi_c^0\Xi_c^0\omega$	$-\frac{g_{VBB1}}{\sqrt{2}}$
$\Xi_c^0\Xi_c^0\phi$	$-g_{VBB1}$						
$\Sigma_c^{++}\Lambda_c^+\rho^+$	$-g_{VBB2}$	$\Sigma_c^{++}\Xi_c^+K^{*+}$	$-g_{VBB2}$	$\Sigma_c^+\Lambda_c^+\rho^0$	$g_{VBB2}$	$\Sigma_c^+\Xi_c^+K^{*0}$	$-\frac{g_{VBB2}}{\sqrt{2}}$
$\Sigma_c^+\Xi_c^0K^{*+}$	$-\frac{g_{VBB2}}{\sqrt{2}}$	$\Sigma_c^0\Lambda_c^+\rho^-$	$g_{VBB2}$	$\Sigma_c^0\Xi_c^0K^{*0}$	$-g_{VBB2}$	$\Xi_c^+\Lambda_c^+\bar{K}^{*0}$	$-\frac{g_{VBB2}}{\sqrt{2}}$
$\Xi_c^+\Xi_c^+\rho^0$	$\frac{g_{VBB2}}{2}$	$\Xi_c^+\Xi_c^+\omega$	$\frac{g_{VBB2}}{2}$	$\Xi_c^+\Xi_c^+\phi$	$-\frac{g_{VBB2}}{\sqrt{2}}$	$\Xi_c^+\Xi_c^0\rho^+$	$\frac{g_{VBB2}}{\sqrt{2}}$
$\Xi_c^0\Lambda_c^+K^{*-}$	$\frac{g_{VBB2}}{\sqrt{2}}$	$\Xi_c^0\Xi_c^+\rho^-$	$\frac{g_{VBB2}}{\sqrt{2}}$	$\Xi_c^0\Xi_c^0\rho^0$	$-\frac{g_{VBB2}}{2}$	$\Xi_c^0\Xi_c^0\omega$	$\frac{g_{VBB2}}{2}$
$\Xi_c^0\Xi_c^0\phi$	$-\frac{g_{VBB2}}{\sqrt{2}}$	$\Omega_c^0\Xi_c^+K^{*-}$	$g_{VBB2}$	$\Omega_c^0\Xi_c^0\bar{K}^{*0}$	$g_{VBB2}$		
$\Sigma_c^{++}\Sigma_c^{++}\rho^0$	$\frac{g_{VBB3}}{\sqrt{2}}$	$\Sigma_c^{++}\Sigma_c^{++}\omega$	$\frac{g_{VBB3}}{\sqrt{2}}$	$\Sigma_c^{++}\Sigma_c^+\rho^+$	$\frac{g_{VBB3}}{\sqrt{2}}$	$\Sigma_c^{++}\Xi_c^+K^{*+}$	$\frac{g_{VBB3}}{\sqrt{2}}$
$\Sigma_c^+\Sigma_c^{++}\rho^-$	$\frac{g_{VBB3}}{\sqrt{2}}$	$\Sigma_c^+\Sigma_c^+\omega$	$\frac{g_{VBB3}}{\sqrt{2}}$	$\Sigma_c^+\Sigma_c^0\rho^+$	$\frac{g_{VBB3}}{\sqrt{2}}$	$\Sigma_c^+\Xi_c^+K^{*0}$	$\frac{g_{VBB3}}{2}$
$\Sigma_c^+\Xi_c^0K^{*+}$	$\frac{g_{VBB3}}{2}$	$\Sigma_c^0\Sigma_c^+\rho^-$	$\frac{g_{VBB3}}{\sqrt{2}}$	$\Sigma_c^0\Sigma_c^0\rho^0$	$-\frac{g_{VBB3}}{\sqrt{2}}$	$\Sigma_c^0\Sigma_c^0\omega$	$\frac{g_{VBB3}}{\sqrt{2}}$
$\Sigma_c^0\Xi_c^0K^{*0}$	$\frac{g_{VBB3}}{\sqrt{2}}$	$\Xi_c^+\Sigma_c^{++}K^{*-}$	$\frac{g_{VBB3}}{\sqrt{2}}$	$\Xi_c^+\Sigma_c^+\bar{K}^{*0}$	$\frac{g_{VBB3}}{2}$	$\Xi_c^+\Xi_c^+\rho^0$	$\frac{g_{VBB3}}{2\sqrt{2}}$
$\Xi_c^+\Xi_c^+\omega$	$\frac{g_{VBB3}}{2\sqrt{2}}$	$\Xi_c^+\Xi_c^+\phi$	$\frac{g_{VBB3}}{2}$	$\Xi_c^+\Xi_c^0\rho^+$	$\frac{g_{VBB3}}{2}$	$\Xi_c^+\Omega_c^0K^{*+}$	$\frac{g_{VBB3}}{\sqrt{2}}$
$\Xi_c^0\Sigma_c^+K^{*-}$	$\frac{g_{VBB3}}{2}$	$\Xi_c^0\Sigma_c^0\bar{K}^{*0}$	$\frac{g_{VBB3}}{\sqrt{2}}$	$\Xi_c^0\Xi_c^+\rho^-$	$\frac{g_{VBB3}}{2}$	$\Xi_c^0\Xi_c^0\rho^0$	$-\frac{g_{VBB3}}{2\sqrt{2}}$
$\Xi_c^0\Xi_c^0\omega$	$\frac{g_{VBB3}}{2\sqrt{2}}$	$\Xi_c^0\Xi_c^0\phi$	$\frac{g_{VBB3}}{2}$	$\Xi_c^0\Xi_c^0K^{*0}$	$\frac{g_{VBB3}}{\sqrt{2}}$	$\Omega_c^0\Xi_c^+K^{*-}$	$\frac{g_{VBB3}}{\sqrt{2}}$
$\Omega_c^0\Xi_c^0\bar{K}^{*0}$	$\frac{g_{VBB3}}{\sqrt{2}}$	$\Omega_c^0\Xi_c^0\phi$	$g_{VBB3}$				

- [arXiv:2109.01056 [hep-ex]].
- [19] F. S. Yu, H. Y. Jiang, R. H. Li, C. D. Lü, W. Wang and Z. X. Zhao, Chin. Phys. C **42**, no.5, 051001 (2018) doi:10.1088/1674-1137/42/5/051001 [arXiv:1703.09086 [hep-ph]].
- [20] V. V. Kiselev and A. K. Likhoded, Phys. Usp. **45**, 455-506 (2002) doi:10.1070/PU2002v045n05ABEH000958 [arXiv:hep-ph/0103169 [hep-ph]].
- [21] D. Ebert, R. N. Faustov, V. O. Galkin, A. P. Martynenko and V. A. Saleev, Z. Phys. C **76**, 111-115 (1997) doi:10.1007/s002880050534 [arXiv:hep-ph/9607314 [hep-ph]].
- [22] S. P. Tong, Y. B. Ding, X. H. Guo, H. Y. Jin, X. Q. Li, P. N. Shen and R. Zhang, Phys. Rev. D **62**, 054024 (2000) doi:10.1103/PhysRevD.62.054024 [arXiv:hep-ph/9910259 [hep-ph]].
- [23] D. Ebert, R. N. Faustov, V. O. Galkin and A. P. Martynenko, Phys. Rev. D **66**, 014008 (2002) doi:10.1103/PhysRevD.66.014008 [arXiv:hep-ph/0201217 [hep-ph]].
- [24] S. S. Gershtein, V. V. Kiselev, A. K. Likhoded and A. I. Onishchenko, Phys. Rev. D **62**, 054021 (2000) doi:10.1103/PhysRevD.62.054021
- [25] W. Roberts and M. Pervin, Int. J. Mod. Phys. A **23**, 2817-2860 (2008) doi:10.1142/S0217751X08041219 [arXiv:0711.2492 [nucl-th]].
- [26] E. Ortiz-Pacheco and R. Bijker, Phys. Rev. D **108**, no.5, 054014 (2023) doi:10.1103/PhysRevD.108.054014 [arXiv:2307.04939 [hep-ph]].
- [27] A. Valcarce, H. Garcilazo and J. Vijande, Eur. Phys. J. A **37**, 217-225 (2008) doi:10.1140/epja/i2008-10616-4 [arXiv:0807.2973 [hep-ph]].
- [28] Q. F. Lü, K. L. Wang, L. Y. Xiao and X. H. Zhong, Phys. Rev. D **96**, no.11, 114006 (2017) doi:10.1103/PhysRevD.96.114006 [arXiv:1708.04468 [hep-ph]].
- [29] G. L. Yu, Z. Y. Li, Z. G. Wang, J. Lu and M. Yan, Eur. Phys. J. A **59**, no.6, 126 (2023) doi:10.1140/epja/s10050-023-01044-1 [arXiv:2211.00510 [hep-ph]].
- [30] Z. Y. Li, G. L. Yu, Z. G. Wang, J. Z. Gu and H. T. Shen, Mod. Phys. Lett. A **38**, no.08n09, 2350052



- (2023) doi:10.1142/S0217732323500529 [arXiv:2210.13085 [hep-ph]].
- [31] B. Eakins and W. Roberts, *Int. J. Mod. Phys. A* **27**, 1250039 (2012) doi:10.1142/S0217751X1250039X [arXiv:1201.4885 [nucl-th]].
  - [32] Z. Shah and A. K. Rai, *Eur. Phys. J. C* **77**, no.2, 129 (2017) doi:10.1140/epjc/s10052-017-4688-x [arXiv:1702.02726 [hep-ph]].
  - [33] J. Soto and J. Tarrús Castellà, *Phys. Rev. D* **102**, no.1, 014013 (2020) [erratum: *Phys. Rev. D* **104**, no.5, 059901 (2021)] doi:10.1103/PhysRevD.104.059901 [arXiv:2005.00551 [hep-ph]].
  - [34] M. J. Savage and M. B. Wise, *Phys. Lett. B* **248**, 177-180 (1990) doi:10.1016/0370-2693(90)90035-5
  - [35] Y. Song, D. Jia, W. Zhang and A. Hosaka, *Eur. Phys. J. C* **83**, no.1, 1 (2023) doi:10.1140/epjc/s10052-022-11136-9 [arXiv:2204.00363 [hep-ph]].
  - [36] T. D. Cohen and P. M. Hohler, *Phys. Rev. D* **74**, 094003 (2006) doi:10.1103/PhysRevD.74.094003 [arXiv:hep-ph/0606084 [hep-ph]].
  - [37] K. W. Wei, B. Chen and X. H. Guo, *Phys. Rev. D* **92**, no.7, 076008 (2015) doi:10.1103/PhysRevD.92.076008 [arXiv:1503.05184 [hep-ph]].
  - [38] T. M. Aliev, K. Azizi and M. Savcı, *Phys. Lett. B* **715**, 149-151 (2012) doi:10.1016/j.physletb.2012.07.033 [arXiv:1205.6320 [hep-ph]].
  - [39] L. Liu, H. W. Lin, K. Orginos and A. Walker-Loud, *Phys. Rev. D* **81**, 094505 (2010) doi:10.1103/PhysRevD.81.094505 [arXiv:0909.3294 [hep-lat]].
  - [40] Z. S. Brown, W. Detmold, S. Meinel and K. Orginos, *Phys. Rev. D* **90**, no.9, 094507 (2014) doi:10.1103/PhysRevD.90.094507 [arXiv:1409.0497 [hep-lat]].
  - [41] M. Padmanath, R. G. Edwards, N. Mathur and M. Peardon, *Phys. Rev. D* **91**, no.9, 094502 (2015) doi:10.1103/PhysRevD.91.094502 [arXiv:1502.01845 [hep-lat]].
  - [42] N. Mathur and M. Padmanath, *Phys. Rev. D* **99**, no.3, 031501 (2019) doi:10.1103/PhysRevD.99.031501 [arXiv:1807.00174 [hep-lat]].
  - [43] N. Mathur, M. Padmanath and S. Mondal, *Phys. Rev. Lett.* **121**, no.20, 202002 (2018) doi:10.1103/PhysRevLett.121.202002 [arXiv:1806.04151 [hep-lat]].
  - [44] C. Albertus, E. Hernandez and J. Nieves, *Phys. Lett. B* **683**, 21-25 (2010) doi:10.1016/j.physletb.2009.11.048 [arXiv:0911.0889 [hep-ph]].
  - [45] M. J. White and M. J. Savage, *Phys. Lett. B* **271**, 410-414 (1991) doi:10.1016/0370-2693(91)90109-4
  - [46] R. H. Li, C. D. Lü, W. Wang, F. S. Yu and Z. T. Zou, *Phys. Lett. B* **767**, 232-235 (2017) doi:10.1016/j.physletb.2017.02.003 [arXiv:1701.03284 [hep-ph]].
  - [47] D. Ebert, R. N. Faustov, V. O. Galkin and A. P. Martynenko, *Phys. Rev. D* **70**, 014018 (2004) [erratum: *Phys. Rev. D* **77**, 079903 (2008)] doi:10.1103/PhysRevD.70.014018 [arXiv:hep-ph/0404280 [hep-ph]].
  - [48] W. Roberts and M. Pervin, *Int. J. Mod. Phys. A* **24**, 2401-2413 (2009) doi:10.1142/S0217751X09043407 [arXiv:0803.3350 [nucl-th]].
  - [49] T. Branz, A. Faessler, T. Gutsche, M. A. Ivanov, J. G. Korner, V. E. Lyubovitskij and B. Oehl, *Phys. Rev. D* **81**, 114036 (2010) doi:10.1103/PhysRevD.81.114036 [arXiv:1005.1850 [hep-ph]].
  - [50] C. Albertus, E. Hernandez and J. Nieves, *Phys. Lett. B* **690**, 265-271 (2010) doi:10.1016/j.physletb.2010.05.042 [arXiv:1004.3154 [hep-ph]].
  - [51] Q. Qin, Y. J. Shi, W. Wang, G. H. Yang, F. S. Yu and R. Zhu, *Phys. Rev. D* **105**, no.3, L031902 (2022) doi:10.1103/PhysRevD.105.L031902 [arXiv:2108.06716 [hep-ph]].
  - [52] H. Bahtiyar, K. U. Can, G. Erkol, M. Oka and T. T. Takahashi, *Phys. Rev. D* **98**, no.11, 114505 (2018) doi:10.1103/PhysRevD.98.114505 [arXiv:1807.06795 [hep-lat]].
  - [53] H. X. Chen, W. Chen, X. Liu, Y. R. Liu and S. L. Zhu, *Rept. Prog. Phys.* **80**, no.7, 076201 (2017) doi:10.1088/1361-6633/aa6420 [arXiv:1609.08928 [hep-ph]].
  - [54] H. Y. Cheng, *Chin. J. Phys.* **78**, 324-362 (2022) doi:10.1016/j.cjph.2022.06.021 [arXiv:2109.01216 [hep-ph]].
  - [55] B. Silvestre-Brac, *Few Body Syst.* **20**, 1-25 (1996) doi:10.1007/s006010050028
  - [56] T. Yoshida, E. Hiyama, A. Hosaka, M. Oka and K. Sadato, *Phys. Rev. D* **92**, no.11, 114029 (2015) doi:10.1103/PhysRevD.92.114029 [arXiv:1510.01067 [hep-ph]].
  - [57] B. Eakins and W. Roberts, *Int. J. Mod. Phys. A* **27**, 1250153 (2012) doi:10.1142/S0217751X12501539 [arXiv:1207.7163 [nucl-th]].
  - [58] L. Y. Xiao, K. L. Wang, Q. f. Lu, X. H. Zhong and S. L. Zhu, *Phys. Rev. D* **96**, no.9, 094005 (2017) doi:10.1103/PhysRevD.96.094005 [arXiv:1708.04384 [hep-ph]].

- [59] T. Mehen, Phys. Rev. D **96**, no.9, 094028 (2017) doi:10.1103/PhysRevD.96.094028 [arXiv:1708.05020 [hep-ph]].
- [60] Y. L. Ma and M. Harada, J. Phys. G **45**, no.7, 075006 (2018) doi:10.1088/1361-6471/aac86e [arXiv:1709.09746 [hep-ph]].
- [61] L. Y. Xiao, Q. F. Lü and S. L. Zhu, Phys. Rev. D **97**, no.7, 074005 (2018) doi:10.1103/PhysRevD.97.074005 [arXiv:1712.07295 [hep-ph]].
- [62] M. J. Yan, X. H. Liu, S. González-Solís, F. K. Guo, C. Hanhart, U. G. Meißner and B. S. Zou, Phys. Rev. D **98**, no.9, 091502 (2018) doi:10.1103/PhysRevD.98.091502 [arXiv:1805.10972 [hep-ph]].
- [63] H. Z. He, W. Liang and Q. F. Lü, Phys. Rev. D **105**, no.1, 014010 (2022) doi:10.1103/PhysRevD.105.014010 [arXiv:2106.11045 [hep-ph]].
- [64] B. Chen, S. Q. Luo, K. W. Wei and X. Liu, Phys. Rev. D **105**, no.7, 074014 (2022) doi:10.1103/PhysRevD.105.074014 [arXiv:2201.05728 [hep-ph]].
- [65] X. H. Hu, Y. L. Shen, W. Wang and Z. X. Zhao, Chin. Phys. C **42**, no.12, 123102 (2018) doi:10.1088/1674-1137/42/12/123102 [arXiv:1711.10289 [hep-ph]].
- [66] Q. F. Song, Q. F. Lü and A. Hosaka, Eur. Phys. J. C **84**, no.1, 89 (2024) doi:10.1140/epjc/s10052-024-12426-0 [arXiv:2308.03261 [hep-ph]].
- [67] Z. X. Zhao, F. W. Zhang, X. H. Hu and Y. J. Shi, Phys. Rev. D **107**, no.11, 116025 (2023) doi:10.1103/PhysRevD.107.116025 [arXiv:2304.07698 [hep-ph]].
- [68] W. Wang, Z. P. Xing and J. Xu, Eur. Phys. J. C **77**, no.11, 800 (2017) doi:10.1140/epjc/s10052-017-5363-y [arXiv:1707.06570 [hep-ph]].
- [69] Y. J. Shi, W. Wang, Y. Xing and J. Xu, Eur. Phys. J. C **78**, no.1, 56 (2018) doi:10.1140/epjc/s10052-018-5532-7 [arXiv:1712.03830 [hep-ph]].
- [70] N. Sharma and R. Dhir, Phys. Rev. D **96**, no.11, 113006 (2017) doi:10.1103/PhysRevD.96.113006 [arXiv:1709.08217 [hep-ph]].
- [71] A. S. Gerasimov and A. V. Luchinsky, Phys. Rev. D **100**, no.7, 073015 (2019) doi:10.1103/PhysRevD.100.073015 [arXiv:1905.11740 [hep-ph]].
- [72] H. Y. Cheng, G. Meng, F. Xu and J. Zou, Phys. Rev. D **101**, no.3, 034034 (2020) doi:10.1103/PhysRevD.101.034034 [arXiv:2001.04553 [hep-ph]].
- [73] T. Gutsche, M. A. Ivanov, J. G. Körner, V. E. Lyubovitskij and Z. Tyulemisov, Phys. Rev. D **99**, no.5, 056013 (2019) doi:10.1103/PhysRevD.99.056013 [arXiv:1812.09212 [hep-ph]].
- [74] R. Dhir and N. Sharma, Eur. Phys. J. C **78**, no.9, 743 (2018) doi:10.1140/epjc/s10052-018-6220-3
- [75] Y. J. Shi, Z. X. Zhao, Y. Xing and U. G. Meißner, Phys. Rev. D **106**, no.3, 034004 (2022) doi:10.1103/PhysRevD.106.034004 [arXiv:2206.13196 [hep-ph]].
- [76] J. J. Han, H. Y. Jiang, W. Liu, Z. J. Xiao and F. S. Yu, Chin. Phys. C **45**, no.5, 053105 (2021) doi:10.1088/1674-1137/abec68 [arXiv:2101.12019 [hep-ph]].
- [77] L. J. Jiang, B. He and R. H. Li, Eur. Phys. J. C **78**, no.11, 961 (2018) doi:10.1140/epjc/s10052-018-6445-1 [arXiv:1810.00541 [hep-ph]].
- [78] R. H. Li, J. J. Hou, B. He and Y. R. Wang, Chin. Phys. C **45**, no.4, 043108 (2021) doi:10.1088/1674-1137/abe0bc [arXiv:2010.09362 [hep-ph]].
- [79] J. J. Han, R. X. Zhang, H. Y. Jiang, Z. J. Xiao and F. S. Yu, Eur. Phys. J. C **81**, no.6, 539 (2021) doi:10.1140/epjc/s10052-021-09239-w [arXiv:2102.00961 [hep-ph]].
- [80] C. P. Jia, H. Y. Jiang, J. P. Wang and F. S. Yu, JHEP **11**, 072 (2024) doi:10.1007/JHEP11(2024)072 [arXiv:2408.14959 [hep-ph]].
- [81] Y. J. Shi, Y. Xing and Z. X. Zhao, Eur. Phys. J. C **79**, no.6, 501 (2019) doi:10.1140/epjc/s10052-019-7014-y [arXiv:1903.03921 [hep-ph]].
- [82] X. H. Hu and Y. J. Shi, Eur. Phys. J. C **80**, no.1, 56 (2020) doi:10.1140/epjc/s10052-020-7635-1 [arXiv:1910.07909 [hep-ph]].
- [83] X. H. Hu and Y. J. Shi, Phys. Rev. D **107**, no.3, 036007 (2023) doi:10.1103/PhysRevD.107.036007 [arXiv:2202.07540 [hep-ph]].
- [84] T. M. Aliev, S. Bilmis and M. Savci, Eur. Phys. J. C **82**, no.10, 862 (2022) doi:10.1140/epjc/s10052-022-10845-5 [arXiv:2206.08253 [hep-ph]].
- [85] T. M. Aliev, M. Savci and S. Bilmis, Phys. Rev. D **106**, no.3, 034017 (2022) doi:10.1103/PhysRevD.106.034017 [arXiv:2205.14012 [hep-ph]].
- [86] W. Wang, F. S. Yu and Z. X. Zhao, Eur. Phys. J. C **77**, no.11, 781 (2017) doi:10.1140/epjc/s10052-017-5360-1 [arXiv:1707.02834 [hep-ph]].

- [87] Z. X. Zhao, Eur. Phys. J. C **78**, no.9, 756 (2018) doi:10.1140/epjc/s10052-018-6213-2 [arXiv:1805.10878 [hep-ph]].
- [88] H. W. Ke, F. Lu, X. H. Liu and X. Q. Li, Eur. Phys. J. C **80**, no.2, 140 (2020) doi:10.1140/epjc/s10052-020-7699-y [arXiv:1912.01435 [hep-ph]].
- [89] H. W. Ke and X. Q. Li, Phys. Rev. D **105**, no.9, 096011 (2022) doi:10.1103/PhysRevD.105.096011 [arXiv:2203.10352 [hep-ph]].
- [90] X. H. Hu, R. H. Li and Z. P. Xing, Eur. Phys. J. C **80**, no.4, 320 (2020) doi:10.1140/epjc/s10052-020-7851-8 [arXiv:2001.06375 [hep-ph]].
- [91] Y. J. Shi, W. Wang and Z. X. Zhao, Eur. Phys. J. C **80**, no.6, 568 (2020) doi:10.1140/epjc/s10052-020-8096-2 [arXiv:1902.01092 [hep-ph]].
- [92] Y. J. Shi, W. Wang, Z. X. Zhao and U. G. Meißner, Eur. Phys. J. C **80**, no.5, 398 (2020) doi:10.1140/epjc/s10052-020-7949-z [arXiv:2002.02785 [hep-ph]].
- [93] T. Gutsche, M. A. Ivanov, J. G. Körner, V. E. Lyubovitskij and Z. Tyulemissov, Phys. Rev. D **100**, no.11, 114037 (2019) doi:10.1103/PhysRevD.100.114037 [arXiv:1911.10785 [hep-ph]].
- [94] R. L. Workman *et al.* [Particle Data Group], PTEP **2022**, 083C01 (2022) doi:10.1093/ptep/ptac097
- [95] H. M. Choi, C. R. Ji, Z. Li and H. Y. Ryu, Phys. Rev. C **92**, no.5, 055203 (2015) doi:10.1103/PhysRevC.92.055203 [arXiv:1502.03078 [hep-ph]].
- [96] T. Feldmann, P. Kroll and B. Stech, Phys. Rev. D **58**, 114006 (1998) doi:10.1103/PhysRevD.58.114006 [arXiv:hep-ph/9802409 [hep-ph]].
- [97] M. Mikhasenko, B. Ketzer and A. Sarantsev, Phys. Rev. D **91**, no.9, 094015 (2015) doi:10.1103/PhysRevD.91.094015 [arXiv:1501.07023 [hep-ph]].
- [98] M. Z. Liu, Y. W. Pan, Z. W. Liu, T. W. Wu, J. X. Lu and L. S. Geng, Phys. Rept. **1108**, 1-108 (2025) doi:10.1016/j.physrep.2024.12.001 [arXiv:2404.06399 [hep-ph]].
- [99] Q. Wu and D. Y. Chen, Phys. Rev. D **100**, no.11, 114002 (2019) doi:10.1103/PhysRevD.100.114002 [arXiv:1906.02480 [hep-ph]].
- [100] Y. K. Hsiao, Y. Yu and B. C. Ke, Eur. Phys. J. C **80**, no.9, 895 (2020) doi:10.1140/epjc/s10052-020-08468-9 [arXiv:1909.07327 [hep-ph]].
- [101] X. Z. Ling, M. Z. Liu, J. X. Lu, L. S. Geng and J. J. Xie, Phys. Rev. D **103**, no.11, 116016 (2021) doi:10.1103/PhysRevD.103.116016 [arXiv:2102.05349 [hep-ph]].
- [102] T. J. Burns and E. S. Swanson, Phys. Rev. D **106**, no.5, 054029 (2022) doi:10.1103/PhysRevD.106.054029 [arXiv:2207.00511 [hep-ph]].
- [103] Y. W. Pan, M. Z. Liu and L. S. Geng, Phys. Rev. D **108**, no.11, 114022 (2023) doi:10.1103/PhysRevD.108.114022 [arXiv:2309.12050 [hep-ph]].
- [104] F. K. Guo, X. H. Liu and S. Sakai, Prog. Part. Nucl. Phys. **112**, 103757 (2020) doi:10.1016/j.ppnp.2020.103757 [arXiv:1912.07030 [hep-ph]].
- [105] F. K. Guo, C. Hidalgo-Duque, J. Nieves and M. P. Valderrama, Phys. Rev. D **88**, 054007 (2013) doi:10.1103/PhysRevD.88.054007 [arXiv:1303.6608 [hep-ph]].
- [106] J. F. Jiang, W. Chen and S. L. Zhu, Phys. Rev. D **96**, no.9, 094022 (2017) doi:10.1103/PhysRevD.96.094022 [arXiv:1708.00142 [hep-ph]].
- [107] M. Bayar, F. Aceti, F. K. Guo and E. Oset, Phys. Rev. D **94**, no.7, 074039 (2016) doi:10.1103/PhysRevD.94.074039 [arXiv:1609.04133 [hep-ph]].
- [108] F. K. Guo, C. Hanhart, U. G. Meißner, Q. Wang, Q. Zhao and B. S. Zou, Rev. Mod. Phys. **90**, no.1, 015004 (2018) [erratum: Rev. Mod. Phys. **94**, no.2, 029901 (2022)] doi:10.1103/RevModPhys.90.015004 [arXiv:1705.00141 [hep-ph]].
- [109] Y. H. Chen, L. Y. Dai, F. K. Guo and B. Kubis, Phys. Rev. D **99**, no.7, 074016 (2019) doi:10.1103/PhysRevD.99.074016 [arXiv:1902.10957 [hep-ph]].
- [110] M. Z. Liu, X. Z. Ling and L. S. Geng, Phys. Rev. D **109**, no.5, 5 (2024) doi:10.1103/PhysRevD.109.056014 [arXiv:2312.01433 [hep-ph]].
- [111] M. Bayar, R. Molina, E. Oset, M. Z. Liu and L. S. Geng, Phys. Rev. D **109**, no.7, 076027 (2024) doi:10.1103/PhysRevD.109.076027 [arXiv:2312.12004 [hep-ph]].
- [112] J. M. Xie, M. Z. Liu and L. S. Geng, Phys. Rev. D **107**, no.1, 016003 (2023) doi:10.1103/PhysRevD.107.016003 [arXiv:2207.12178 [hep-ph]].
- [113] Y. H. Lin, C. W. Shen, F. K. Guo and B. S. Zou, Phys. Rev. D **95**, no.11, 114017 (2017) doi:10.1103/PhysRevD.95.114017 [arXiv:1703.01045 [hep-ph]].
- [114] M. Ablikim, D. S. Du and M. Z. Yang, Phys. Lett. B **536**, 34-42 (2002) doi:10.1016/S0370-

- 2693(02)01812-9 [arXiv:hep-ph/0201168 [hep-ph]].
- [115] H. Y. Cheng, C. K. Chua and A. Soni, Phys. Rev. D **71**, 014030 (2005) doi:10.1103/PhysRevD.71.014030 [arXiv:hep-ph/0409317 [hep-ph]].
  - [116] C. D. Lu, Y. M. Wang, H. Zou, A. Ali and G. Kramer, Phys. Rev. D **80**, 034011 (2009) doi:10.1103/PhysRevD.80.034011 [arXiv:0906.1479 [hep-ph]].
  - [117] H. n. Li, C. D. Lu and F. S. Yu, Phys. Rev. D **86**, 036012 (2012) doi:10.1103/PhysRevD.86.036012 [arXiv:1203.3120 [hep-ph]].
  - [118] T. M. Aliev, K. Azizi and M. Savci, Phys. Lett. B **696**, 220-226 (2011) doi:10.1016/j.physletb.2010.12.027 [arXiv:1009.3658 [hep-ph]].
  - [119] T. M. Yan, H. Y. Cheng, C. Y. Cheung, G. L. Lin, Y. C. Lin and H. L. Yu, Phys. Rev. D **46**, 1148-1164 (1992) [erratum: Phys. Rev. D **55**, 5851 (1997)] doi:10.1103/PhysRevD.46.1148
  - [120] R. Casalbuoni, A. Deandrea, N. Di Bartolomeo, R. Gatto, F. Feruglio and G. Nardulli, Phys. Rept. **281**, 145-238 (1997) doi:10.1016/S0370-1573(96)00027-0 [arXiv:hep-ph/9605342 [hep-ph]].
  - [121] U. G. Meissner, Phys. Rept. **161**, 213 (1988) doi:10.1016/0370-1573(88)90090-7
  - [122] N. Li and S. L. Zhu, Phys. Rev. D **86**, 014020 (2012) doi:10.1103/PhysRevD.86.014020 [arXiv:1204.3364 [hep-ph]].
  - [123] T. M. Aliev, K. Azizi and M. Savci, Nucl. Phys. A **852**, 141-154 (2011) doi:10.1016/j.nuclphysa.2011.01.011 [arXiv:1011.0086 [hep-ph]].
  - [124] J. W. Li, M. Z. Yang and D. S. Du, HEPNP **27**, 665-672 (2003) [arXiv:hep-ph/0206154 [hep-ph]].
  - [125] X. Q. Li and B. S. Zou, Phys. Lett. B **399**, 297-302 (1997) doi:10.1016/S0370-2693(97)00308-0 [arXiv:hep-ph/9611223 [hep-ph]].
  - [126] Y. S. Dai, D. S. Du, X. Q. Li, Z. T. Wei and B. S. Zou, Phys. Rev. D **60**, 014014 (1999) doi:10.1103/PhysRevD.60.014014 [arXiv:hep-ph/9903204 [hep-ph]].
  - [127] M. P. Locher, Y. Lu and B. S. Zou, Z. Phys. A **347**, 281-284 (1994) doi:10.1007/BF01289796 [arXiv:nucl-th/9311021 [nucl-th]].
  - [128] C. D. Lu, Y. L. Shen and W. Wang, Phys. Rev. D **73**, 034005 (2006) doi:10.1103/PhysRevD.73.034005 [arXiv:hep-ph/0511255 [hep-ph]].
  - [129] M. He, X. G. He and G. N. Li, Phys. Rev. D **92**, no.3, 036010 (2015) doi:10.1103/PhysRevD.92.036010 [arXiv:1507.07990 [hep-ph]].
  - [130] Z. Zhang, R. G. Ping, T. Liu, J. J. Song, W. Yang and Y. j. Zhou, Phys. Rev. D **110**, no.3, 034034 (2024) doi:10.1103/PhysRevD.110.034034 [arXiv:2404.04787 [hep-ph]].
  - [131] K. Nakayama, Y. Oh, J. Haidenbauer and T. S. H. Lee, Phys. Lett. B **648**, 351-356 (2007) doi:10.1016/j.physletb.2007.03.034 [arXiv:nucl-th/0611101 [nucl-th]].
  - [132] T. M. Aliev, K. Azizi and M. Savci, Eur. Phys. J. C **71**, 1675 (2011) doi:10.1140/epjc/s10052-011-1675-5 [arXiv:1012.5935 [hep-ph]].
  - [133] R. Aaij *et al.* [LHCb], Phys. Rev. Lett. **121**, no.5, 052002 (2018) doi:10.1103/PhysRevLett.121.052002 [arXiv:1806.02744 [hep-ex]].
  - [134] Q. X. Yu and X. H. Guo, Nucl. Phys. B **947**, 114727 (2019) doi:10.1016/j.nuclphysb.2019.114727 [arXiv:1810.00437 [hep-ph]].
  - [135] F. S. Yu, Sci. China Phys. Mech. Astron. **63**, no.2, 221065 (2020) doi:10.1007/s11433-019-1483-0 [arXiv:1912.10253 [hep-ex]].
  - [136] H. Y. Cheng and Y. L. Shi, Phys. Rev. D **98**, no.11, 113005 (2018) doi:10.1103/PhysRevD.98.113005 [arXiv:1809.08102 [hep-ph]].
  - [137] A. V. Berezhnoy, A. K. Likhoded and A. V. Luchinsky, Phys. Rev. D **98**, no.11, 113004 (2018) doi:10.1103/PhysRevD.98.113004 [arXiv:1809.10058 [hep-ph]].
  - [138] C. W. Liu, Phys. Rev. D **109**, no.3, 033004 (2024) doi:10.1103/PhysRevD.109.033004 [arXiv:2308.07754 [hep-ph]].
  - [139] S. Zeng, F. Xu, P. Y. Niu and H. Y. Cheng, Phys. Rev. D **107**, no.3, 034009 (2023) doi:10.1103/PhysRevD.107.034009 [arXiv:2212.12983 [hep-ph]].
  - [140] C. W. Liu and C. Q. Geng, Phys. Rev. D **107**, no.1, 013006 (2023) doi:10.1103/PhysRevD.107.013006 [arXiv:2211.12960 [hep-ph]].
  - [141] A. K. Leibovich, Z. Ligeti, I. W. Stewart and M. B. Wise, Phys. Lett. B **586**, 337-344 (2004) doi:10.1016/j.physletb.2004.02.033 [arXiv:hep-ph/0312319 [hep-ph]].
  - [142] S. Mantry, D. Pirjol and I. W. Stewart, Phys. Rev. D **68**, 114009 (2003) doi:10.1103/PhysRevD.68.114009 [arXiv:hep-ph/0306254 [hep-ph]].